Assessment of Air Pollution and Carbon Emission from Fuel Consumption Activities

Xuelin Tian

A Thesis
in
The Department
of
Building, Civil and Environmental Engineering

Presented in Partial Fulfillment of the Requirements
for the Degree of Master of Applied Science (Civil Engineering) at
Concordia University
Montreal, Quebec, Canada

October 2021

CONCORDIA UNIVERSITY

School of Graduate Studies

This is to certify that the thesis prepared

By: Xuelin Tian

Entitled: Assessment of Air Pollution and Carbon Emission from Fuel Consumption Activities

and submitted in partial fulfillment of the requirements for the degree of

Master of Applied Science (Civil Engineering)

Complies with the regulations of the University and meets the accepted standards with respect to originality and quality.

Signed by the final examining committee:

Dr. Fuzhan Nasiri Chair

Chair's name

Dr. Mazdak Nik-Bakht Examiner

Examiner's name

Dr. Fuzhan Nasiri Examiner

Examiner's name

Dr. Chunjiang An Supervisor

Supervisor's name

Approved by Dr. Mazdak Nik-Bakht Graduate Program Director

Dr. Mourad Debbabi Dean

ABSTRACT

Assessment of Air Pollution and Carbon Emission from Fuel Consumption Activities

Xuelin Tian

The consumption of fuel is associated with a number of environmental issues. One of the major environmental concerns is the increasing greenhouse gas (GHG) emissions and air pollution. GHG emissions and air pollution are mainly from the human activities such as transportation, non-renewable electricity production, oil and gas production, and heating and cooling of buildings. In this thesis, a comprehensive review was conducted to assess the impact of elements in urban form on on-road vehicles GHG emissions. A small-medium North American city case study was given to track the progress in reducing real-world emissions over time and to estimate the future air quality impacts based on the trends of fleet mixes. It helps gain understanding of detailed source apportionment information to quantify the contributions to total emission made by different vehicle body types, different fuels, and manufacturer models in recent decades and how the fuel economy of the vehicle fleet has changed over the years. Following that, an assessment was conducted to analyze the impact of COVID-19 pandemic on GHG emissions from urban transportation and air quality in Canadian cities. The reduced traffic experienced throughout several lockdowns offers a glimpse of what air quality in cities would look like if the country switched to low-carbon transportation modes. Finally, the reductions in NO_2 emissions from thermal power plants in Canada were assessed to evaluate the government commitment of switching from fossil fuels to clean energy. The satellite observation was developed as a supplementary information management tool to verify the effect of technologies and policies on emissions changes from threshold perspective on a smaller spatial scale. Overall, this thesis provides some new insights on assessing air pollution and carbon emission levels from transportation and electricity sectors.

ACKNOWLEDGEMENTS

I would first like to thank my supervisor Dr. Chunjiang An. The door to Dr. An's office was always open whenever I ran into a trouble spot or had a question about my research or writing. He consistently allowed this paper to be my own work, but steered me in the right the direction whenever he thought I needed it.

I would also like to thank Dr. Mazdak Nik-Bakht, Dr. Fuzhan Nasiri, Dr. Zhiqiang Tian for their valuable comments on my works, as well as the help from Mr. Ziyang Song on modelling analysis.

I would also express my thanks to my friends and colleagues in Concordia University for their assistance in various aspects of my research and for their support with constant friendship. They are Mr. Zhikun Chen, Ms. Huifang Bi, Ms. Qi Feng, Mr. Zheng Wang, Ms. Mengfan Cai.

Finally, I must express my very profound gratitude to my parents for providing me with unfailing support and continuous encouragement throughout my years of study and through the process of researching and writing this thesis. This accomplishment would not have been possible without them.

TABLE OF CONTENTS

LIST OF TABLES

LIST OF FIGURES

LIST OF ABBREVIATIONS

GHG	Greenhouse Gas
VMT	Vehicle-Miles Traveled
FEAT	Fuel Efficiency Automobile Test
SGA	Smart Growth America
TA	Total Area
AI	Aggregation Index
CI	Compactness Index
LPI	Largest Patch Index
AWMSI	Area-Weighted Mean Shape Index
AWMPFDI	Area-Weighted Mean Patch Fractal Dimension Index
PARA_MN	Perimeter Area Ratio Distribution
AWM	Aera Weighted Mean
PLADJ	Percentage of Like Adjacencies
COHESION	Patch Cohesion Index
LSI	Landscape Shape Index
CONTIG	Contiguity
OLS	Ordinary Least Squares
FE	Fixed Effect
RE	Random Effect
ME	Mixed Effect
LLC	Levin-Lin-Chu
SEM	Structural Equation Model
LPD	Linear Population Density
CBD	Central Business District
BCI	Buffer Compactness Index
DENSITY	Gross Density of Cities
MIXITE	The Ratio Between Jobs and Residents
RURAL	The Rate of Agricultural Areas in The Built Environment
PCA	Principal Component Analysis
SHAREPUB	Metric to Represent Accessibility

ITS	Intelligent Transport Systems
VICS	Vehicle Information and Communication System
LDVs	Light-Duty Vehicles
HDVs	Heavy-Duty Vehicles
XGBoost	Extreme Gradient Boosting
SVR	Support Vector Regression
SGI	Saskatchewan Government Insurance
ICCT	International Council on Clean Transportation
OECD	Organization for Economic Co-Operation and Development
MAPE	Mean Absolute Percentage Error
GWP	Global Warming Potential
Kt	Kilotonnes
ACA	Alberta Capital Airshed
CASA	Clean Air Strategic Alliance
NAPS	National Air Pollution Surveillance
AQI	Air Quality Index
CIEEDAC	Canadian Industrial Energy End-Use Data Analysis Centre
AQHI	Air Quality Health Index
ESA	European Space Agency
TVCDs	Tropospheric Vertical Column Densities
OMI	Ozone Monitoring Instrument
NPRI	National Pollutant Release Inventory
KNMI	Royal Netherlands Meteorological Institute
TEMIS	Tropospheric Emission Monitoring Internet Service
NGCC	Natural Gas Combined Cycle
FDFC	Four Door Car Fuel Consumption
VRQ	Van Registration Quantity
TRQ	Truck Registration Quantity
SWRQ	Station Wagon Registration Quantity
DP	Diesel Price
TFC	Truck Fuel Consumption

VFC	Van Fuel Consumption
GP	Gasoline Price
POM	Proportion of Males
DRQ	Diesel Vehicle Registration Quantity
SWFC	Station Wagon Fuel Consumption
EHGFQ	Electric Hybrid Gas Vehicle Registration Quantity
EMPL	Employment Rate
PRQ	Propane Vehicle Registration Quantity
TDFC	Two Door Car Fuel Consumption

CHAPTER 1. INTRODUCTION

The consumption of fuel is associated with a number of environmental issues. One of the major environmental concerns is the increasing greenhouse gas (GHG) emissions and air pollution (Cai et al., 2020; Chen et al., 2020b; Hu and Xia, 2020; Zhang et al., 2019). GHG emissions and air pollution are mainly from the human activities such as transportation, non-renewable electricity production, oil and gas production, and heating and cooling of buildings. Their contributions in these sectors vary in different regions. This is because the characteristics of various regions are different in energy structure, land use, transportation networks, and relationships between buildings, road, and infrastructure that directly affect fuel consumption and emissions (Fang et al., 2015; Senbel and Church, 2010; Song et al., 2019). In order to reduce the negative effects of GHG emission as well as air pollution on climate change, human health, and welfare, to examine the costs imposed on society by these effects, and to explore energy technology and policy options for encouraging more desirable outcomes, assessing the air pollution and carbon emission from fuel consumption activities is critical. It is necessary to develop appropriate strategies to reduce air pollution and carbon emission based on regional characteristics.

Urban form is used to describe the physical characteristics that make up a city. The features of urban form can be considered at different scales ranging from localized scale like individual building to regional scale like layout of the city. Studying urban form can help better understand the spatial structure and character of a metropolitan area, city, district, or neighborhood by examining the patterns of its component parts (Dempsey et al., 2010). Rational urban form can effectively reduce energy use and GHG emissions. Therefore, many scholars have studied the relationship between the spatial allocation of urban development and GHG emissions. For example, Ishii et al. (2010) tested energy-saving technologies such as photovoltaic cells and combined heat and power (CHP) in three urban forms as predicted in scenarios for the years 2030 and 2050. In terms of the benefits of both photovoltaic cells and CHP, their results showed that medium density typically outperformed the high-density centralized and low-density decentralized forms. A wide range of research has been conducted to study GHG emissions from residential sources

such as space heating and household electricity use in the context of different patterns of urban development. It has been found that lower density in residential settings gives rise to more heat island formation than higher density, as it brings about more radiant heat energy (Yao et al., 2020). Policy makers should consider compact moderate-to-high-density residential development patterns for reducing emission of radiant heat energy (Glaeser and Kahn, 2010; Stone Jr and Rodgers, 2001).

Urban form has also been proved to have a significant impact on traffic-related emissions. The spatial evolution of urban development mainly affects the travel behaviour from private vehicle (Hawkes, 2014). Dulal et al. (2011) examined the empirical evidence linking land-use policy to transport emissions and investigated the impact of residential and employment density on travel demand. Anderson et al. (1996), meanwhile, targeted urban transport energy use in order to evaluate the current state of integrated urban form models and energy utilization in the environment. Although the transformation of urban form has a limited influence on traffic-related emissions in the short term because of the long period in building up the supporting infrastructure, it can have significant impact on citizens' travel behaviour in the long term, including the travel mode choices, travel frequency, vehicle-miles traveled (VMT) and vehicle choice. Therefore, it is important to understand how urban development, and the elements in different urban forms, affect citizens' travel behaviour and, ultimately, the mitigation of GHG emissions from on-road private vehicles.

In addition to the impacts from urban forms, the restructuring of energy mix in different regions in recent years has also influenced the GHG emissions. The overall energy mix is becoming more diverse as many countries and regions commit to switching from fossil fuels to clean energy. However, shutting down plants and replacing them with new sources will take time and most countries still rely on fossil fuels. Therefore, it is important to quantify the emissions reductions that result from the transition to to low-carbon energy system. That will help develop low-carbon policies and evaluate the effects of implementing decarbonization measures. The satellite inversion of tropospheric air pollutants has been applied for monitoring and tracing the interannual and geospatial

variation, especially the emissions from anthropogenic activities such as coal-fired power generation (Jiao et al., 2020; Lu and Streets, 2012; Russell et al., 2010). Apart from direct quantitative monitoring, scholars have taken a combined approach comparing ground data with emission estimates based on satellite observation. For instance, an approach comparing satellite retrievals with emissions estimates from a bottom-up inventory has been used to double-measure the emission variation from power plants (Liu et al., 2018; Lu and Streets, 2012). More recently, satellite pollutant monitoring has been used to verify the effect of technologies and policies intended to control and reduce emissions from coal-fired power plants (Jiao et al., 2020; Wu et al., 2019). In order to verify the effects of implementing decarbonization measures, satellite pollutant observation can be regarded as a supplementary tool to draw connections with ground emission data, showing thresholds or concentration trends for specific pollutants and a particular jurisdiction from both digital and visual perspectives (Danilina and Grigoriev, 2020; Tang and Mudd, 2014).

Therefore, the aim of this thesis is to explore the detailed source apportionment for emissions from transportation and electricity sectors, and develop supplementary information management tools to investigate the air pollutant variations. To achieve this aim, there are four objectives proposed as follows:

- Conduct comprehensive literature review of the impact of elements in urban form on on-road vehicle GHG emissions (CHAPTER 2);
- Analyze the impact from evolution of private vehicle fleet composition on traffic-related emissions in small-medium cities based on a North American case study (CHAPTER 3);
- Assess the impact of COVID-19 pandemic on GHG emissions from urban transportation and air quality in Canadian cities (CHAPTER 4).
- Assess the reductions in NO_2 emissions from thermal power plants in Canada based on the analysis of policy, inventory, and satellite data (CHAPTER 5).

CHAPTER 2. LITERATURE REVIEW

2.1. Theoretical background of identifying the relationship between vehicle GHG emissions and urban form

2.1.1. Characteristics of data using in GHG emissions estimation and urban form measurement

The quantitative analysis was mainly used in the existing studies to explore the relationship between urban form and GHG emissions. Therefore, the data using in GHG emissions estimation and urban form measurement are the foundation of corresponding studies (Newman and Kenworthy, 1996). The data trend summarized from the existing studies is that the data used changed from single year to long time span, and the urban form data shifted from single elements to multiple elements for comprehensive studies (Ewing and Rong, 2008; Kahn, 2009). A dataset with the above characteristics is concluded as panel data. Panel data is different from cross-sectional data and time series data. Cross-sectional data are a collection of observations for multiple subjects at a single point in time, which means it is a one-time survey with no relation to time. Time series data, meanwhile, are a collection of observations for a single subject at different time intervals. It reflects the state of degree of change of a thing or phenomenon over time. Panel data are usually collected over time and for different subjects. Figure 1 compare the similarities and differences among three kinds of data. The notable feature of panel data is the time continuity of samples. Panel data is hard to collect due to the number of elements involved and the long-time span. It is widely used in fields of social science, epidemiology, and econometrics for its high power to control individual heterogeneity (Al-mulali, 2012; Fang et al., 2015).

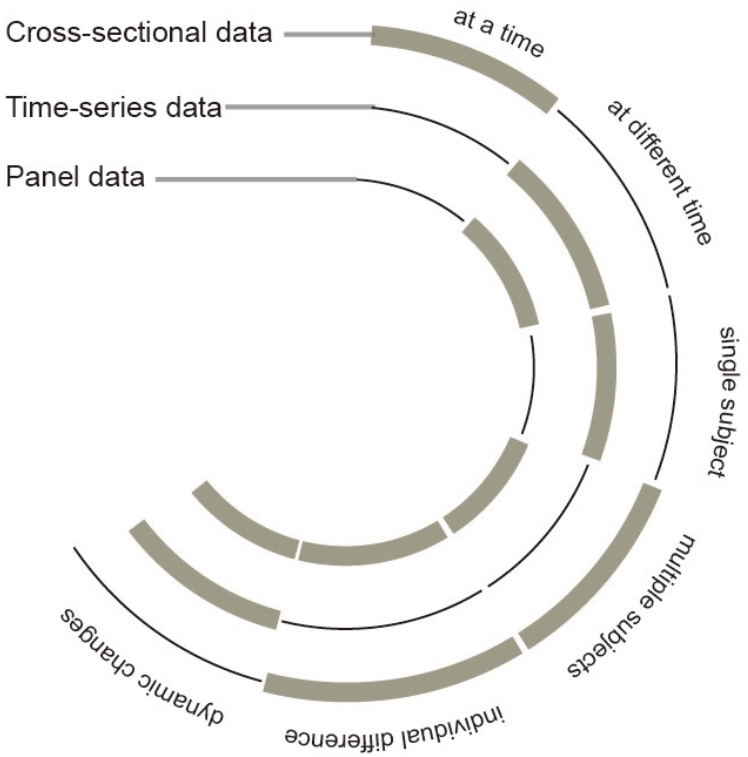

Figure 1. Comparison among cross-sectional data, time-series data and panel data.

2.1.2. Methods for GHG emissions estimation

The estimation for GHG emissions is an important part in quantitative studies that identify the relationships between GHG emissions and urban form. In the field testing of the real-world emissions, the most common methods used in current studies are top-down and bottom-up emissions estimation methods. Both methods aim at obtaining statistical emission data or monitoring emission data. Figure 2 presents the bottom-up to top-down vehicle emissions monitoring methods from time scale and spatial scale. Scholars have been developing the estimation of GHG emissions from both top-down and bottom-up approaches to improve the accuracy of the GHG emissions inventory (Farren et al., 2020; Sun et al., 2017).

- Top-down GHG emissions estimation

Top-down GHG emissions estimation refers to obtaining existing statistical data, sectoral

data or estimation inventory data from official agencies or monitoring station. The advantages of this method are that the official data are generally accepted as well as the time and cost required for collecting process is relatively less. The disadvantages are that the level of detail of the data may not meet the segmentation requirements, and it is hard to do an in-depth analysis of the emission structure. Fang et al. (2015) applied the coefficients published by Intergovernmental Panel on Climate Change (IPCC) and collected the consumption data of coal, gas, electricity, and liquefied petroleum gas data in 1991, 2001 and 2011 for 30 provincial capital cities to estimate the approximate CO_2 emissions data. Yang et al. (2015) also referred the transportation carbon-emission model from IPCC, and collected the final energy consumption data in the transportation sector to estimate the amount of CO_2 emissions for 30 provinces from 2000 to 2012. In addition to GHG emissions, top-down estimation can also be used for vehicle-miles travelled (VMT) data, that also indirectly affects GHG emissions. Su (2010) collected the average daily VMT for 85 US urban areas from 1982 to 2003 from the Urban Mobility Report to examine the relationships between travel demand and urban form characteristics. Anenberg et al. (2017) adapted a global transportation emission inventory model to generate the NO_X emissions from diesel light-duty vehicles (LDVs) and heavy-duty vehicles (HDVs) in 11 major vehicle markets and found that HDVs contributed to excess diesel NO_X emissions in almost all regions.

The satellite inversion has also been applied by many scholars as a top-down method for monitoring and tracing the interannual and geospatial variation of emissions, especially the emissions from anthropogenic activities such as coal-fired power generation (Jiao et al., 2020; Lu and Streets, 2012; Russell et al., 2010). Moreover, the emergence of remote sensing presents a novel approach for quantitative monitoring of emissions or empirical study of other ecological issues (Karimi et al., 2020; Tian et al., 2021; Xiao et al., 2020a). More recently, satellite pollutant monitoring has been used to verify the effect of

technologies and policies intended to control and reduce emissions from coal-fired power plants (Jiao et al., 2020; Wu et al., 2019). The combination of ambient measurements and satellite retrievals can also be used to verify the emission inventory (Li et al., 2019a). However, there is a lack of studies having used a combined (ground–satellite) approach to further process and validate the threshold changes on a smaller spatial scale. Meanwhile, satellite pollutant observation is also regarded as a supplementary information management tool that can be used to draw connections with national pollutant release inventory, showing thresholds or concentration trends for specific pollutants and a particular jurisdiction from both digital and visual perspectives (Danilina and Grigoriev, 2020; Tang and Mudd, 2014).

- Bottom-up GHG emissions estimation

Bottom-up GHG emission estimation refers to the collection and aggregation of data from end-consumers, mainly through research and sample surveys. The advantage of this method is that the data are comprehensively classified, that is conducive to analyzing the emission structure and identifying key emission sources. The disadvantage is that it requires a high level of data detail and more time and resources. Barla et al. (2011) considered the distance, mode choice, vehicle make-model-year, speed and number of passengers to compute the amount of travel GHG emissions from 400 respondents in the Quebec City region in a survey on household activities from 2002 to 2006. Based on a survey from 5% of the households in Montreal for over 4 years, Zahabi et al. (2012) also considered the speed, vehicle fleet characteristics, vehicle occupancy and travel distance to calculate the GHG emissions a the trip level. Glaeser and Kahn (2010) and Lee and Lee (2014) both used the 2001 National Household Transportation Survey (NHTS) data to estimate the household level annual CO_2 emissions from private vehicle by using the VMT, fuel efficiency and emission factor data, and CO_2 emissions from public transportation by using household annual transit rides, trip length, and emission factor data .

Apart from using statistical data, on-site emission mobile measurements have also been conducted using various technologies for traffic emissions estimation such as Fuel

Efficiency Automobile Test (FEAT) (Bishop and Haugen, 2018; Farren et al., 2020). In addition, on-vehicle measurements deployed the monitoring equipment in instrumented vehicles such as conventional probe vehicles studies and car chaser studies (Ropkins et al., 2009). However, most of these studies have focused on the emissions from vehicles categorized in vehicle weight or fuel types, whereas the variations in emissions from different vehicle body types in recent decades have received far less attention due to the limited data available. With the increase of different types of vehicles and inadequate design of traditional traffic systems, quantifying vehicle emissions have become one of the key issues to be addressed in urban areas to devising appropriate mitigation strategies (Orun et al., 2018). It is important to gain understanding of how vehicle emissions have distributed in different vehicle body types in recent decades and how the fuel economy of the vehicle fleet has changed over the years in order to improve environmental impact assessment of road vehicles for regulatory purposes.

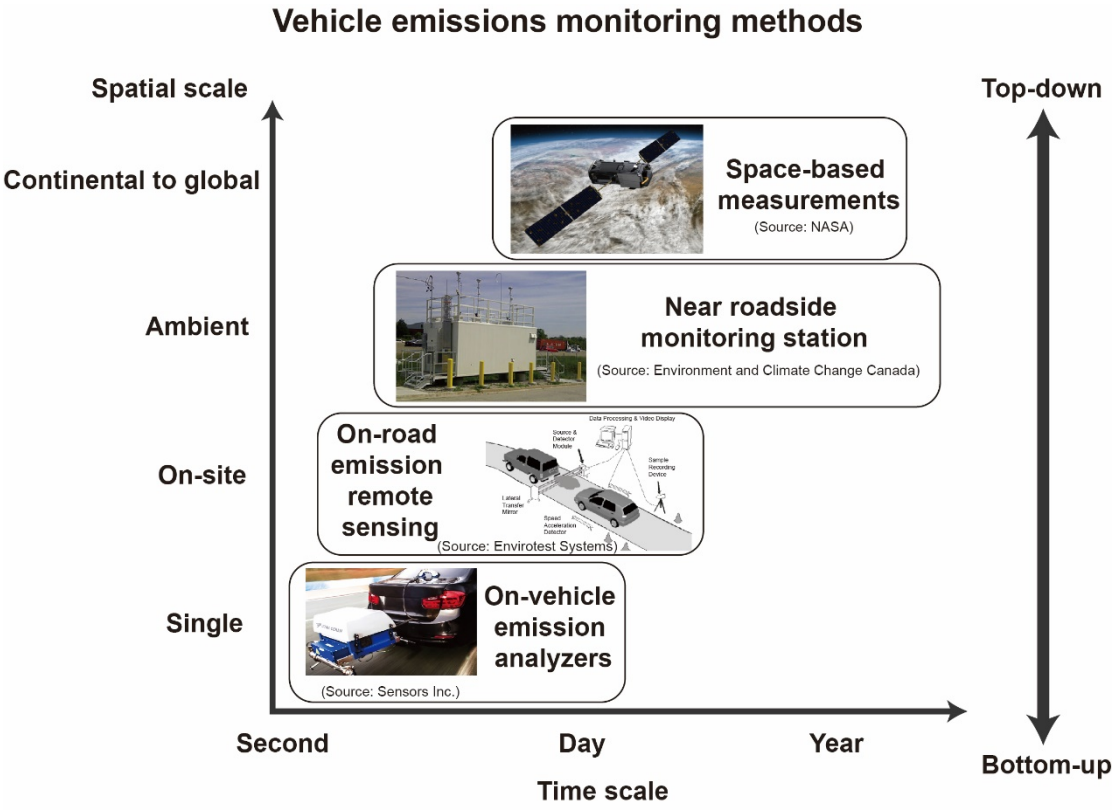

Figure 2. Vehicle emission monitoring methods from different scale.

2.1.3. Methods for urban form elements measurement

Quantitative methods of elements in urban form are mainly used to better analyze the relationships between urban form and GHG emissions. However, operationally defining and objectively measuring elements in urban form is not a simple task due to the unduplicated nature of each area. Besides, the data sources from household level to city level make the measurement of urban form more complicated. From the existing studies, the spatial morphology of built-up area obtained by remote sensing is the main data source, and combined with application of urban form index become the main method to measure the elements in urban form. Table 1 concluded measurement methods of urban form in the previous studies that evaluate the direct relationships between urban form and air quality. The studies related to travel demand and energy use will also be included in the next two paragraphs.

Table 1. Published studies about urban form variables and air quality adapted by Bereitschaft and Debbage (2013)

Scale	Pollutant variables	Urban form variables	References
City level scale			
83 U.S. metropolitan areas and 449 counties	O_3 concentration	Residential density, street accessibility, clustering of development	(Ewing and Rong, 2008)
45 U.S. metropolitan regions	O_3 exceedance, VOC, NOx emissions	Centeredness, connectivity, density, land use mix, SGA sprawl index	(Stone Jr, 2008)
80 U.S. metropolitan regions	O_3 concentration, $PM_{2.5}$ concentration,	Centeredness, connectivity, density, land use mix, SGA sprawl index	(Schweitzer and Zhou, 2010)
83 global urban areas	NO_2 concentration	Contiguity, compactness	(Bechle et al., 2011)
111 U.S. urban areas	EPA's criteria pollutants, long-term air quality index	City shape, jobs–housing imbalance, population centrality, population density, road density, transit supply	(Clark et al., 2011)
30 provincial capital cities in China	CO_2 emissions	TA, LPI, AWMSI, AWMPFDI, PARA_MN, PLADJ, COHESION, AI, LSI, CONTIG	(Fang et al., 2015)
33 provincial capital cities in China	CO_2 emissions	Average city size, urban population density, urban road density, per capita GDP, per capita disposable income of urban households	(Yang et al., 2015)
86 U.S. metropolitan areas	NOx emissions, VOC, $PM_{2.5}$, CO_2 emissions	Residential density, land use mix, street accessibility, degree of centering, urban continuity, urban shape complexity	(Bereitschaft and Debbage, 2013)
50 cities in Japan	CO_2 emissions	Buffer compactness index, compactness index (CI), CI of the largest patch, aera weighted mean (AWM) shape index, AWM patch fractal dimension	(Makido et al., 2012)

Household level scale			
Household level	CO_2 emissions	Nine-cell grid approach, land use mix, transit accessibility	(Zahabi et al., 2012)
Household level	CO_2 emissions	Residential zone classification approach, land use, transit supply	(Barla et al., 2011)
Household level	CO_2 emissions	Population density, population centrality, polycentricity	(Lee and Lee, 2014)

- City level scale

Su (2010) considered the population distribution, road network, urban congestion, alternative transportation modes, and transit use as explanatory variables for the annual VMT per capita. Ewing and Rong (2008) adopted the county sprawl index from Ewing et al. (2003). The sprawl index incorporates six variables to measure the residential density, street accessibility, and clustering of development. The value of the index increases with the compactness of the area. Stone Jr (2008) and Schweitzer and Zhou (2010) employed the Smart Growth America (SGA) urban sprawl index from Ewing et al. (2002) to observe the relationships among transportation impact, air pollution, climate change, and the level of urban sprawl. The SGA sprawl index was developed based on principal components analysis on an integration of these four urban form factors including centeredness, connectivity, density and land use mix. The contiguity and compactness measurement were used by Bechle et al. (2011) to explore the effects from urban form to urban NO_2 emission in global cities. Yang et al. (2015) considered the urban population density, average city size, and urban road density. The measurement of average city size is to calculate the total built-up area of the city divided by the number of cities. The value of the total length of urban roads to the total built-up area of the city represents the urban road density. Fang et al. (2015) applied visual interpretation and vectorization in ENVI/IDL 5.1 software and ArcGIS 10.1 software to process the characteristics of spatial and temporal dynamics of urban form. Ten pattern metrics including total area (TA), the largest patch index (LPI), the area-weighted mean shape index (AWMSI), the area-weighted mean patch fractal dimension index (AWMPFDI), perimeter area ratio distribution (PARA_MN), the percentage of like adjacencies (PLADJ), the patch cohesion index (COHESION), the aggregation index (AI), the landscape shape index (LSI) and contiguity (CONTIG) to describe the changes in urban form.

- Household level scale

The fine-scale grid pattern approach is often used when doing the cluster analysis of urban from. Manaugh et al. (2010) divided the Metropolitan region of Montreal into $150 \times 150\ m$ grid cells to measure the land use, employment, economics, demographics and service accessibility, and to explain the different impacts on commuting distances from

neighborhoods types. Zahabi et al. (2012) applied the nine-cell grid approach from Miranda-Moreno et al. (2011) to measure the land use mix and transit accessibility. The Montreal census metropolitan area was divided into $500 \times 500\ m$ grid cells. Compared with simply dividing large grid with $1500\ m$ sides, the nine-cell grid defines a central grid to where the observation is, making sure the absolute distance is the same from an observation to the outer edge of these nine cells. The resulting neighborhood typology clusters were classified as five Clusters, including Rural/Suburban, Outer suburb, Inner suburb, Downton core, and Urban core. Barla et al. (2011) divided address from 250 households in the survey into four zones in Quebec City and characterized the land use differences in these four zones. They also characterized transit supply by measuring the percentage of the trips from a respondent that can be hard for taking public bus. Lee and Lee (2014) measured urban form from three dimensions: population density, centrality, and polycentricity. They derived centrality index from central business district's population share, area-based centrality index, ratio of weighted to unweighted average distance, population density gradient. The polycentricity index is consist of subcenters' share of center employment, the number of extra subcenters, slope of rank-size distribution, primacy and commuter shed ratio. Liu and Shen (2011) chose density, street network connectivity, diversity and accessibility to examine the impacts from urban form on household travel demand.

2.1.4. Methods used for identifying the relationship between urban form and vehicle GHG emissions

- Linear model

Multiple linear regression analysis was often used to verify the causal relationship between multiple independent variables and individual dependent variable. Makido et al. (2012) employed stepwise multiple linear regression analysis to analyze the causal relationship between independent variables such as average urban area per capita, BCI, CI and AWMPFD. CO_2 emissions per capita from industrial, commercial, residential,

transportation, passenger transport, freight transport sectors were set as dependent variables separately. Stepwise linear regression was also used by Clark et al. (2011) to quantify the relationships between urban form, climate, transportation, land area, income, region and air pollutants concentrations. Bechle et al. (2011) constructed linear regression model to determine the dependence of NO_2 concentration on the urban characteristics. Ordinary least squares (OLS) analysis was also used separately to examine the household characteristics on household energy use (Ewing and Rong, 2008), and to explain the level of individual GHG emissions influenced by household characteristics, land use and transit supply indicators (Barla et al., 2011). A standard regression model (OLS) can be used in the first step and a two simultaneous equation can be combined in the second step to identify the factors such as socio-economic characteristics, neighbourhood types and accessibility related to commuting distances and GHG emissions (Manaugh et al., 2010; Zahabi et al., 2012).

Panel data model is often used in previous studies when dealing with panel data. There are two types of panel data models, the unobserved effect model and the pooled regression model. Usually there are unobservable variables affecting urban form, so the unobserved effect model is applied in this field of study as a way of characterizing relationships. The unobserved effect model can be further divided into the fixed effect (FE) model, the random effect (RE) model, and the mixed effect (ME) model. The FE model is used to study only the internal variation of sample data with time, while it does not consider the variation between different data. It can effectively eliminate time-invariant factors and tends to make the results more accurate. As such it is proven to be a superior option when studying individuals as the whole study population. Many scholars have used the FE model to analyze the factors that influence GHG emissions (Al-mulali, 2012; Baltagi, 2008; Du et al., 2012). Hausman test can be used to select the RE model or FE model (Yang et al., 2015).

Zhang and Zeng (2013) and Su et al. (2011) also applied panel data model to explore the impacts of socio-economic factors and urban form elements on CO_2 emissions from transportation. In common research procedures, a panel unit root test is needed for testing the stationarity of the variables. Fang et al. (2015) and Yang et al. (2015) both employed the Levin-Lin-Chu (LLC) unit root test for the common unit root that is identical among cross-sections. Fang et al. (2015) chose panel model to for its advantages of controlling individual heterogeneity, reducing effects of multicollinearity and increasing the degrees of freedom.

- Structural equation model (SEM)

SEM is also often used in examining the relationships causal relationship among variables. Unlike linear regression model analysis, SEM can handle multiple dependent variables simultaneously. Considering that the existing relationships between latent variables and their structures in the same study will influence each other, SEM can simultaneously estimate the structure of a single latent variable and the relationships among all latent variables. Lee and Lee (2014) used multilevel SEM based on weighted least squares estimation in conjunction with the missing variable method to examine the relationships between total household CO_2 emissions from transportation and residence and multiple endogenous variables. Multilevel SEM is a combination of multilevel linear modelling and conventional SEM. When analyzing the data, it can moderate bias and enhance statistical power (Preacher et al., 2011). Liu and Shen (2011) examined the effects of urban land use characteristics on household travel and transportation energy consumption, and applied SEM to model the linkage between urban form and household transportation energy consumption in the Baltimore metropolitan area. In their SEM, the endogenous variables included VMT, vehicle gasoline consumption, and vehicle characteristics, while characteristics such as travel mode, vehicle type, and speed were considered as intermediate variables. The structural coefficient, it should be noted, is the direct effect of a variable, while the mechanism of indirect effect is that it is exerted through one or more endogenous variables. It was found that urban form had total effects rather than direct

effects on VMT, which means urban form may influence the travel speed primarily and thus indirectly influence VMT. Moreover, they found that denser form had both direct and total effects on the travel mode, especially for inducing walking as a travel mode choice.

2.2. Variables in urban form that affect vehicle GHG emissions

A variety of variables have been introduced to study the relationship between urban form and vehicle emissions (Figure 3). The size of the blue circle on the world map in the figure represents the amount of current research activity. It can be clearly seen from the figure that relatively little research in this area is underway in developing countries. This section will mainly analyze the essential variables based on the frequency of their appearance in previous studies.

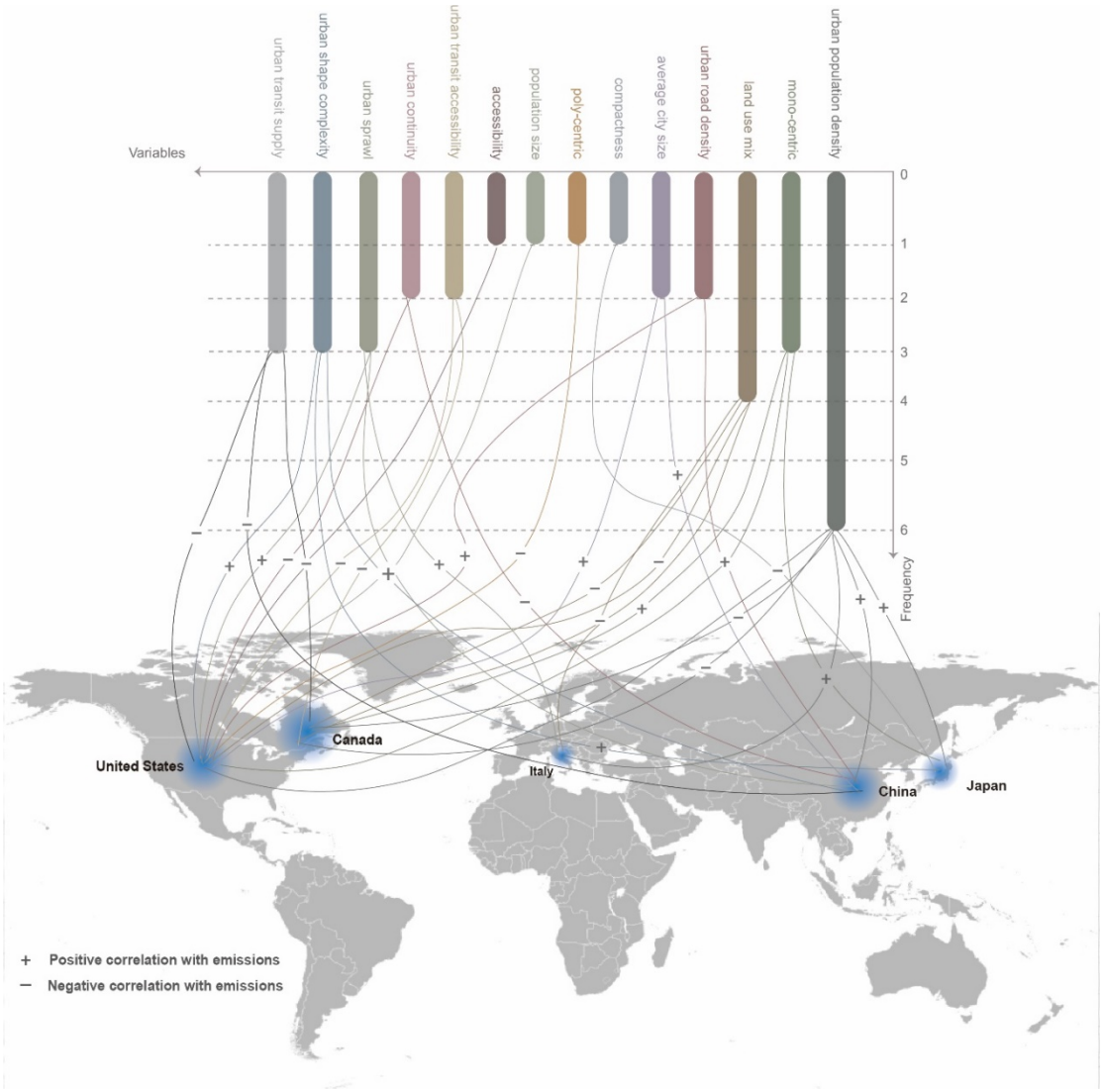

Figure 3. Correlations between variables in urban form and emissions in published studies.

2.2.1. Density—A tool to analyze social and physical qualities of urban environments

Density as a concept in urban development was introduced in the 19th century as a way of diagnosing and analyzing sprawling and overcrowded cities. The focus of studies in urban density then shifted from city development and migration to quantitative and qualitative analyses of the social and physical qualities of urban environments for the purpose of encouraging sustainability and vital human interaction in urban environments (Berghauser Pont and Haupt, 2009). Yang et al. (2015), for instance, employed urban population density

and urban road density as the key variables in examining the relationship between density and CO_2 emissions in China. They found that a 1% increase in urban population density and urban road density would result in 0.22% and 0.16% increases in per capita CO_2 emissions, respectively. Studies of urban area in the United States have shown similar results in terms of road density. For instance, Su (2010) found that VMT increases along with incremental road density, while more frequently travelled and longer distances result in less burdensome and less time-consuming travel in the United States. This suggests that simply complicated road density may actually result in more travel time and may increase per capita GHG emissions. In a similar study, Liu and Shen (2011) selected population density at the block group level from NHTS data to represent urban density in their analysis. They found that population density has indirect negative effects on VMT through intermediate variables such as vehicle speed, particularly the relationship between on-road vehicle emissions and changes in vehicle speed and engine load when driving conditions change. Emissions of CO and NOx have also been proven to have significant positive correlations with vehicle speed (Kean et al., 2003).

When looking at the direct effects, density can have a positive influence on walking mode choice, meaning that people in a denser area are more likely to prefer walking as a travel mode choice than are people in a less dense area. Residents of higher density neighbourhoods are also more likely to have smaller and more fuel-efficient vehicles. These indicated that the per capita CO_2 emissions will be lower in a denser area. Lee and Lee (2014) used a population-weighted density as an alternative to conventional population density measurement to better capture density at a block group level. Their results showed the relatively prominent effects of density on household CO_2 emissions. Under the same conditions, if all the direct and indirect elastic factors are combined, they found that the population-weighted density increases by 10%, and the CO_2 emissions generated by travel are reduced by 4.8% correspondingly. They proposed two possible explanations of this result. First, high-density developments can provide more alternative transportation modes and reduce the distance between different destinations, thus mitigating household VMT. Second, the passenger load of public transit is higher in high-density communities, and this increases carbon efficiency per passenger mile. Regarding population density, Zahabi et al.

(2012) have argued that calculating the approximate population in each grid cell based on land use data (such as data from Desktop Mapping Technologies Inc., for example) can be an accurate method for allocating population. Their study in Montréal tried to figure out the relationship between transportation GHG emissions and urban form. Based on the fact that the Montréal region has a slightly higher population density and larger transit load than some U.S. cities, the results found that a 10% increase in population density would result in a 2.49% mitigation of household GHG, a finding seemingly more intuitive than those of previous North American studies. Bereitschaft and Debbage (2013), meanwhile, applied four system indices to represent urban sprawl level, population density being one of most the important measurements among four of them. Having conducted a regression test, they found that the level of population density also has a significant positive relationship with ozone concentration. In terms of the CO_2 emissions from on-road sources, residential density was the only variable in urban form in their study which was shown to have a significant impact. With the same standard increase in residential density, they found that there would be a 22% reduction in CO_2 emissions from on-road sources.

As an improvement upon the simple average population density metric used in other studies to capture population concentration, Makido et al. (2012) have argued that spatial determinants such as CI and BCI can be used to explain urban density in terms of distinguished patterns of settlement. They concluded that well-organized settlements with higher populations can reduce emissions in general, while massive density and mono-centric urban settlement could aggravate the residential emissions as well. As a possible explanation, they pointed to the compromising with the flexibility of building design principles in compact settlements. Zahabi et al. (2012) examined the case of Québec City and found that the average residential densities (people/km^2) in the center, the old suburbs, the new suburbs, and the periphery in as of 2011 were 4,351, 2,082, 1,307, and 506, respectively. Accordingly, compared with the travel emission in the center, the emission in the old suburbs was found to be 19% higher, in the new suburbs 27% higher, and in the periphery 70% higher.

To provide insights into the expansion of road networks in the city over time, Hankey and

Marshall (2010) introduced the Linear Population Density (LPD) as one variable of urban form to measure the number of people along a transect of an urban area. They then predicted the VKT based on the average population density in one urban area from transportation data. In the most-dense city considered in their study, Miami, where the population density is 2,480/km^{-2}, they predicted the VKT to be 30.9 km/day^{-1}/person^{-1}. In the least-dense city under study, Kansas City, the density is 530/km^{-2} and accordingly they predicted the VKT to be 46.7 km/day^{-1}/person^{-1}.

2.2.2. Mono-centric—A single and prespecified center with production activities

With regard to mono-centricity, one assumption that has been widely adopted within the field of "New Urban Economics" is that any given city has a single center which is the focal point of production activities. It is also called the central business district (CBD) which has a fixed size and provides places of employment for the entire population. In terms of patterns of urban sprawl in the classical monocentric-city model, there are three land-use patterns: leapfrog development, scattered development, and mixed development (Mills, 1981). Radial discontinuity is a notable characteristic of leapfrog development while the other two forms feature circumferential discontinuity (Fujita and Ogawa, 1982). Boarnet (1994) noted that, in the case of the monocentric urban model, there are important links between transportation access and the structure of the city. Furthermore, as noted by Veneri (2010), the spatial characteristics of urban areas, such as degree of polycentricity and or of urban configurations, can affect the externalities of commuting. Makido et al. (2012) developed a Buffer Compactness Index (BCI) to determine the distance between the central business area and surrounding areas and the density at various distances from the city center. This index was based on the percentage of urban area in separate ring buffers defined by 1-km intervals from the city center toward the exterior. Among the various results of their stepwise regression analysis of spatial metrics, BCI was the only positive correlative variable in increasing residential emissions per capita, which means that highly monocentric urban settlement likely increases residential emissions. Similarly, Cirilli and Veneri (2014) measured urban form in an urban area in Italy from intensity-based and

spatial structure-based perspectives, estimating the level of urban mono-centricity by comparing the share of intensive employment in the central municipality. Compared with the polycentric development model, they noted, the monocentric model may entail less accessible amenities, especially in large urban areas, but either model may have high compactness. They concluded that, in large urban areas, the degree of mono-centricity is closely associated with GHG emissions. Bereitschaft and Debbage (2013), meanwhile, defined the degree of centricity in a city in terms of the proximity of housing and jobs for citizens to the CBD area. They found that the degree of centricity had a significant negative correlation with nonpoint source emissions.

2.2.3. Urban sprawl—Major source of environmental problems

One of the major environmental issues worldwide is urban sprawl, which is associated with consumption of agricultural and forested land, decreases in natural habitats and biodiversity, and progressive air pollution (Cai et al., 2020). Furthermore, the locations of households and businesses within cities will affect levels of GHG emissions and land consumption in urban structures (Legras and Cavailhès, 2016). As mentioned above, Fang et al. (2015) reviewed existing indices available in the literature and applied spatial metrics based on remote sensing data on land-use and land-cover. Tsai (2005) distinguished compact city and sprawled city by using quantitative methods with four metropolitan-form variables, namely, metropolitan size, density, degree of equal distribution, and degree of clustering. Matsuhashi and Ariga (2016) compared two population distribution scenarios for Sagamihara, Japan, in 2030, one a compact distribution and the other a dispersed distribution. The city was plotted using large-population meshes of cells representing the compact distribution scenario and the dispersed distribution scenario. In other words, in the compact scenario the city will have a denser urban structure than the dispersed scenario. According to their forecast results, under the condition of compact distribution, the annual per capita CO_2 emission level associated with passenger cars decreases with time, while under the condition of dispersed distribution, annual per capita passenger car CO_2 emissions increase with time. The annual per capita passenger car CO_2 emissions generated

in the dispersed distribution scenario was estimated to be roughly 10% higher than the estimate of the same in the compact distribution scenario.

Travisi et al. (2010) analyzed the relationship between urban sprawl and commuting in Italy using multivariate cross-section regression analysis and Causal Path Analysis, and their empirical results confirmed that urban sprawl is accompanied by intensive travel and associated environmental effects. They also noted that sprawl is one of the explanatory variables for the dependent variable "mobility impact index". The level of sprawl was controlled by three factors in Travisi's work: DENSITY (urban density was estimated as the gross density of cities), MIXITE (the ratio between jobs and residents) and RURAL (the rate of agricultural areas in the built environment). Car ownership by urban residents and urban sprawl itself have also been found to affect one another in a trade-off relationship—urban expansion has exacerbated residents' dependence on car travel, while the growing dependence on cars has, in turn, contributed to urban sprawl (Dulal et al., 2011).

2.2.4. Urban shape complexity—Physical features of urban landscapes

Complexity is one of the spatial metrics employed to represent the physical features of urban landscapes. The AWMSI and the aera AWMPFD were applied by Huang et al. (2007), Makido et al. (2012), and Fang et al. (2015) to measure the irregularity of the patch shape, representing complexity index. About AWMSI and AWMPFD, Fang et al. (2015) added another index, the landscape shape index, to measure the perimeter-to-area ratio of a given landscape as a way of describing urban shape complexity. AWMSI, it should be noted, represents the shape irregularity of the landscape structure by measuring the patches, while AWMPFD describes the raggedness of the urban boundary and implies an unplanned growth urban area. It is derived from the fractal dimension using remote sensing, which is a suitable method for measuring real-world cities (Longley and Mesev, 2000). Their results mentioned above in this paragraph showed different relationships among urban complexity, residential CO_2 emissions, and transport CO_2 emissions. The effect of urban complexity on

residential CO_2 emissions was found to be negligible (Makido et al., 2012), while on-transport CO_2 emissions was significant. Residents who lived in higher-regularity and higher-density settlements tended to produce less per capita transport emissions, as their commuting activities were less influenced by the irregular edges of the cities. Nevertheless, compared with other factors, the role of complexity in reducing CO_2 emissions has been found to be relatively insignificant Makido et al. (2012).

In the research of Fang et al. (2015), a high value of shape complexity implies a more irregular urban form, as indicated by increased commuting time and distance. Thus, increased CO_2 emissions is closely associated with urban shape complexity in their research. Based on the notion of perimeter-to-area ratio, it should be noted, shape complexity can be understood as the "jaggedness" of the urban boundary. Bereitschaft and Debbage (2013) used principal component analysis (PCA) to categorize the multiple landscape metrics for measuring the shape complexity of urban development. As they noted, there are total four landscape metrics derived from multiple satellite-based metrics for measuring urban complexity: area-weighted mean shape index, landscape shape index, area-weighted mean patch fractal dimension, and edge density. They found that, after running a regression model, an increase of one standard deviation in urban shape complexity will result in an 8.7% increase in NOx emissions and a 12.4% increase in PM2.5 emissions. The reason for this is that highly convoluted landscapes will lead to a rise in the number and duration of automotive trips.

2.2.5. Continuity—A method to measure the uninterrupted level in urban areas

Continuity refers to the extent to which land is developed in an uninterrupted manner in urban contexts. Continuity provides a way to measure the size of the development and the distance between the developed metropolitan area and any discontinuous areas (Tsai, 2005). It also provides a way to measure the level of polymerization or fragmentation between patches, i.e., "leapfrog" development (Bereitschaft and Debbage, 2013). Galster et al. (2001) defined continuity as a function of density, and they assessed the level of

continuity in urban development by observing the number of the housing units and places of employment. The quantitative operationalization they proposed is divided into two steps. The first step is to determine whether a given cell in a grid of 1.5-mile square cells contains over 10 housing units or over 50 employees. The second step is to calculate the proportion of all such cells in the grid as way of measuring continuity (Galster et al., 2001). Fang et al. (2015), meanwhile, used COHESION, AI, and CONTIG to represent the degree of urban continuity, which contributes to the connection and aggregation of a city. The average commuting distance in a fragmented and interspersed developed area, they noted, will be much farther than that in high aggregation and highly connected areas. They also found that urban expansion with a pattern of high connectedness is beneficial in terms of curbing CO_2 emissions. In a similar study, Bereitschaft and Debbage (2013) used urban continuity to represent the degree of fragmentation of an urban landscape, where an area with highly integrated development is described as having high urban continuity. In such an area, they found, residents will typically have shorter automotive trips and thus less carbon emissions from nonpoint sources due to there being less open space separating different parts of the city. In their study, they found that one standard deviation increased in urban continuity contributed to an 8,647-ton (or 9%) reduction in annual VOC emissions.

2.2.6. Land use mix—Reducing the distance between origin and destination

Land use mix within a neighbourhood is important in terms of its effect on residents' lifestyle, where the key advantage of mixed use is that it brings various origins and destinations closer together. The location of destinations within an acceptable distance can encourage residents to walk or bicycle instead of driving, thus reducing vehicle dependence (Duncan et al., 2010). In terms of assessing the impacts of land use mix on travel, the land use mix index evaluates the balance between distance from workplace to residence and the diverse functions such as recreational function and commercial function within the area under study. Liu and Shen (2011), for instance, considered land use mix as one of the variables in urban form. They captured the even level of square footage of various land uses such as commercial, residential, and official floor area located within a given

household's 1-mile buffer distribution. The results of their study were found to be consistent with the finding of a previous study in which land use mix has a modest effect on the elasticity of VMT (Ewing and Cervero, 2001). Stone et al. (2010) and Bereitschaft and Debbage (2013) both applied three elements, the ratio of jobs to population, the diversity of land uses, and the accessibility of residential uses to non-residential uses, at the level of the transportation analysis zone and within a 1-mile radius to represent land-use mix attribute. Zahabi et al. (2012), meanwhile, combined with the nine-cell grid approach, defined land use mix in terms of an entropy index with residential, commercial, institutional and governmental, resource and industrial, and parks and recreation. They found that the promotion of land use mix plays a negligible role in reducing the carbon footprint of daily travel. Hankey and Marshall (2010) noted with respect to the U.S. context that encouraging policy measures such as zoning for mixed use is a common strategy for compact growth, as there are inherent connections among energy, environment, and land-use patterns. Cervero (1988) considered that mixed land-use planning policies could serve to mitigate energy consumption in the transportation system as an alternative strategy to trip chaining and curtailment of trip length. In another study, based on a survey conducted in the San Francisco Bay Area, Cervero and Duncan (2006) examined the degree to which job accessibility is associated with reduced work travel and how closely retail and service accessibility is correlated with miles and hours logged travelling to shopping destinations. They found that improving the jobs to housing land-use mix strategy can reduce travel. Ewing and Cervero (2010), meanwhile, conducted a meta-analysis of the literature on built environment and travel. They concluded that land use diversity can strongly influence the choice to walk and is a secondary factor for bus and train use. Similarly, other researchers have noted that, in order to reduce drive-alone travel, communities are increasingly seeking mixed land use planning strategies to mitigate GHG emissions from vehicles (Krizek, 2003; Srinivasan, 2002).

2.2.7. Accessibility—Describing the performance of road network

Accessibility is one of the fundamental factors in shaping the dimensional organization of

economic activities and contributing to traffic flow. Indeed, controlling the level of accessibility with regards to transport infrastructure endowment is critical in analyzing the relationship between spatial structure and the external effects of commuting (Cirilli and Veneri, 2014). Travisi et al. (2010) considered accessibility as one of the prominent factors in characterizing the relationship between travel impacts and the quality of public transport services. They used the variable, SHAREPUB, which captures the market share of public transport calculated with the proportion of all trips made by public transport used as the metric to represent accessibility. Kitamura et al. (2001) studied the effect of the level of accessibility on long-term and short-term travel behaviour. The prism-based measures used in their research showed that people might easily obtain opportunities to participate in activities in urban areas. In a similar manner, McConville et al. (2011) analyzed the accessibility of non-residential land use and its influence on the choice of walking as a mode of transportation. They measured the street distance from the participant's home to the closest instance of various land uses such as physical activity uses and social uses. Liu and Shen (2011) determined accessibility based on the number of jobs within a given zone, the travel time from zone to zone, and the travel flow matrices. In the initial regression outcomes, when controlling the other urban form variables and household characteristics, accessibility was found to be the most significant factor influencing household VMT. Zahabi et al. (2012) found, based on the grid approach, that higher transit accessibility is correlated with public transit stops being closer to the cell centroid (i.e., a smaller headway). They calculated this by aggregating each line's closest stops to each cell, and found that a 10% increase in public transit accessibility is associated with a 5.17% decrease in household GHG emissions. They thus considered the promotion of transit accessibility to be just as important as improvements in the fuel-efficiency of vehicles in reducing GHG emissions.

2.3. Vehicle GHG emissions in different urban forms

2.3.1. Dispersed city

The distinguishing features of a dispersed city are low residential density, low accessibility

for newly built settlements, and a central business district with a small concentration of population and employment (Muñiz et al., 2006). Among the wide range of factors that have accelerated new housing construction and urban dispersion in recent decades, the mass diffusion of cars is one of the most influential factors. Furthermore, the cost for constructing new settlements in suburban areas is much lower than that in the historic center as the revitalization of mature areas is costly (Balsas, 2000). In addition to these economic considerations, political factors may also be key determinants of urban development patterns. The high degree of administrative fragmentation and local autonomy may cause unfair financial competition in the process of attracting land investment, which will lead to decentralized urban development (Carruthers, 2003).

Urban dispersion can bring about two groups of environmental implications. The first is the direct environmental costs resulting from scattered development of new housing. Contrary to the compact pattern of development, isolated housing patterns lead to more waterproof land and water consumption. It also entails the loss of rich soil, and a higher degree of land fragmentation and homogeneous land use patterns. The second group of effects has to do with the pattern of commuting in dispersed urban areas. The associated effects on the environment include noise and air pollution, land occupancy, and traffic accidents. Urban dispersion uses up land that would otherwise be available for ecological uses, while the excessive energy consumption leads to air pollution, exhaustion of non-renewable energy, and gas emissions, which ultimately contribute to climate change (Anderson et al., 1996; Chen et al., 2020b; Liu et al., 2020; Wu and Xia, 2019).

Ewing and Rong (2008) conducted a study investigating the relationship between the choice of housing type and urban form, and found that multifamily housing is seven time less popular in dispersed areas than in compact areas. With their study combining path analysis, they concluded that residential energy use will be higher in sprawling urban development due to the low density and the prominence of large, single-family detached housing. Yang et al. (2015), meanwhile, obtained the result that a 1% increase in the built-up area will contribute to a 0.08% increase per capita in the CO_2 emissions of the transportation sector. Especially when public transportation is limited and there is a spatial

mismatch in the dispersed areas of the city, this will lead to increasing use of motor vehicles rather than sustainable travel modes such as public transportation, cycling, and walking. They noted that a polycentric structure, alternatively, can reduce commuting distance through the establishment of commercial, and entertainment subcenters (Lee and Lee, 2014). They used several measurements to create a polycentricity index: subcenters' share of center employment, the number of subcenters, the slope of the rank-size distribution, and the primacy and commuter shed ratio.

Several studies have sought to characterize the causal connection among shorter average commute time, polycentricity, and carbon emissions (Crane and Chatman, 2002; Gordon and Lee, 2015; Meijers and Burger, 2010). In the United States, the use of private cars in medium and large cities tends to supersede transit use due to the lack of convenient public transport station design and extensive coverage of route arrangements. As a result, for mitigating the carbon emissions, the public transportation networks should be highly compatible with polycentric urban area. Furthermore, they found policy strategies such as transit subsidies to greatly reduce the VMT (by nearly 46%) and transportation-related CO_2 emissions (by 18%). Meanwhile, Bereitschaft and Debbage (2013) showed that the irregular boundaries with highly complex characteristics in the less compact urban landscapes commonly found in the dispersed city increase the number of cars and the duration of car travel times. In their experiment, they found that the annual PM2.5 emissions would increase by 3,055 tons (12.4%) as a result of a standard increase in urban shape complexity. In another study, Barla et al. (2011) proposed polycentric urban development to help reduce the level of emission, with their results demonstrating that a 2.7% curb in emission would result from a 10% reduction in commuting time.

According to World Resource Institute, CO_2 emissions from transport occupied 24% of global emissions in 2018. In turn, 74.5% of global transport emissions consists of emissions from road vehicles, including passenger and freight travel (Ritchie, 2020). The issue of traffic-related emissions is particularly acute in North American cities. According to the International Energy Agency (2019b), Canada and the United States rank first and second in the world in average fuel consumption per vehicle and CO_2 emissions per kilometer

driven. In 2019, the transportation sector was identified as the second largest contributor to greenhouse gas (GHG) emissions in Canada, with the emissions from this sector growing by 54% in the past 30 years (Government of Canada, 2021a). Unlike in Japan, Korean, Europe, and China, in North America most cities have adopted a grid street plan and a mono-centric pattern of development that is conducive to vehicle circulation and therefore encourages use of private vehicles (Attoe and Logan, 1989). Moreover, cities in North America typically feature extreme clustering in the downtown area, fragmented distribution of service facilities, and clear boundaries of urban functional zoning . As of 2021, there are 18 only metropolitan areas in North America with their metro systems. For most of the small-medium cities in North America, the density of public transportation coverage does not meet the needs of citizens. Instead, residents tend to rely on private vehicle to commute, leading to high traffic-related emissions.

2.3.2. Compact city

Opposite to the form of urban sprawl, compact city has since the 1990s been the consensus choice among researchers for promoting energy-efficiency and reducing pollution, as it encourages walking, cycling, and public transit use within the city (Abdullahi et al., 2015; Chang and Chen, 2016; Lee et al., 2015). Several compact city indicators have been developed, such as density, land use, trip distance, and availability of public transport services (Lee et al., 2015; Lee and Lim, 2018; Mizutani et al., 2015; OECD, 2012). When considering carbon emission in the private transport sector, many scholars have connected the indicators of compact city development with commuting behaviour and analyzed their relationships. Fang et al. (2015), for instance, demonstrated that travel distances can be reduced in a more compact city through the use of private vehicles, since the time and distance of commuting will be increased along with the decreasing degree of compactness associated with intricate and irregular boundaries. They also noted that the efficiency of city operation and urban land use intensity have positive correlations with the degree of compactness. They considered that, for a fast-growing city, the compact and continuous form is favorable for mitigating CO_2 emissions once an optimum degree of compactness

and matching public service system investment are achieved; otherwise, problems such as overcrowding will have a detrimental environmental effect. Liu and Shen (2011), meanwhile, in a study of U.S. cities, found that the choice of compact cars and non-motorized travel modes would increase in a denser city area. The compact car is a vehicle size class which is predominantly used than other vehicle classes in North America. It has better gas mileage than larger vehicles and thus reduces fuel consumption. From the perspective of spatial structure, the compact city emphasizes central development rather than a polycentric urban spatial structure (Gordon and Richardson, 1997).

Lee and Lee (2014) derived a centrality index based on the central business district's population share, area-based centrality index ratio of weighted to unweighted average distance, and population density gradient. They argued that population density can serve as a catch-all variable to represent compact urban form. The results of their multilevel SEM demonstrated a reduction in CO_2 emission from household travel and energy consumption by 48% and 35%, respectively, relative to population-weighted density. As Bereitschaft and Debbage (2013) have asserted, compared with the tree-lined suburb, a compact area with denser population, convenient transportation, low per capita car ownership, and shorter distances to pedestrian and cycling destinations will have far lower carbon emissions. In terms of the CO_2 emissions from the passenger transport sector, Makido et al. (2012) have suggested that regular shape and compact density of urban settlements could result in lower per capita emissions. However they noted that residential emissions can increase along with excessive density and mono-centric urban development. Hankey and Marshall (2010), meanwhile, referenced three scenarios of urban development for the purpose of predicting future GHG emissions. Looking at these scenarios, per capita VKT was found to increase in the Constant Density mode and Suburban Nation mode but decrease in the Complete Infill mode. They predicted that the emissions in the Complete Infill mode in 2020 would see an 18% decrease compared to the year 2000, while the emissions in 2020 in the Suburban mode would see a 17% increase compared to 2000. However, Marshall et al. (2005) considered that if the density elasticity magnitude is minimal or if the standards for vehicle emission system are low, compact cities may actually see worse air pollution than a conventional compact urban mode. Indeed, factors that reduce the average vehicle speed

through intensive congestion, whether in low- or high-density cities, may worsen emissions and individual exposures to the vehicle pollutants. Furthermore, because of the density of compact cities, the exposure to air pollutants such as PM may also increase. In order to enhance the function of compact development in mitigating emissions, then, corresponding improvements in fuel and vehicle technologies should be pursued (Hankey and Marshall, 2010).

2.4. Opportunities in urban form planning for the mitigation of household vehicle GHG emissions

Based on the above review, the rational allocation of land, as well as the relationship between urban form and intelligent development and low-carbon transportation (and the associated opportunities), in various jurisdictions around the world can be summarized in terms of five notable aspects.

The first is the relationship between the model of urban space utilization and low-carbon development. The utilization pattern of urban space encompasses urban density and land use mix, where the density of a city can be represented as population density or employment density. Rises in the degree of urban density and mixed function can effectively reduce the per capita car usage, thereby reducing fuel consumption and GHG emissions. It is thus necessary to strengthen mixed land use and diversified development, and to move away from the practice of zoning for a single function. It can help mitigate unnecessary traffic demand from the source, including reducing the number of trips and shortening the distance of travel, while simultaneously strengthening access to employment and services, and creating employment, leisure, and shopping opportunities within an acceptable proximity. This can significantly reduce the demand for travel, enabling people to reach work and shopping locations within a shorter time and lesser distance and thus reduce energy consumption and carbon emissions.

The second aspect is the relationship between urban spatial form and low-carbon

development. The impact of urban space morphology on carbon emissions is mainly reflected in the continuity of urban space and the dispersion of centers. Continuous urban space helps improve accessibility between various urban activities, thereby reducing travel distance and keeping carbon emissions in check. A decentralized trend in development and construction of urban land, even in the form of leapfrog or enclave, is not conducive to the realization of low-carbon goals. The polycentric development model not only reduces travel distance, but also makes travel more balanced, controls urban sprawl, reduces the traffic congestion caused by excessive concentration in the center, and reduces the pollution and carbon emissions from traffic. At the same time, it can alleviate the strong heat island effect caused by the excessive concentration in a single center and thereby reduce the energy consumption required for space-cooling in the built environment.

The third aspect is the relationship between urban transportation mode and low-carbon development, specifically the changes in transportation structure as a result of low-carbon development. Based on the scale of the urban area, the development of urban public transportation and non-motorized travel in the transportation system should be supported, and the integrated development and operation of the public transportation system should be emphasized to make the regional transportation network adaptable to the spatial layout. Based on the scale of the neighbourhood area, the accessibility of walking and public transportation systems should be considered in order to reduce the dependence of residents on private cars. Increasing the density of urban public transport coverage, guiding public transport as a priority, designing optimal transfer plans, shortening bus travel time, and improving bus travel efficiency are all strategies that can enhance the attractiveness of public transport travel to residents. From the perspective of urban form and street design, replacing the development of major roads and street blocks with the development of small blocks and pedestrian paths can play an important role in encouraging low-carbon travel.

The fourth aspect is the promotion of energy-saving and energy-efficient vehicles, where governments can promote the use of energy-saving and low-carbon vehicles through policy measures such as financial incentives and taxation. Not only can this reduce the dependence on fossil energy, but it can also reduce the emission of automobile exhaust.

The fifth aspect is the promotion of low-carbon development through urban smart management. The CO_2 emitted by vehicles in congested traffic is much more than that during high-speed driving. Intelligent transport systems (ITS) refer to a system designed to integrate residents, road networks and vehicles in order to resolve traffic problems such as traffic congestion, traffic accidents and environmental degradation. In this context, ITS, which is widely-used in Japan, can improve road use efficiency and thereby reduce congestion. The intelligent transportation technology, vehicle information and communication system (VICS), meanwhile, can alleviate traffic congestion by increasing vehicle speed, thereby improving fuel efficiency and reducing emissions. The intelligentization and informatization of transportation represent an important trend influencing future urban development patterns. Moreover, the combination of intelligent information technology and low-carbon technology, as well as urban scientific management, and the development and application of technologies such as big data can be used to promote smart energy management. Furthermore, the development and integration of technologies and management systems such as transportation, building energy efficiency, and circular economy will play a strong role in promoting the integration of resource allocation and the optimization of low-carbon technologies in urban settings.

2.5. Knowledge and research gaps

Many recent efforts have been made in the analysis of traffic-related GHG emission based on different urban form characteristics but there remains a significant knowledge gap in the adequate understanding of on-road vehicle emissions in North American cities, where people more rely on private vehicle to commute. Further study is required for making detailed vehicle emission source apportionment information and supplementary information management tools to verify the air pollutants variations to inform the development of appropriate environmental policy. The future research gaps are as follows.

1. Most of these studies have focused on the emissions from vehicles categorized in vehicle weight or fuel types, whereas the variations in emissions from different vehicle

body types in recent decades have received far less attention due to the limited data available. A unique data set that supports the tracking of progress in reducing real-world emissions over time and the estimation of future air quality impacts based on the trends of fleet mixes are important. It is important to gain understanding of detailed source apportionment information to quantify the contributions to total emission made by different vehicle body types, different fuels, and manufacturer models in recent decades and how the fuel economy of the vehicle fleet has changed over the years in order to improve environmental impact assessment of road vehicles for regulatory purposes.

2. Unlike in Japan, Korean, Europe, and China, in North America most cities have adopted a grid street plan and a mono-centric pattern of development that is conducive to vehicle circulation and therefore encourages use of private vehicles (Attoe and Logan, 1989). Moreover, cities in North America typically feature extreme clustering in the downtown area, fragmented distribution of service facilities, and clear boundaries of urban functional zoning. For most of the small-medium North American cities without metro systems, the density of public transportation coverage does not meet the needs of citizens. According to the International Energy Agency (2019b), Canada and the United States rank first and second in the world in average fuel consumption per vehicle and CO_2 emissions per kilometer driven. The issue of traffic-related emissions is particularly acute in North American cities. However, there still lacks studies related to the environmental pressure exerted by on-road vehicle emissions in small-medium North American cities, in which residents tend to rely on private vehicle to commute, leading to high traffic-related emissions.

3. One of the frustrations with the analysis of air quality data is the lack of representative vehicle activity data. Such data has the potential to generate useful information on source apportionment and hence provide insights into the most effective mitigation measures that should be considered to improve air quality. Previous studies usually build or simulated scenarios of different levels of vehicle activity to predict the traffic-related emissions and air quality. The reduced traffic experienced throughout several lockdowns over the past year offers us a glimpse of what air quality in cities would

look like if the country switched to low-carbon transportation modes. If the ultimate objective is a decarbonized urban transportation system, it is important for us to think about the long-term panacea for future urban transportation patterns.

4. Satellite observations have been used for visualizing how carbon emission and air pollution are distributed globally, including studies that have focused on anthropogenic emissions. More recently, satellite monitoring has been used to verify the effect of technologies and policies intended to control and reduce emissions from coal-fired power plants (Jiao et al., 2020; Wu et al., 2019). However, there is a lack of studies having used a combined (ground–satellite) approach to further process and validate the threshold changes on a smaller spatial scale. In order to verify the effects of implementing decarbonization measures, satellite observation can be developed as a supplementary information management tool to draw connections with national pollutant release inventory, showing thresholds or concentration trends for specific pollutants and a particular jurisdiction from both digital and visual perspectives

CHAPTER 3. IMPACT FROM THE EVOLUTION OF PRIVATE VEHICLE FLEET COMPOSITION ON TRAFFIC RELATED EMISSIONS IN SMALL-MEDIUM CITIES—— A NORTH AMERICAN CASE STUDY

3.1. Background

Carbon dioxide (CO_2), carbon monoxide (CO), nitrogen oxides (NO_X), particle matter with aerodynamic diameter less than 10 microns (PM_{10}) and less than 2.5 microns ($PM_{2.5}$), and sulfur dioxide (SO_2) are among the principal sources of ambient air pollution, having been associated with not only environmental issues like soil acidification, but also with adverse effects of human health such as heart attacks and lung diseases (Haugen et al., 2018). According to the World Resources Institute (2019), CO_2 emissions from transport occupied 24% of global emissions in 2018. In turn, 74.5% of global transport emissions consists of emissions from road vehicles, including passenger and freight travel (Ritchie, 2020). The issue of traffic-related emissions is particularly acute in North American cities. According to the International Energy Agency (2019b), Canada and the United States rank first and second in the world in average fuel consumption per vehicle and CO_2 emissions per kilometer driven. In 2019, the transportation sector was identified as the second largest contributor to GHG emissions in Canada, with the emissions from this sector growing by 54% in the past 30 years (Government of Canada, 2021a). Unlike in Japan, Korean, Europe, and China, in North America most cities have adopted a grid street plan and a mono-centric pattern of development that is conducive to vehicle circulation and therefore encourages use of private vehicles (Attoe and Logan, 1989). Moreover, cities in North America typically feature extreme clustering in the downtown area, fragmented distribution of service facilities, and clear boundaries of urban functional zoning. As of 2021, there are 27 cities in North America with their metro, underground, subway or urban trains (Mapa Metro, 2021). For most of the small-medium cities in North America, the density of public transportation coverage does not meet the needs of citizens. Instead, residents tend to rely on private vehicle to commute, leading to high traffic-related emissions.

Researchers have been developing both top-down and bottom-up approaches to improving

the accuracy of vehicle emissions inventories (Farren et al., 2020; Sun et al., 2017). Anenberg et al. (2017) adapted a global transportation emission inventory model to generate the NO_X emissions from diesel light-duty vehicles (LDVs) and heavy-duty vehicles (HDVs) in 11 major vehicle markets and found that HDVs contributed to excess diesel NO_X emissions in almost all regions. Apart from using statistical data, on-site emission mobile measurements have also been conducted using various technologies for traffic emissions estimation such as FEAT (Bishop and Haugen, 2018; Farren et al., 2020). However, most of these studies have focused on the emissions from vehicles categorized in vehicle weight or fuel types, whereas the variations in emissions from different vehicle body types in recent decades have received far less attention due to the limited data available. With the increase of different types of vehicles and inadequate design of traditional traffic systems, quantifying vehicle emissions have become one of the key issues to be addressed in urban areas to devising appropriate mitigation strategies (Orun et al., 2018). It is important to gain understanding of how vehicle emissions have distributed in different vehicle body types in recent decades and how the fuel economy of the vehicle fleet has changed over the years in order to improve environmental impact assessment of road vehicles for regulatory purposes.

In addition to estimating vehicle emissions, researchers have also adopted statistical methods and machine learning methods to forecast air pollutants concentrations and identify the factors affecting changes in air pollutants. Orun et al. (2018) used optimized Bayesian Networks to increase the accuracy of predictions of traffic-related air pollution (SO_2, NO_2 and CO) and uncovered the associations between dynamic traffic parameters. Ma et al. (2020) used Extreme Gradient Boosting (XGBoost) to model the relationship between air quality and 171 environmental, demographic, economic, meteorological, and energy features on a national scale. Ebrahimi-Khusfi et al. (2021) evaluated the performance of support vector regression (SVR) in the prediction of ground-level pollutant concentrations, identifying potential contributing factors such as climatic changes, terrestrial conditions, and human impacts. However, these previous studies have mainly developed air quality prediction models that offer one-step-ahead forecast at an hourly and daily resolution. What is still needed is an approach that focuses on prediction of long-term

annual traffic-related air pollutants and investigates the potential influence on air quality of changes in the composition and fuel economy of the vehicle fleet resulting from the growth or reduction of the proportion of the overall vehicle fleet that a given vehicle classification accounts for and various technological developments over the years.

To fill these research gaps, in this chapter we collected comprehensive private vehicle fleet composition data at the city scale, downtown air quality data, as well as data encompassing various demographic, economic, and energy features. The data spanned the period 2001 to 2018, and the city of Regina, Canada, was selected as a case study for the analysis. Regina is a typical small-medium city without metro systems in North America. Along with the extreme weather in winter, people more dependent on traveling by vehicles, thereby increasing the per capita GHG emissions. In this chapter, an analysis of trends in vehicle fleet composition, including changes in six vehicle body type classifications and seven fuel types, is presented in the first section of results. Then, Section 3.3.3 describes trends in downtown air pollutants, including the concentrations of CO, NO_X, PM_{10}, $PM_{2.5}$, and SO_2 during the period, 2001 to 2018. Section 3.3.4 examines the estimation of total GHG emission inventories from on-road private vehicles and how vehicle emissions have been distributed among different vehicle body types in Regina in recent decades. The analysis of historical trends in the fuel economy of six vehicle body types is presented in Section 3.3.5. To evaluate the relationship between the environmental pressure exerted by on-road vehicles and economic growth, a decoupling analysis considering data from both Regina in particular and Canada in general is presented in Section 3.3.6. Section 3.3.7 and 3.3.8 demonstrate the annual pollution level prediction results based on the XGBoost model. Meanwhile, the vehicle fleet composition, demographic, economic, and energy features that influence traffic-related air pollutions levels are identified based on the importance ranking generated by the XGBoost algorithm.

3.2. Materials and methods

3.2.1. Data preparation for GHG emission estimation

The quantities of private vehicles registered in Regina during the period from 2001 to 2018 by make and model was obtained from Saskatchewan Government Insurance (SGI). The physical characteristics of each individual vehicle, including engine size and fuel type, were also obtained from the data set. The conventional private vehicle fleet from SGI was categorized into six body types: four-door car, sport utility vehicle, station wagon, truck, two-door car, and van. In analyzing variations in the private vehicle fleet for the period between 2001 and 2018, this study considered gasoline, diesel, flexible fuel, gas–electric hybrid, natural gas, and propane as fuel types, and gasoline and diesel were adopted as the representative fuel types for the GHG emissions inventory estimation, given that they are the most common fuel types. We combined the fuel consumption rating search tool from Natural Resources Canada (2021) and EPA's fuel economy information website www.fueleconomy.gov in order to obtain the fuel consumption (L/100 km) data of each vehicle by fuel type, make, and model. The fuel consumption data for 27,901 models and brands was collected based on the registration quantities of private vehicles. According to Vorano (2015), 96.4% of new car buyers in Canada in 2015 opted to purchase an automatic vehicle. Accordingly, in the process of accessing the fuel consumption, we defaulted all models to automatic. We also adopted the national value of GHG emission factors for energy mobile combustion sources in Canada (Environment and Canada, 2019). The average distance traveled by vehicle per year for six body types was obtained from Natural Resources Canada (2009). (The 2009 issue of the Canadian Vehicle Survey is the final release, as this survey has been discontinued. As such, for the purpose of the GHG emission estimation conducted in this study, the mean value of the Canadian Vehicle Survey data spanning the survey years 2001 to 2009 was used as the average distance traveled by vehicle per year.

3.2.2. Data preparation for prediction of air pollutants

Air pollutant data, including the concentration of CO, NO_X, PM_{10}, $PM_{2.5}$, and SO_2, was collected from the air monitoring station in downtown Regina (latitude: 50.45017°, longitude: −104.61722°) (Government of Canada, 2021b). The hourly data spanning the period 2001 to 2018 for five air pollutants was collected from this continuous monitoring

station, amounting to some 789,000 data points. Regarding emissions from vehicles, the air pollutant data used in the prediction model was drawn from the morning (9am) and afternoon (6pm) rush-hour periods. The concentrations of each pollutant during rush hour were considered as the targeted variables in this study. Since the aim of this study was to explore the significant factors influencing air pollutant concentrations and predict the future trends, different aspects of possible significant variable data needed to be collected. Along with the vehicle data used in GHG emissions estimation and the data from Statistics Canada, we gathered data on transportation, demographic, economic, and energy features. The transportation variables included weighted average fuel consumption for six vehicle classes (four-door car, SUV, station wagon, truck, two-door car and van), and the vehicle fleet composition data (number of vehicles registered under each of these six body types). The demographic variables included the total population, the sex breakdown of the workforce, proportion of children between 0 to 14 years, median age, and employment rate (Statistics Canada, 2021a). In terms of economic features, annual median total income and annual average retail price for regular gasoline and diesel fuel were considered as variables. The energy-related feature considered was the breakdown of private vehicles by fuel type (i.e., gasoline, diesel, flexible fuel, electric, gas–electric hybrid, natural gas, and propane). The gross domestic product data for both Canada and Regina for the period 2001 to 2017, used in the decoupling analysis, was obtained from Statistics Canada (2014) and Statistics Canada (2020b). Data on estimated GHG emissions from Canada's transportation sector (2001 to 2017) was also obtained for the decoupling analysis (Government of Canada, 2021a).

3.2.3. GHG emissions estimation

The 2006 IPCC guidelines provide methods to quantify the national GHG inventories that have been used widely in various countries (Seo and Kim, 2013). For the quantification of GHG emissions from mobile combustion in this study, we applied the Tier 1 approach from the 2006 IPCC guidelines (Eggleston et al., 2006a). The calculation of GHG emissions (kg/year) from road transport was carried out as follows:

$$E_{GHG} = \sum_{a} fuel_a \times EF_a$$
$$= \sum_{i=1}^{i=n} Q_{iam} \times D_{im} \times C_{iam} \times EF_{ia} \quad (1)$$

where E_{GHG} is the total GHG emissions inventory of private vehicle in one year (e.g., CO_2, CH_4, and N_2O.) (kg/year), $fuel_a$ is the fuel sold (TJ), EF_a is the emission factor for CO_2, CH_4, and N_2O (kg/TJ), a is the type of fuel (e.g., gasoline, and diesel.), Q_{iam} is the registration quantity of a private vehicle, D_{im} is the estimation of the average vehicle-kilometers in Saskatchewan (100 km/year), C_{iam} is the fuel consumption of a private vehicle (L/100 km), m is the vehicle models in different bands. In this study, the fuel sold can be estimated by the multiplication of Q_{iam}, D_{im}, and C_{iam}. All the GHG emissions were converted into CO_2 equivalents (CO_2 eq) for the purpose of comparison.

3.2.4. Weighted average fuel economy of vehicle fleet

The fuel economy by vehicle body type for Regina and spanning the period 2001 to 2018 was also calculated, reflecting the level of fuel consumption of the existing vehicle fleet composition in Regina. Based on the national data from the International Council on Clean Transportation (ICCT) (Yang and Bandivadekar, 2017), the results for Regina were also compared with the historical trends and future targets for Canada at the national level. It should be noted that the fuel economy (miles per gallon) by vehicle body type was calculated using weighted arithmetic mean, where the weight assigned to each make, model, and year was based on its share of the total number of registered vehicles for the period and jurisdiction under study.

3.2.5. Decoupling index

To assess the linkage between environmental pressure exerted by the transportation sector and economic growth, decoupling analysis was carried out in order to better understand the degree of decoupling between gross domestic product and CO_2 emissions from the

transportation sector at both the city level (Regina) and national level (Canada). Because of the differing methods used in estimating CO_2 emissions at the city level versus the national level, it was not always as straightforward as simply comparing the amounts. However, given that the diverse methods do not create a bias in terms of the rate of time growth, this issue is less problematic when determining whether decoupling has occurred (Tapio, 2005). In this context, it should be noted, decoupling means that the growth rate of environmental pressure is lower than that of the economic drivers over the given period of time, a phenomenon which will contribute to more sustainable development patterns (Caïd, 2006).

In contrast to the Organization for Economic Co-operation and Development (OECD) index, which popularized the concept of decoupling, Tapio's elastic analysis method calculates the decoupling degree with the elasticity value of the pressure variable and economic factor (Shan et al., 2021). Tapio separated the decoupling indices into eight categories (as shown in Table 2), making the decoupling index more flexible in terms of time scale, and the final results of the analysis more comprehensive (Li et al., 2019b). The decoupling index was calculated according to Equation 2 (Tapio, 2005).

$$DI_{GDP\ elasticity\ of\ transport\ CO_2} = \frac{\Delta CO_2\%}{\Delta GDP\%} = \frac{\frac{CO_2^{t2} - CO_2^{t1}}{CO_2^{t1}}}{\frac{GDP^{t2} - GDP^{t1}}{GDP^{t1}}} \quad (2)$$

Table 2. The degrees of coupling and decoupling types

The degrees of coupling and decoupling types		ΔCO_2	ΔGDP	DI
Coupling	Recessive connection	<0	<0	(0.8, 1.2)
	Expansive coupling	>0	>0	(0.8, 1.2)
Decoupling	Recessive decoupling	<0	<0	(1.2, +∞)
	Strong decoupling	<0	>0	(-∞, 0)
	Weak decoupling	>0	>0	(0, 0.8)
Negative decoupling	Expansive negative decoupling	>0	>0	(1.2, +∞)
	Strong negative decoupling	>0	<0	(-∞, 0)

	Weak negative decoupling	<0	<0	(0, 0.8)

Source: Tapio (2005)

3.2.6. Prediction model based on machine learning

Compared with the traditional statistical and air quality models, the new prediction approaches based on regression decision trees that have been developed in recent years have proven to be better suited to air quality weather detrending, since they reduce the variance and error in highly dimensional dataset (Grange et al., 2018; Vu et al., 2019). After preprocessing, the non-linear machine learning model, XGBoost, can be deployed to characterize the non-linear relationship between air pollution and related features and predict the level of pollutants accordingly (Chen and Guestrin, 2016). XGBoost is a decision tree-based ensemble technique that extends the gradient tree boosting algorithm to improve speed and performance. It has been shown to yield state-of-the-art results on a wide range of machine learning challenges, and runs much faster than traditional gradient boosting models (Friedman, 2002).

For a given dataset, there are n data samples, and m features are learned in order to predict target label s simultaneously, $D = \{(x_i \in R^m, y_i \in R^s),\ |D| = n\}$j . The ensemble tree models learn the input with K additive functions and predict the output as follows:

$$\hat{y}_i = \sum_{k}^{K} f_k(x_i) \tag{3}$$

where each $f_k(\cdot)$ corresponds to a regression tree with leaf weight w that is learned from the space of regression trees, $F = \{f_k(x) = w_{q(x)}\}$. Here q represents the structure of each tree that maps an example to the corresponding leaf index in the total of T leaves. To learn the set of functions used in the model, we minimize the following regularized objective consisting of the training loss function and the regularization term:

$$L = \sum_{i}^{n} l(y_i, \hat{y}_i) + \sum_{k}^{K} \Omega(f_k)$$

$$\Omega(f_k) = \gamma T + \frac{1}{2}\lambda\left|\left|w\right|\right|^2 \quad (4)$$

Compared with traditional gradient tree boosting algorithms, XGBoost includes an additional regularization term that selects simple and predictive functions in order to avoid over-fitting. To further prevent over-fitting, XGBoost employs a shrinkage technique to reduce the influence of each individual tree, and encourages the future tree to improve its prediction performance. Moreover, it adopts a column (feature) subsampling technique to randomly choose a subset of features for tree building (Hastie et al., 2009).

Given that the XGBoost model includes regression tree functions $f_k(\cdot)$ as parameters where stochastic gradient descent cannot be employed, XGBoost is trained with an additive learning function by incorporating the best tree model f_t into the loss function in the objective to execute the prediction for step t.

$$L^t = \sum_{i}^{n} l\left(y_i, \hat{y}_i^{(t-1)} + f_t(x_i)\right) + \Omega(f_t) \quad (5)$$

XGBoost can quickly optimize the additive learning objective with a Taylor expansion up to the second order. The approximated objective at step t can be simplified as follows:

$$\widetilde{L^t} = \sum_{i}^{n} [g_i f_t(x_i) + \frac{1}{2} h_i f_t^2(x_i) + \Omega(f_t) \quad (6)$$

where g_i and h_i represent the first- and second-order gradient statistics on the differentiable convex loss function.

In our study, the Mean Absolute Percentage Error (MAPE) was used to measure the accuracy of the prediction model for downtown Regina air pollutant levels. The calculation of this evaluation metric is presented in Equation (7).

$$MAPE = \frac{1}{n}\sum_{i=1}^{n}\frac{|y_i - y_i^*|}{y_i} \quad (7)$$

where n represents the number of samples, y_i represents the observed value of the i^{th} sample, and y_i^* represents the predicted value of the i^{th} sample. A lower value for this metric means that the accuracy of the prediction is higher and the performance of the model is better.

3.2.7. Feature importance and selection

Like tree-based machine learning algorithms, XGBoost is capable of evaluating the relative importance of features that indicate how influential each feature is in the building of decision trees within the model (Hastie et al., 2009). In this experiment, we adopt the metric of gain which is computed for each decision tree by the average amount that each feature split point contributes to performance improvement. As XGBoost optimizes one level of the tree at a time, it splits a leaf into two leaves, and the score it gains is defined as follows:

$$Gain = \frac{1}{2}\left[\frac{G_L^2}{(H_L+\lambda)} + \frac{G_R^2}{(H_R+\lambda)} - \frac{(G_L+G_R)^2}{(H_L+H_R+\lambda)}\right] - \lambda \quad (8)$$

where the subscripts L and R correspond to the new left leaf and the new right leaf, respectively. The gain score can be interpreted as the score increase after the leaf split and subtracting the regularization cost on the additional leaf. The feature importance is then averaged across all trees within the model.

3.3. Results and discussions

3.3.1. Analysis of vehicle fleet composition trends in vehicle body type

An exhaustive segmentation of the vehicle fleet composition was carried out in this study to obtain the variations by vehicle body type in Regina for the period under study. In the period 2001–2018, the total quantity of private vehicles registered in Regina increased by 36.6%, from 120,112 to 164,082. Figure 4 shows the private vehicle fleet composition by vehicle body type for the period under study. Another notable observation is that there was a gradual decreasing trend in the quantity and proportion of two-door cars during the period

of study, with the quantity of this vehicle class declining by 59.9% during the period. A sharp upward trajectory was observed in the quantity of SUVs (from 8,565 in 2001 to 54,761 in 2018). Among the fluctuations in quantities of four-door car, station wagon, truck, and van, what can be clearly seen in the figure is the dominance of the quantity of four-door cars, which peaked in 2009 and has since been in decline. In fact, the quantity actually dropped to 52,623 units by the end of the period of study, lower than it was in 2001. The quantity of station wagons initially declined from 2001 to 2004, then rose beginning in 2005 before once again declining. It ultimately reached its lowest value at the close of the period of study, after having peaked in 2009. The quantity of trucks, meanwhile, rose beginning in 2001 and peaked in 2009. It then declined between 2009 and 2011, then increased to its highest point by the end of the study, accounting for 18.9% of all private vehicles registered in 2018. The quantity of vans increased from 2001 to 2008, then declined steadily from 2009 to 2018. What is striking in this data is the simultaneous ceasing of increasing trends of these four vehicle body types circa 2008–2009. This may be attributable to the impact of the global financial crisis in Canada serving to disrupt automobile sales (Walks, 2015). With the injection of government capital, North America's automobile sector was ultimately able to recover, and automobile sales eventually rebounded (Gordon, 2017).

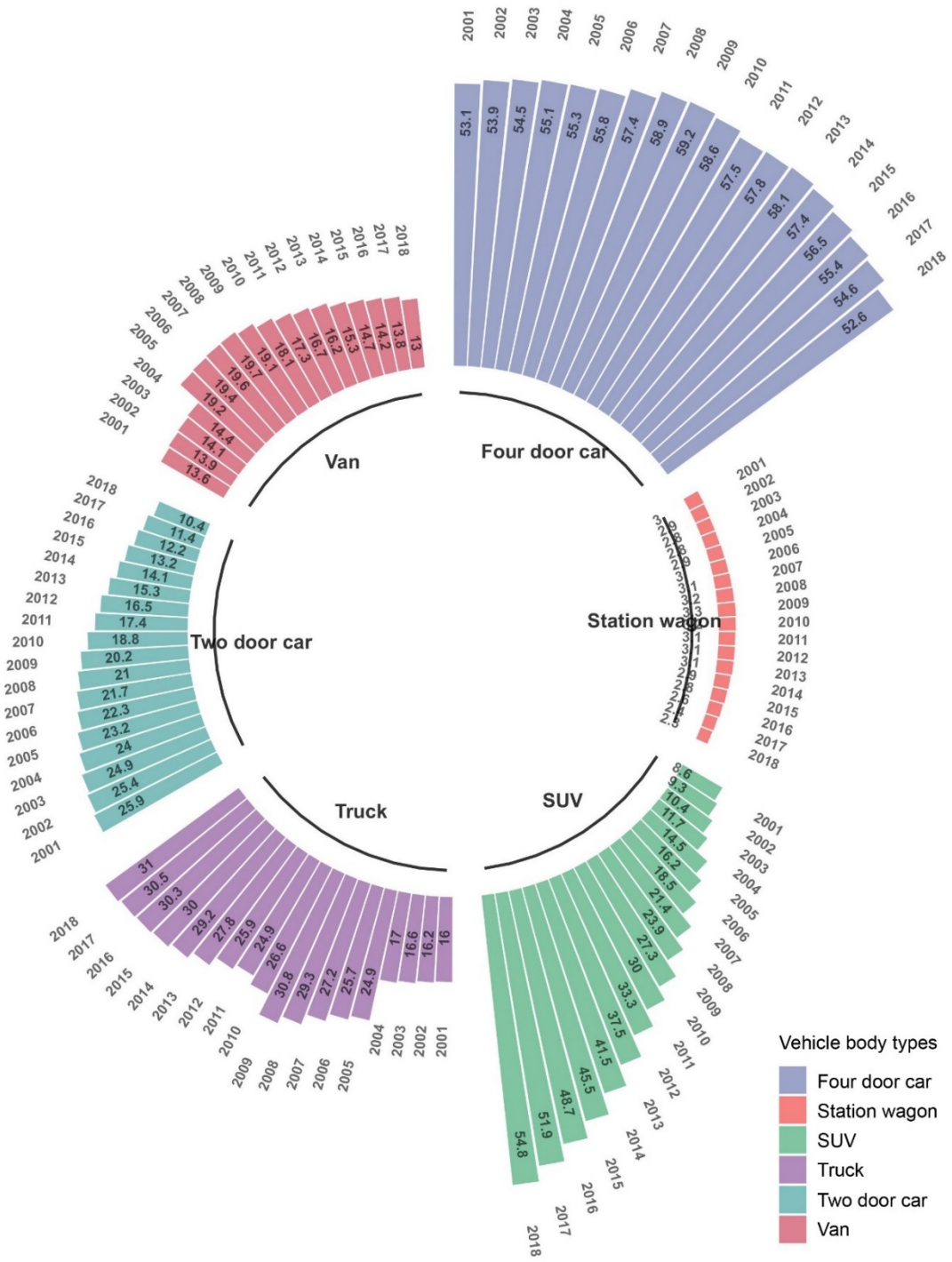

Figure 4. Registration quantity of private vehicles by vehicle body type in Regina from 2001 to 2018 (in thousands).

Figure 5 shows the variation of percentage of six vehicle body types from 2001 to 2008. It

reflects the changes in people's vehicle body type preferences over the course of the last two decades. For instance, in 2001, four-door cars represented the highest proportion of private vehicles, followed by two-door cars, trucks, SUVs, and station wagons. From 2001 to 2018, the percentage of four-door cars dropped from 44.2% to 32.1%. Similarly, two-door car, van, and station wagon declined by 15.2%, 3.6%, and 1.1%, respectively. By contrast, Figure 5 reveals that there has been a rise in the percentage of SUV and trucks, particularly SUVs, which increased in proportion from 7.1% in 2001 to 33.4% in 2018, supplanting the four-door car as the dominant vehicle body type. This trend is not unique to Regina, as national sales figures for 2019 show that pickup trucks and SUVs have continued to increase their market share at the expense of other private vehicle classes across the Canadian fleet (Antich, 2019). This trend in Canada is a significant factor in Canada's position as the highest ranking country in average fuel consumption per vehicle and CO_2 emissions per kilometer driven (International Energy Agency, 2019b). Moreover, the low occupancy rates per vehicle combined with the trend larger (less fuel efficient) vehicles may increase future CO_2 emissions, underscoring the need to improve transportation efficiency (Shiraki et al., 2020). In this regard, other studies have shown that it is the proportion of larger vehicles in the fleet rather than the traffic volume that plays the most significant role in determining the air pollution from the road transportation sector (Dabek-Zlotorzynska et al., 2019; Wang et al., 2018).

In North America, the recent trend towards buying larger vehicles has emerged as a significant environmental issue. As shown in the research results of Bishop and Haugen (2018), the American cities of Chicago, Denver, and Tulsa have also seen a distinct shift from small vehicles to SUVs and trucks, particularly after 2016. The reasons for this trend are diverse. For private vehicles, compared with other developed countries, low interest rates and lower fuel costs are the most significant reasons (Schoettle and Sivak, 2017), while financial incentives from retailers have made it more feasible for consumers to be able to afford an SUV or truck. Recent studies have also shown that, as fuel costs decrease, consumers are more inclined to purchase larger vehicles (Leard et al., 2019). Especially in Canada, the vastness of the country and the cold winter weather make the combination of robust and roomy vehicles more practical for consumers, particularly families (Mohamed

et al., 2018). Apart from private vehicles trends, the rising freight intensity of the economy has also brought about a rise trade within and among provinces as well as internationally (Nasreen et al., 2018). In this context, knowledge of current trends in vehicle purchase preferences and the types of vehicles that contribute most to private vehicle emissions will allow for the measures taken to address air pollution and climate change to be designed correctly (Pérez et al., 2019).

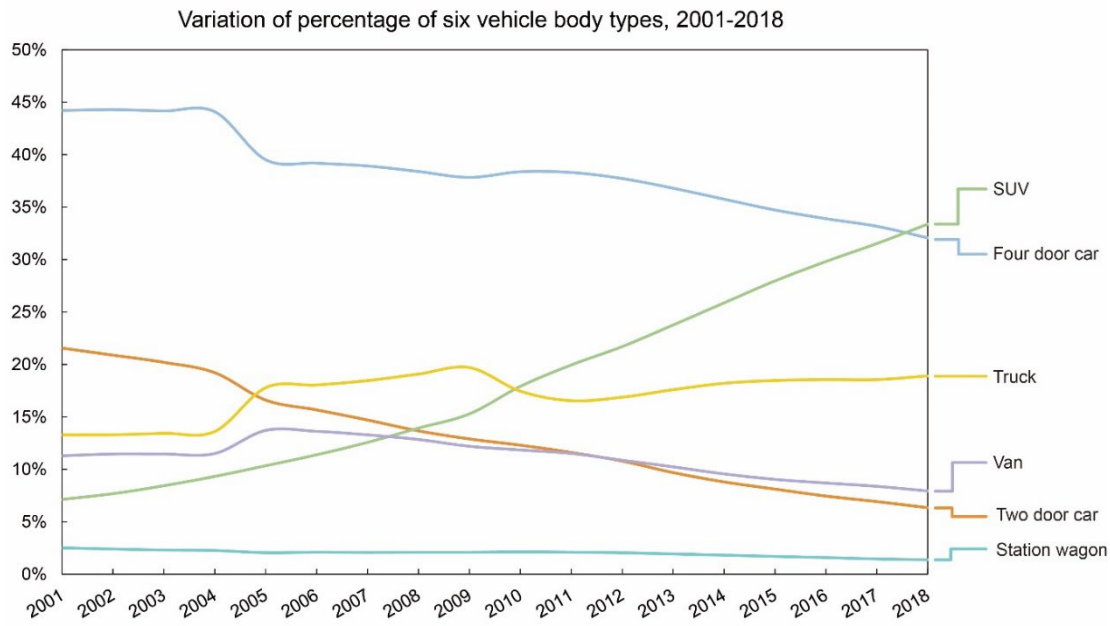

Figure 5. Variation of percentage classified by vehicle body type in Regina, 2001–2018 (two-door car, four-door car, SUV, truck, van and station wagon).

3.3.2. Analysis of vehicle fleet composition trends in fuel types

As shown in Figure 6, most private vehicles registered in Regina are gasoline vehicles, which account for 99.2% of all vehicles registered in 2001. It is notable that this dropped to 88.6% in 2018 due to the rise of clean fuel alternatives over the years. Meanwhile, there has been a slight increase in the proportion of diesel vehicles since 2001, rising from 0.7% to 2.4%. The proportion of flexible fuel vehicles (FFVs), designed to run gasoline blended with either ethanol or methanol fuel, increased from 0.02% to 8.56% from 2001 to 2018. Compared with vehicles that use conventional gasoline or diesel fuel, FFVs offer improved

energy efficiency and emission performance (Bailey, 2018). As for gas–electric hybrids, though accounting for less than 0.5% of the total private vehicle registrations in 2018, they experienced substantial growth in numbers from 2001 to 2018. With the combination of a standard-sized engine and a large electric motor, the hybrids outperform their conventional counterparts in the same vehicle class in terms of overall fuel economy range. The flexible powertrain of today's hybrid vehicles has also addressed the initial concern from electric vehicles drivers related to limited battery range and charging station availability (Thomas, 2009). Historical data from Regina shows that the predominance of gasoline vehicles in the vehicle market is gradually declining. The future of clean fuel for vehicles will rely on the portfolio of fuels and technologies. In this regard, the Clean Fuel Standard was published by the Government of canada (2020a) and the reduction requirements will come into force in 2022. It is designed to incentivize innovation and adoption of clean technologies such as ethanol in gasoline and hydrogen in vehicles, and expand the use of low carbon fuels throughout the economy.

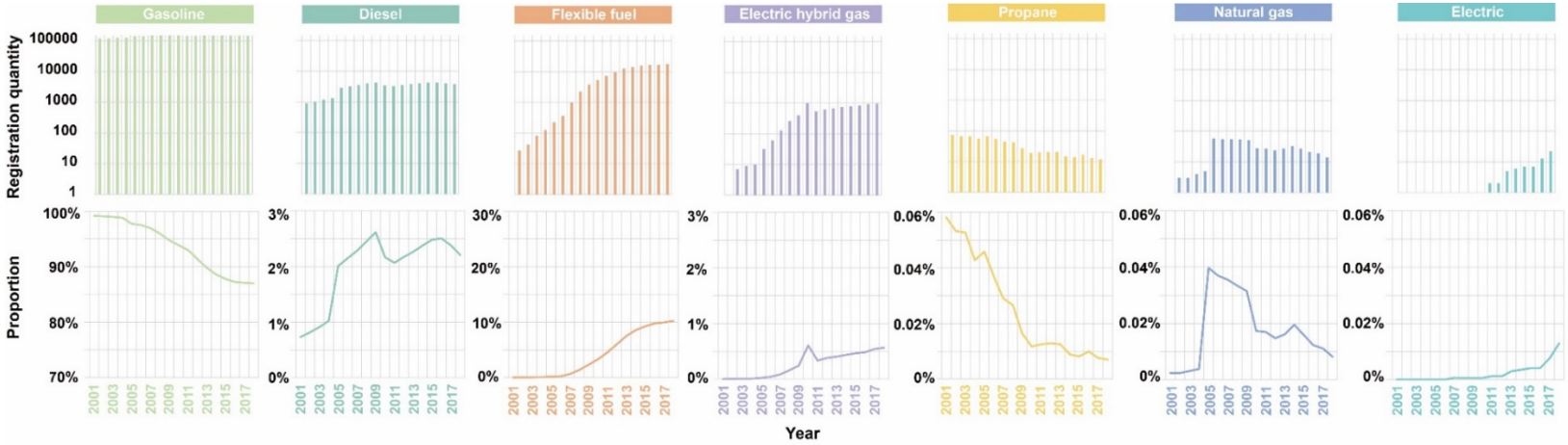

Figure 6. Registration quantity and proportion of vehicles disaggregated by type of consumed fuel in Regina from 2001 to 2018 (diesel, gasoline, propane, flexible fuel, natural gas, electric and electric hybrid gas).

3.3.3. Air quality from 2001 to 2018

The *Federal Agenda on Cleaner Vehicles, Engines and Fuels* having been set out in 2001 to accelerate actions on clean air, emission regulations in Canada for new on-road vehicles and engines came into force in 2004 (Government of canada, 2013, 2017). Aligned with the emission standards in the United States, it applied to light-duty vehicles, light-duty trucks, heavy-duty vehicles, heavy-duty engines, and motorcycles. In this context, although the total quantity of private vehicles in Regina actually rose from 120,112 to 164,082 during the period under study, the air quality benefits of increasing fuel efficiency of vehicles was found to be significant. Figure 7 to Figure 16shows the hourly air pollutant concentrations during rush hour in the downtown area of Regina during the period under study. As can be seen, average pollution levels for most parameters have been dropping over time. Compared to 2001 levels, concentrations of CO, NO_X, $PM_{2.5,}$ PM_{10}, and SO_2 had fallen by more than 30% by 2018. The largest reduction was in CO concentration, which dropped 78.3% from 0.73 ppm in 2001 to 0.19 ppm in 2018. According to Figure 7 and Figure 8, the range of hourly CO concentration was widespread until about 2011, as high as 3.8 ppm in 2001. By 2018, the CO concentrations in 298 samples were found to be less than 1 ppm and the range was more concentrated. Similarly, the range of NO_X and SO_2 concentration became smaller and more concentrated over the course of the period under study.

The concentration of fine particulate matter ($PM_{2.5}$ or PM_{10}), meanwhile, increased slightly in the years after 2010, although this is most likely attributable to wildfire smoke (Dreessen et al., 2016; Wu et al., 2018). These fires were considered "exceptional events" and the spread of smoke led to a short-term decline in urban air quality. Without the wildfires, the overall average concentration of fine particulate matter in Regina would have actually decreased during this period (Government of saskatchewan, 2021).

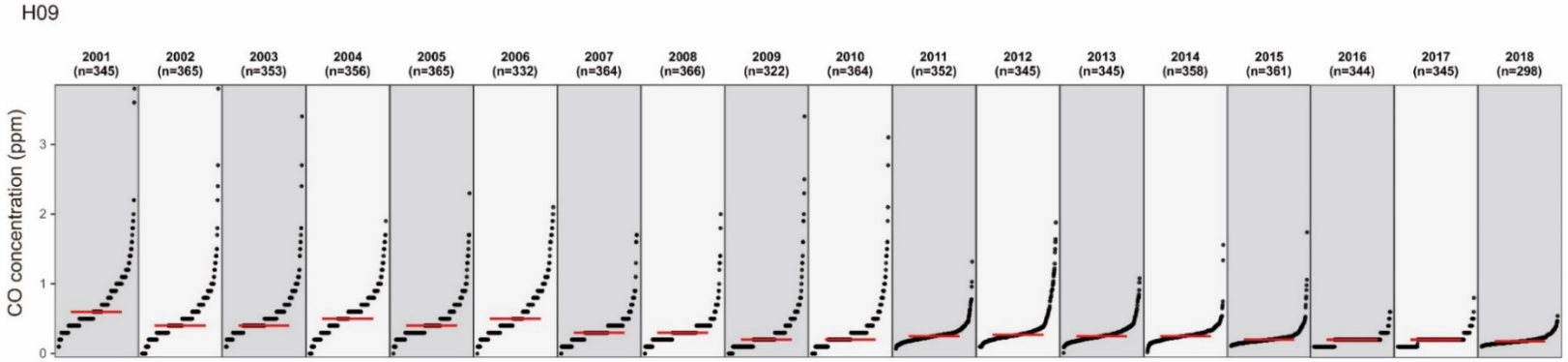

Figure 7. Hourly CO concentration (ppm) on H09 in downtown, Regina, 2001-2018.

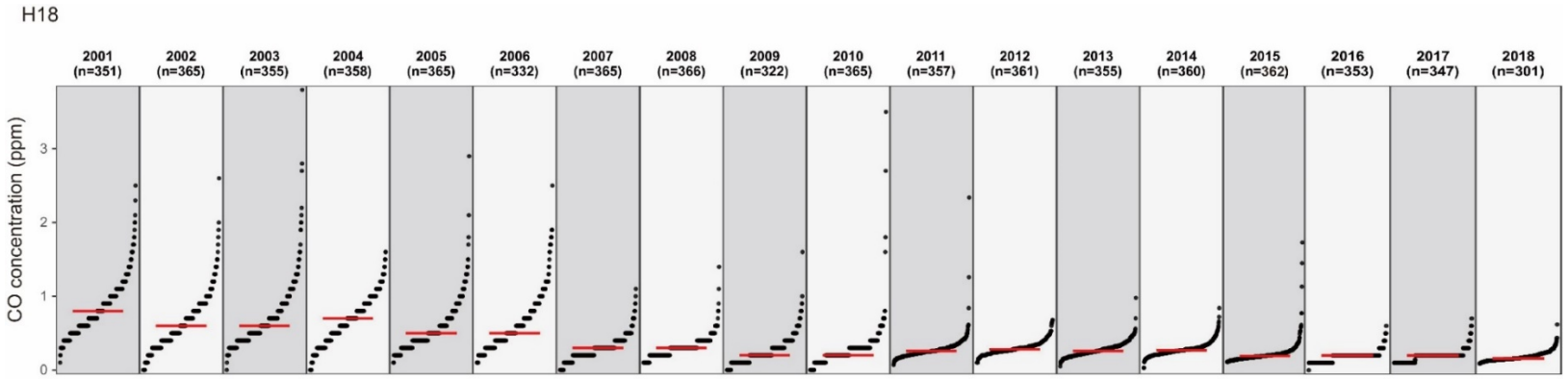

Figure 8. Hourly CO concentration (ppm) on H18 in downtown, Regina, 2001-2018.

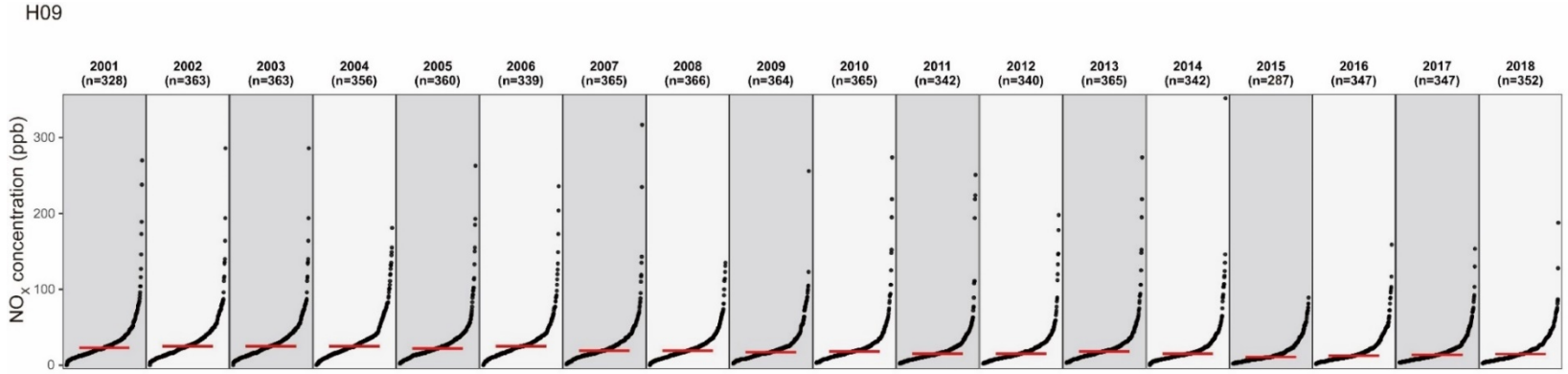

Figure 9. Hourly NO_X concentration (ppb) on H09 in downtown, Regina, 2001-2018.

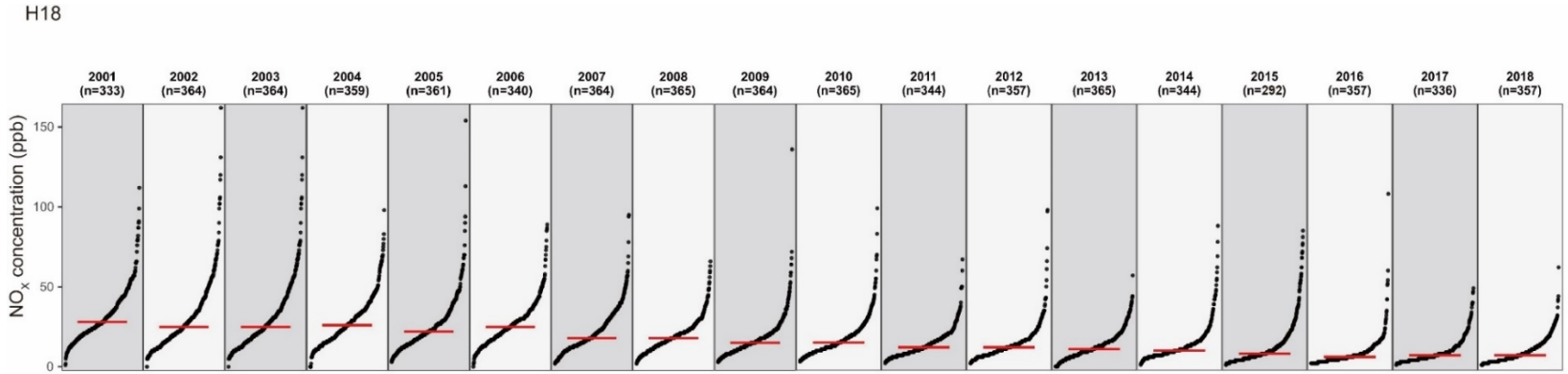

Figure 10. Hourly NO_X concentration (ppb) on H18 in downtown, Regina, 2001-2018.

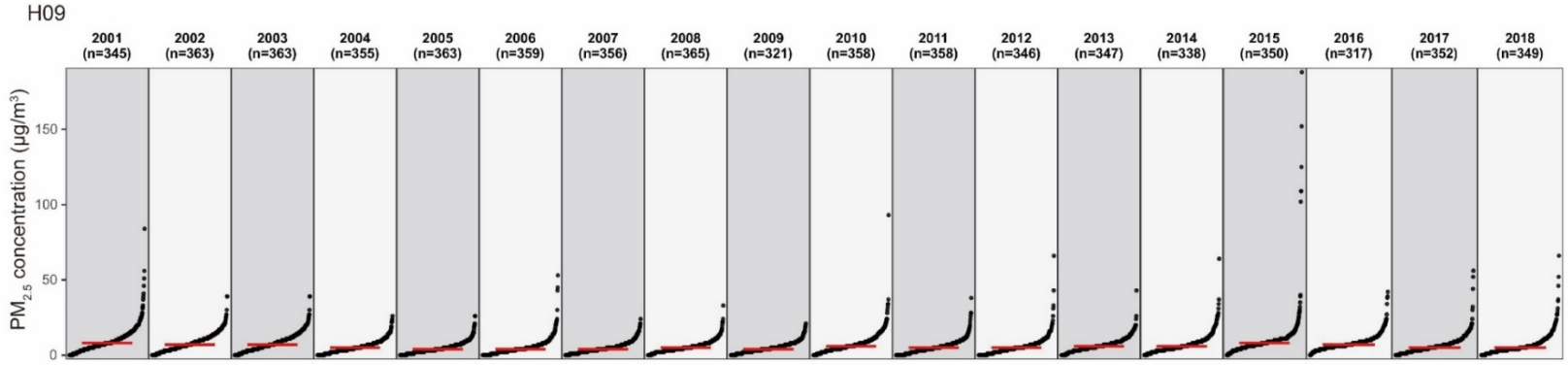

Figure 11. Hourly $PM_{2.5}$ concentration ($\mu g/m^3$) on H09 in downtown, Regina, 2001-2018.

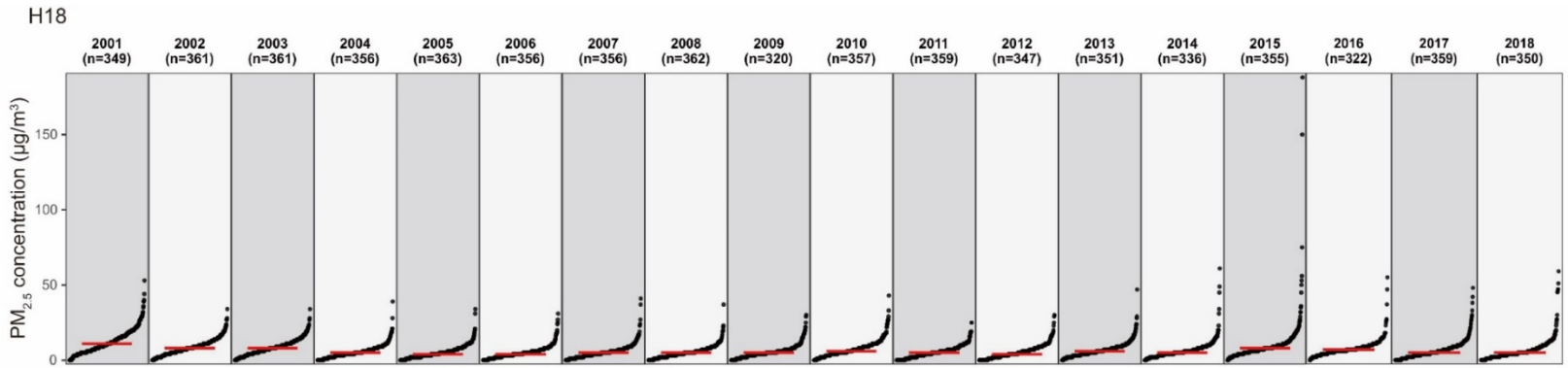

Figure 12. Hourly $PM_{2.5}$ concentration (µg/m3) on H18 in downtown, Regina, 2001-2018.

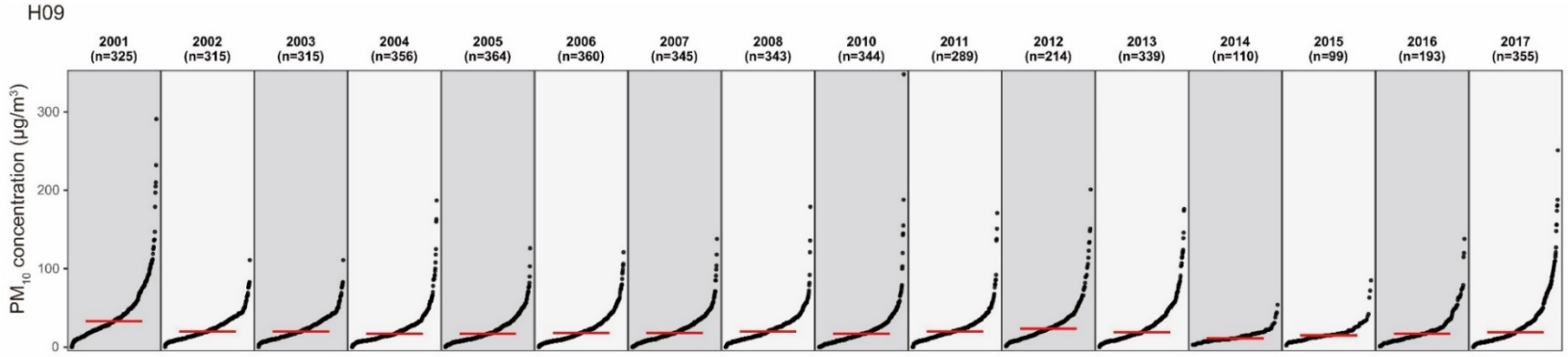

Figure 13. Hourly PM_{10} concentration (µg/m^3) on H09 in downtown, Regina, 2001-2018.

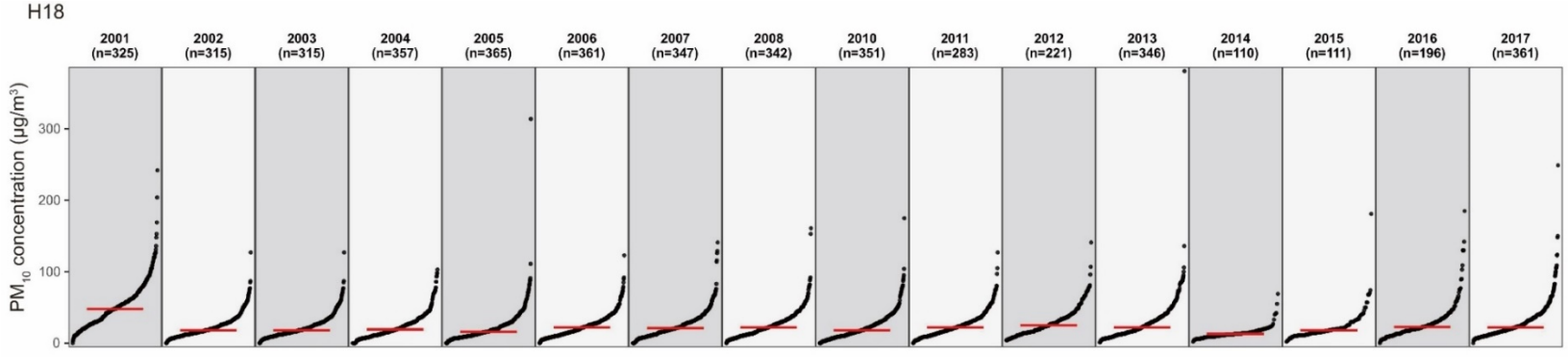

Figure 14. Hourly PM_{10} concentration (µg/m3) on H18 in downtown, Regina, 2001-2018.

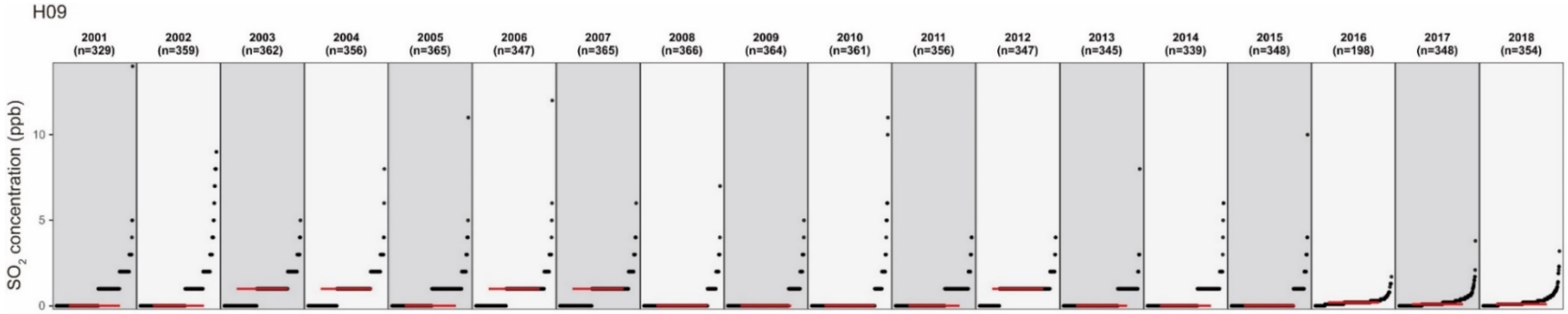

Figure 15. Hourly SO_2 concentration (ppb) on H09 in downtown, Regina, 2001-2018.

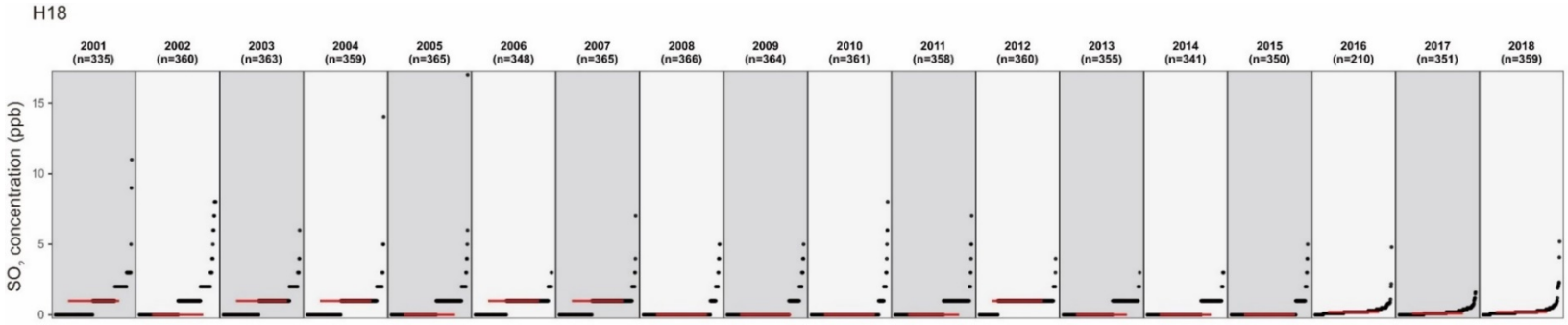

Figure 16. Hourly SO_2 concentration (ppb) on H18 in downtown, Regina, 2001-2018.

3.3.4. Estimation of GHG emissions inventories from on-road private vehicles

This study considered three key GHGs and their 100-year global warming potential (GWP): CO_2, CH_4, and N_2O (Forster et al., 2007). Figure 17 presents the estimation of CO_2 eq for the six vehicle classes, the jurisdiction, and the period under study. As can be seen, for 2018, total GHG emissions from private vehicles were estimated at 655 kilotonnes (Kt) CO_2 eq. In fact, this metric peaked in 2009 and began to level off beginning in 2010. Notwithstanding these fluctuations, though, GHG emissions from the private vehicle sector actually grew by 25.0% overall. This is attributable to a significant shift in the GHG emissions emitted from vehicle types used for passenger transport: emissions from SUVs and trucks rose by 374.0% and 69.3%, respectively, whereas emissions from four-door cars, two-door cars, station wagons, and vans all decreased. These increases from bigger vehicles were only partially offset by a 124.7 Kt CO_2 eq decrease in emissions from four-door cars, two-door cars, station wagons, and vans. SUVs' share of total private vehicle emissions rose from 9.7% in 2001 to 36.6% in 2018 (the largest share of any vehicle class by the end of the period under study). Trucks' share of emissions also increased, from 18.1% in 2001 to 24.6% in 2018.

According to data from the Government of Canada (2020b), the trend of GHG emissions incurred by the transportation sector in Canada overall from 1990 to 2019 is similar to the trend seen in Regina, especially the changes in vehicle type used. The CO_2 eq from cars declined by 21%, while emissions from trucks, vans, and SUVs more than doubled. Variations in the mixture of vehicle type used, such as the increasing popularity of SUVs and light trucks at the expense of more fuel-efficient vehicles, have played a significant role in determining the evolution of GHG emissions.

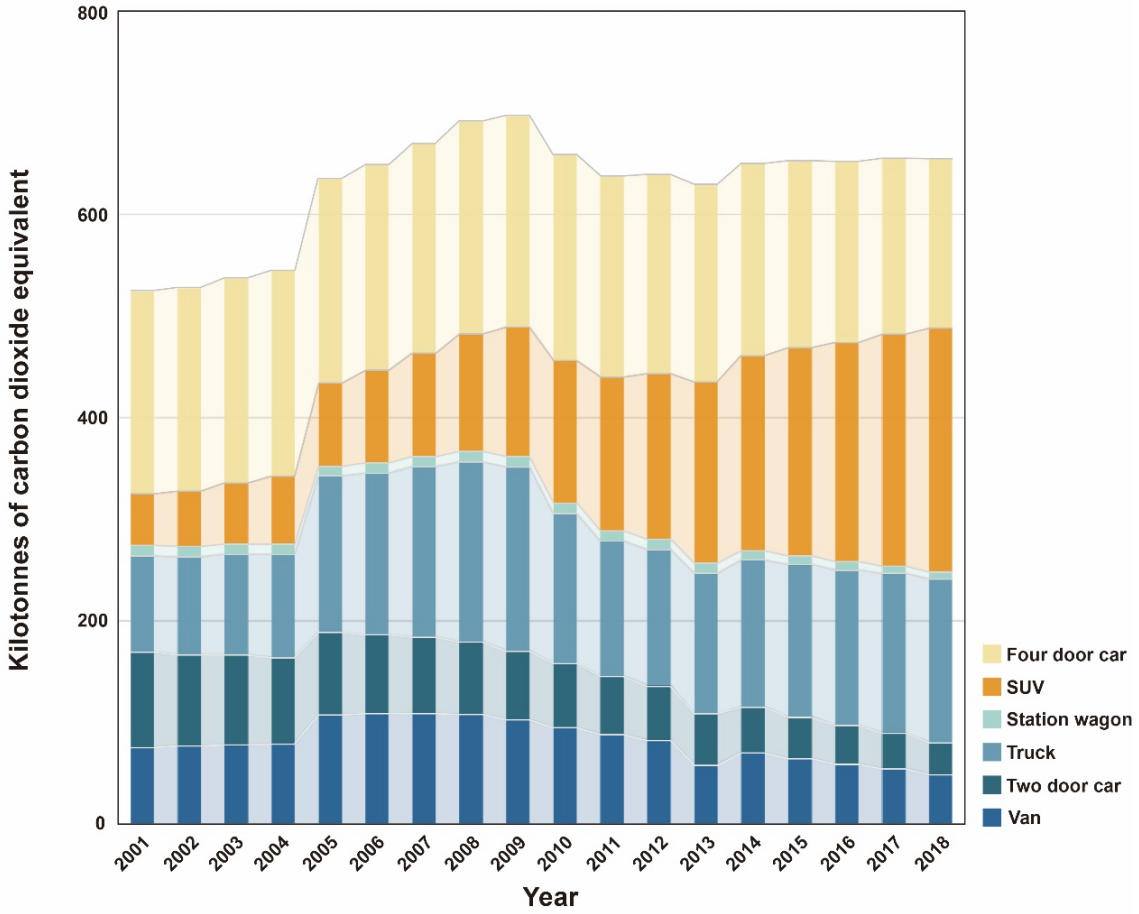

Figure 17. Estimation of carbon dioxide equivalent from private vehicle sector in Regina from 2001 to 2018.

3.3.5. Analysis of fuel economy historical trend

The total GHG emissions from private vehicles in Regina has been on a steady flat trend since 2014. The changes in vehicle composition, along with the steady trend in GHG emissions, may be a response to the establishment of fuel economy standards and improved fuel economy (Doremus et al., 2019). Figure 18 to Figure 23 show the historical trend of average weighted fuel economy and the annual improvement rate of the six private vehicle body types under study. The fuel economy of four-door cars, two-door cars, and SUVs continued to improve during the course of the period of study. The fuel economy standards for vehicles, similarly, have seen significant progress in recent years both in Canada and

around the world. Moreover, continued advances in vehicle engine and emission control technology will play a critical role in reducing future emissions from on-road vehicle use. Prior to the past decade ago, only China, Japan, South Korea, and the United States had a legislative framework in place for fuel economy or GHG emission standards. Today, most of the countries among the top 15 vehicle markets worldwide, including Canada, have put in place legislative frameworks for regulating fuel economy to encourage continued innovations to reduce vehicle GHG emissions. In 2014, the Government of Canada announced on-road vehicle and engine emission regulations that lower the limits on the sulfur content of gasoline and impose stricter limits on air pollutant emissions from various types of vehicles beginning with the 2017 model year (Government of Canada, 2014). These types include new passenger cars, light-duty trucks, and certain heavy-duty vehicles.

According to the International Council on Clean Transportation (ICCT) (Yang and Bandivadekar, 2017), the simulated efficiency results for passenger vehicles based on a series of test cycles (US Corporate Average Fuel Economy standards) in Canada was 21.3 mpg in 2001 and 27.7 mpg in 2016. The enacted target for passenger vehicles by 2025, meanwhile, is 40.6 mpg. However, while there have been notable improvements in the fuel efficiency of mainstream cars in Regina in recent decades—even relative to the country's historical levels and future target—these have not been sufficient to offset the increases in emissions due to changes in the vehicle fleet composition. Given this, determining the weighted average fuel economy of the vehicle fleet at the city level will aid in understanding of fuel-economy standards, thereby benefitting policy makers seeking to set appropriate targets for the future.

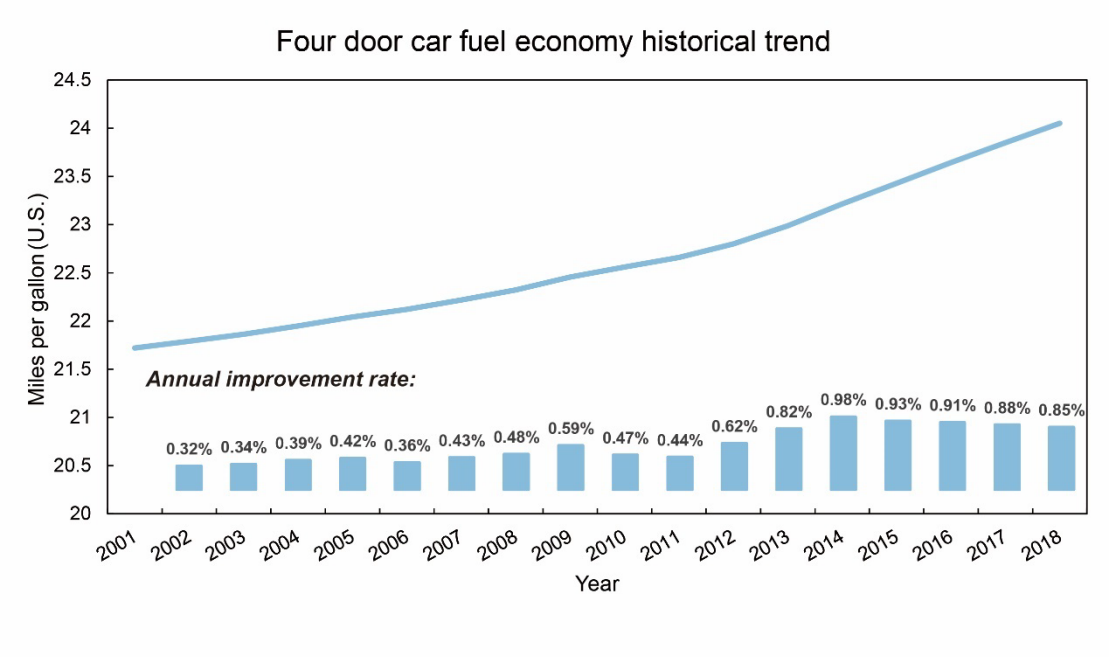

Figure 18. Four door car fuel economy historical trend and annual improvement rate in Regina from 2001 to 2018.

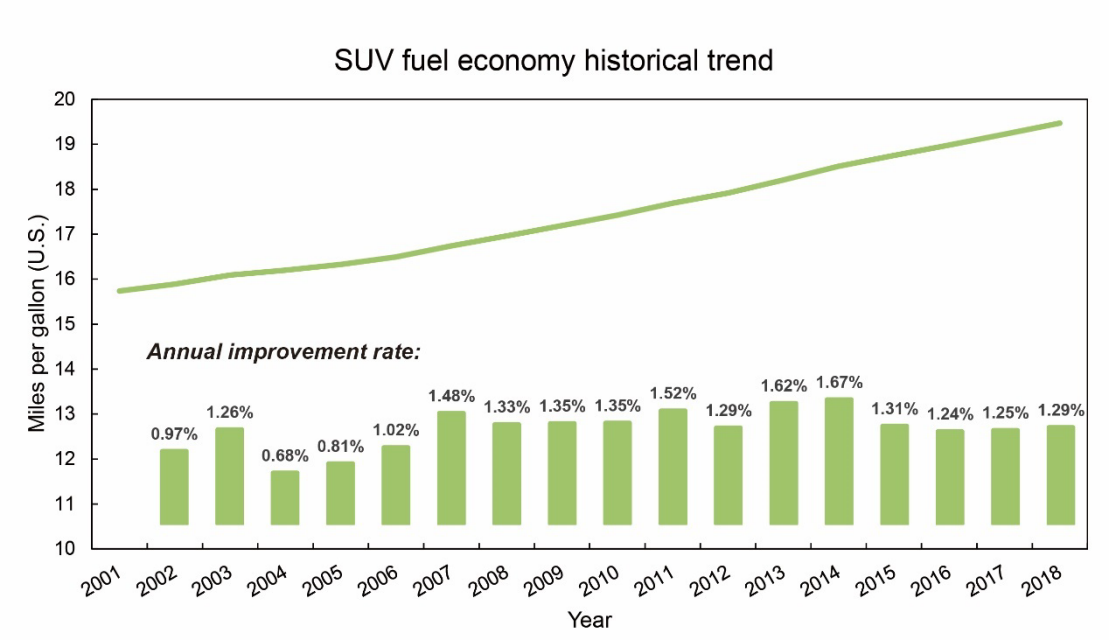

Figure 19. SUV fuel economy historical trend and annual improvement rate in Regina from 2001 to 2018.

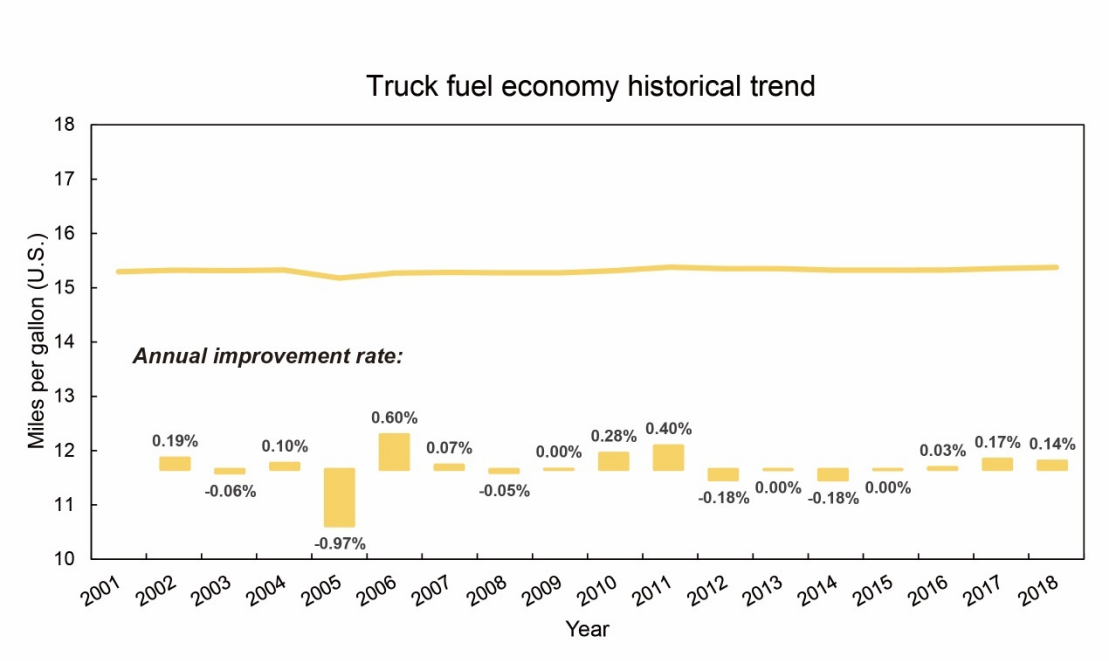

Figure 20. Truck fuel economy historical trend and annual improvement rate in Regina from 2001 to 2018.

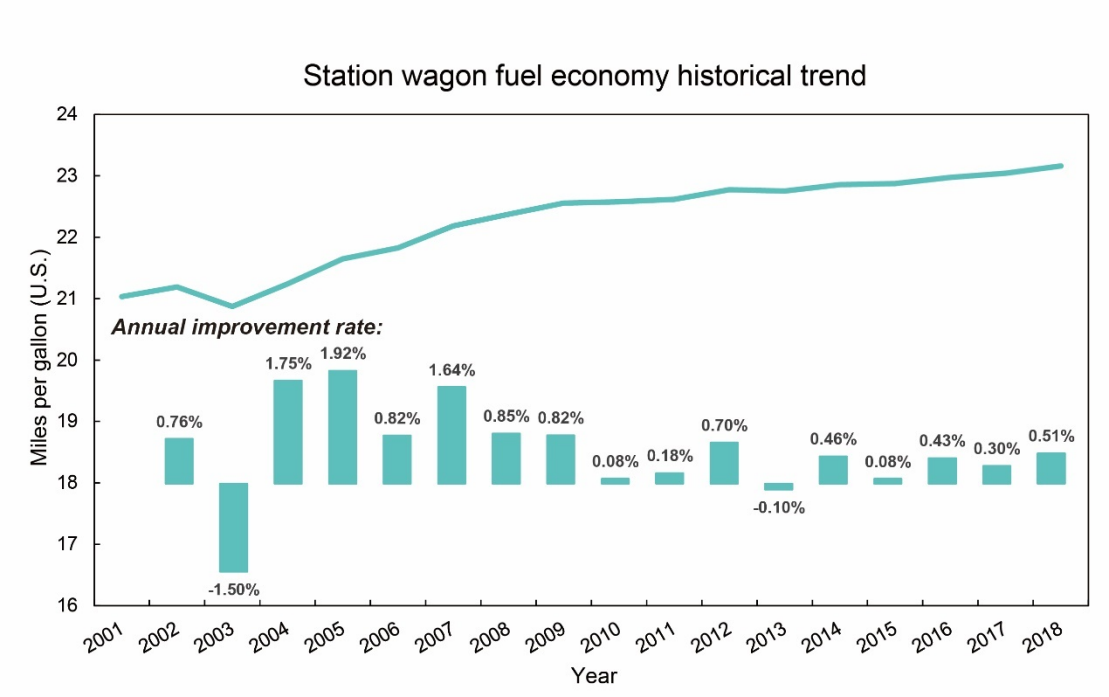

Figure 21. Station wagon fuel economy historical trend and annual improvement rate in Regina from 2001 to 2018.

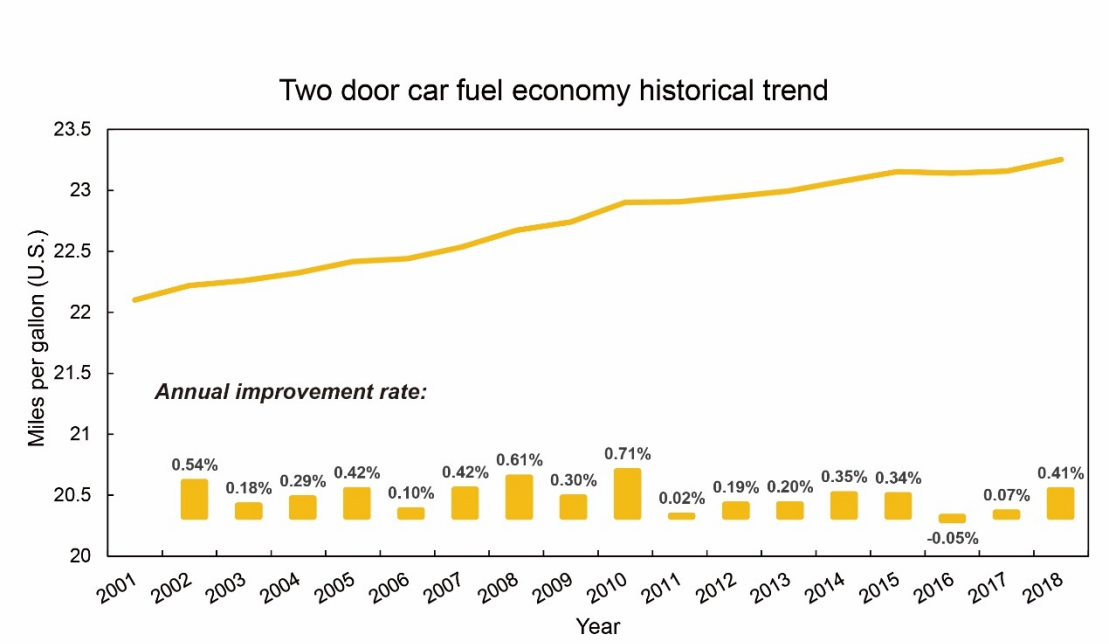

Figure 22. Two door car fuel economy historical trend and annual improvement rate in Regina from 2001 to 2018.

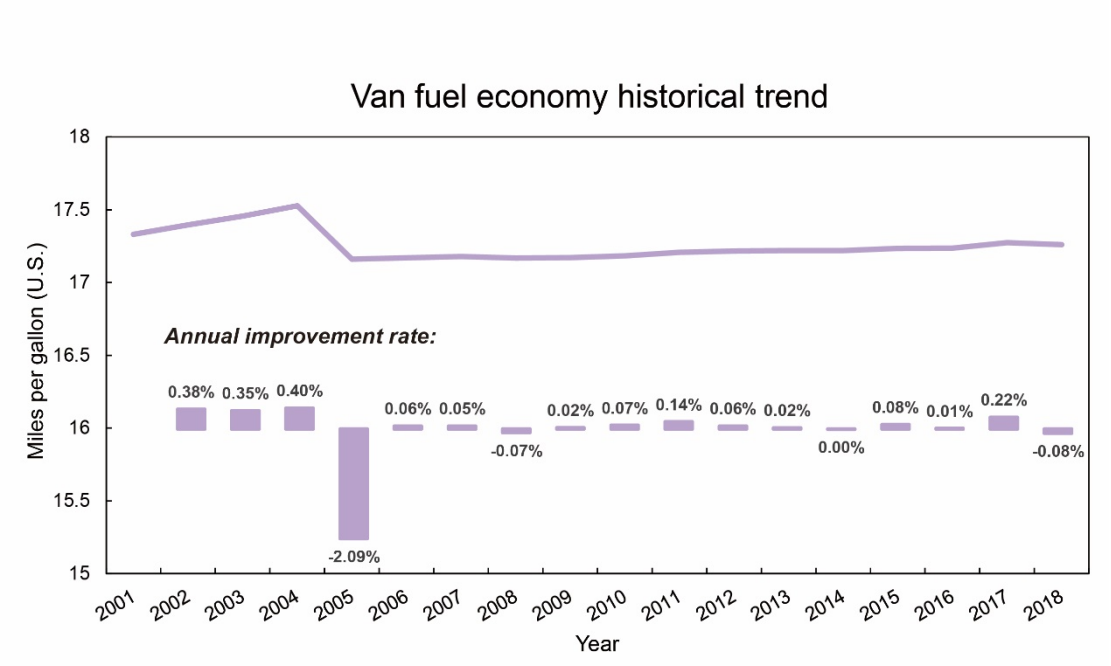

Figure 23. Van fuel economy historical trend and annual improvement rate in Regina from 2001 to 2018.

3.3.6. Decoupling analysis between GDP and CO_2 emissions from the transportation sector in Regina and Canada

Figure 24 shows the degrees of coupling and decoupling of passenger transport CO_2 emission from economic growth in both Regina and Canada. The numbers in the figure represent the interval between the corresponding two years; for example, "1" represents the interval from year 2001 (the first year under study) to year 2002. Relative decoupling was observed in aggregate as shown in the figure for Regina and Canada in most of the years. It may be concluded that weak decoupling occurred in Regina from 2001 to 2008 and in Canada from 2001 to 2007 except for 2005–2006. Both Regina and Canada subsequently experienced strong decoupling, in the years 2009–2010, 2012–2013, and 2015–2016 in the case of Regina, and 2010–2012 and 2013–2014 in the case of Canada nationally. The increase in decoupling degree observed indicates that the economic development increased while the release of CO_2 from passenger transport vehicles declined due to the improvement of fuel economy over these years.

From 2013 to 2015, the relationship between passenger transport CO_2 emission and GDP in Regina was unstable and fluctuated between strong negative decoupling (elasticity of −3.83) and expansive negative decoupling (elasticity of 1.81). Similarly, this phenomenon occurred in Canada from 2014 (elasticity of −4.76) to 2016 (elasticity of 2.29). Due to global over-supply, the crash in oil prices in 2014 strained the local economy. Both Regina and Canada experienced economic downturns and increases in environmental pressure in the form of emissions during this period. Additionally, from 2016 to 2017, at the country level, the linkage effect of CO_2 emissions and GDP in Canada once again exhibited a weak coupling phenomenon. At the city level, meanwhile, the linkage effect presented strong decoupling from 2015 to 2016, then strong negative decoupling after 2016.

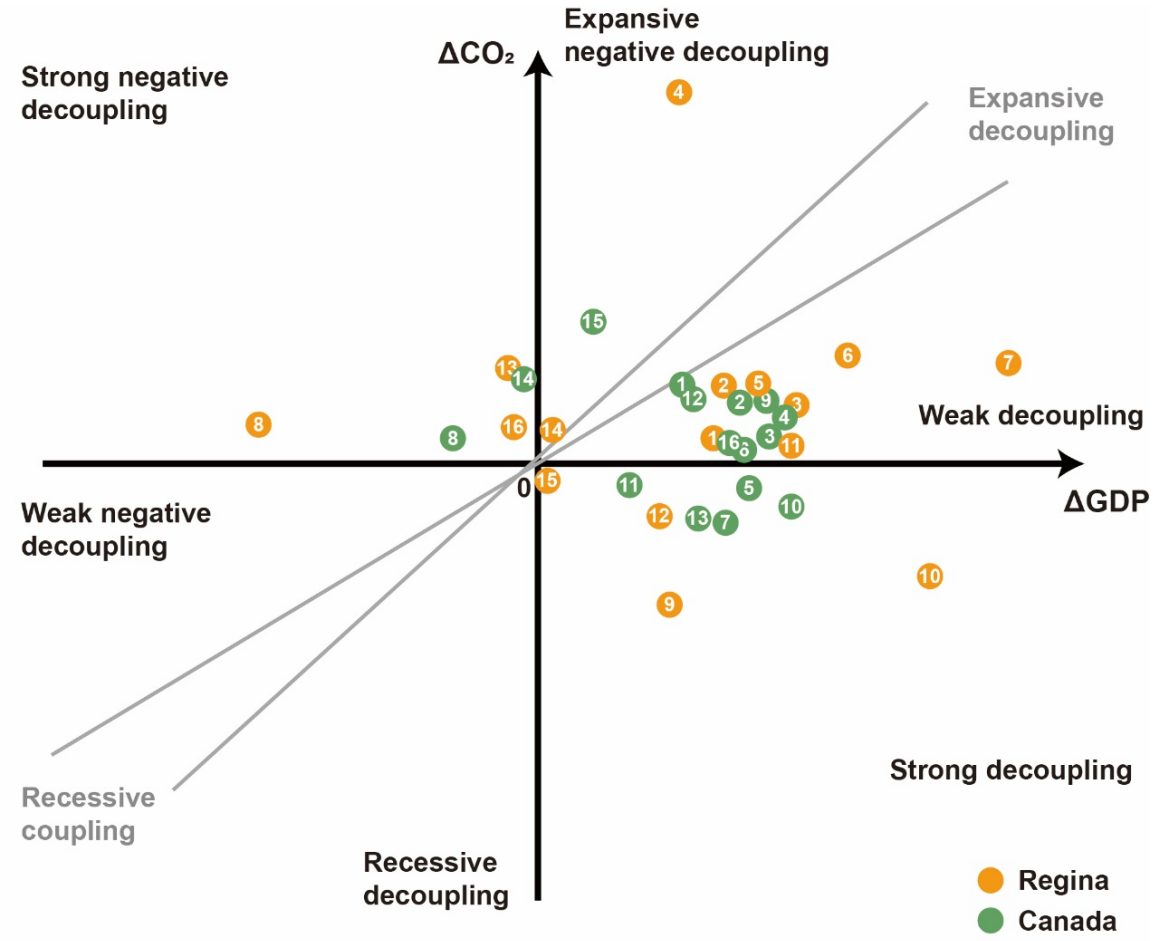

Figure 24. Decoupling of passenger transport CO_2 emission from GDP in Regina and Canada from 2001 to 2017.

3.3.7. Performance of XGBoost model for predicting air pollutants

Due to the missing value of PM_{10} in rush hour H09 and H18 in 2009 and 2018, XGBoost was used for predicting the remaining air pollutants, including CO, NO_X, $PM_{2.5}$, and SO_2. Hourly air pollutant concentration data for each day of the year, obtained from monitoring station data, was used to establish the annual average level. Data for the period 2001 to 2015 was taken as the training set, while the remaining data (2016 to 2018) was used as

the testing set in a train–test split. Before inputting the data into XGBoost and modeling the results, the parameters of the algorithms, such as the number of boosted trees, learning rate, the maximum depth a tree can grow, and the minimum sum of instance weight needed in a tree child, were all fine-tuned. Moreover, a grid search method of parameter was adopted for the selection of optimal ensemble model. The actual values and predicted values of annual average air pollutant levels as generated by the XGBoost model are displayed in Table 3. The efficiency of this model was evaluated based on the metrics of MAPE. According to the outcomes obtained, the result with the smallest error was observed in the prediction of NO_X in H18 in 2018. In predicting the NO_X concentration, the MAPE value decreased from 2.52% in 2016 to 0.91% in 2018. Also, with the exception of the results of SO_2 in H09, the model performed well in the prediction of CO, PM2.5, and NO_X in rush hour in these three years. Overall, these results demonstrate the high capability of the XGBoost model in predicting the annual concentration of air pollutants.

Table 3. Prediction performance of XGBoost model for air pollutants in the study area

Pollutants		2016	2017	2018		2016	2017	2018
CO_H09 (ppm)	Obs.	0.191	0.197	0.193	CO_H18 (ppm)	0.183	0.191	0.181
	Pred.	0.195	0.200	0.196		0.189	0.186	0.188
	MAPE (%)	1.89	1.72	1.34		3.54	2.83	3.72
NOx_H09 (ppb)	Obs.	17.245	17.452	18.176	NOx_H18 (ppb)	8.728	9.653	9.852
	Pred.	17.609	17.938	17.822		8.948	9.817	9.762
	MAPE (%)	2.11	2.76	1.95		2.52	1.7	0.91
$PM_{2.5}$_H09 (ug/m^3)	Obs.	8.256	6.622	6.900	$PM_{2.5}$_ H18 (ug/m^3)	7.783	6.579	6.609
	Pred.	7.830	6.900	7.112		7.537	6.924	7.006
	MAPE (%)	5.15	4.19	3.07		3.16	5.24	6.02
SO_2_H09 (ppb)	Obs.	0.231	0.224	0.255	SO_2_H18 (ppb)	0.271	0.181	0.286
	Pred.	0.279	0.259	0.298		0.239	0.191	0.262
	MAPE (%)	20.91	15.24	16.87		12.03	5.21	8.37

3.3.8. Features influencing downtown air pollutant levels

Changes in air pollutant levels resulting from passenger and freight transport in a given region are influenced by a number of factors, including trends in population and economic growth, vehicle type, fuel efficiency, and fuel type (Government of Canada, 2021a). In this regard, transportation, demography, economics, and energy features may have contributed to the changes in downtown air pollutant levels in Regina during the period of study. Based on the computation of feature importance as expressed in Eq. (8), possible influencing factors and the most important factors influencing downtown air pollutant levels can be identified on a city scale. Table 3 presents the top 15 features that were identified as having the highest importance in the prediction of air pollutant levels. The most important feature was found to be FDFC (four-door fuel consumption, FI = 0.398), followed by VRQ (FI = 0.202), TRQ (FI = 0.122), SWRQ (FI = 0.044), DP (FI = 0.041), etc. According to the findings, it was determined that FDFC plays an important role in changes in downtown air pollutant levels. The standing of FDFC as the number one factor influencing air pollution levels may be attributable to the fact that fuel consumption of vehicles is an important factor in air pollution, and that personal motorized travel has been dominated by a reliance on four-door vehicles in recent decades (Tian et al., 2021). The factors ranking 2 to 4 were the number of van, truck, and station wagon registrations in the private vehicle fleet, and ranking 6 to 7 were the fuel economy of the corresponding vehicle types. In Canada, urban transit systems are less likely to be used for family-based trips, daily commute and commercial activity than in other jurisdictions because of the sparseness of the population distribution, the limited road public transportation coverage, and the cold weather. Given the trends in personal and family travel demand in recent decades, the change in fleet composition of medium and heavy vehicles is evident, and this in turn may exert environmental pressure in the form of elevated air pollution levels from urban traffic. Improvements in fuel economy, meanwhile, help to offset the air pollution effects associated with changes in vehicle fleet composition. In the future, governments in "personal vehicle-oriented cities" with a large number of private vehicles relative to the population should place increasing emphasis on the establishment of robust multi-mode travel systems and countermeasures that strike an appropriate balance between environmental, energy, demography, and planning development features to achieve the

optimal level of service for travel (Chen et al., 2020a).

Table 4. Top 15 factors based on feature importance measurement

Rank	Feature abbreviation	Description	Feature Importance
1	FDFC	Four door car fuel consumption	0.398
2	VRQ	Van registration quantity	0.202
3	TRQ	Truck registration quantity	0.122
4	SWRQ	Station wagon registration quantity	0.044
5	DP	Diesel price	0.041
6	TFC	Truck fuel consumption	0.038
7	VFC	Van fuel consumption	0.036
8	GP	Gasoline price	0.025
9	POM	Proportion of males	0.023
10	DRQ	Diesel vehicle registration quantity	0.020
11	SWFC	Station wagon fuel consumption	0.016
12	EHGFQ	Electric hybrid gas vehicle registration quantity	0.012
13	EMPL	Employment rate	0.008
14	PRQ	Propane vehicle registration quantity	0.006
15	TDFC	Two door car fuel consumption	0.003

3.4. Summary

In this chapter, an account of the evolution and development of the private vehicle fleet in Canadian cities over the last twenty years was presented in particular reference to six vehicle body types and seven fuel types. From 2001 to 2018, the percentage of four-door cars in the vehicle fleet dropped from 44.2% to 32.1%. The shift in preference toward larger vehicles contributed to the increasing dominance of SUVs and trucks in the fleet. This trend was particularly pronounced in the case of SUVs, where the percentage increased from 7.1% in 2001 to 33.4% in 2018. In terms of changes in vehicle fuel type, due to the rise of clean fuel alternatives and the support from the national Clean Fuel Standard in recent years, historical data from Regina shows that the domination of gasoline vehicles in the vehicle market is gradually declining. In addition, we investigated how the fuel economy

of the whole vehicle fleet is changing, as well as how the downtown air quality has changed. In reference to the case study, although the total number of vehicles in Regina rose over the course of the period of study, the increasing fuel efficiency of vehicles contributed to the improvement of downtown air quality. Compared to 2001, concentrations of CO, NO_X, $PM_{2.5}$, PM_{10}, and SO_2 fell by more than 30% in 2018. Moreover, this study characterized changes in the distribution of GHG emissions from private vehicles in Regina in recent decades by vehicle body type. It was found that there was a significant shift in the total GHG emissions emitted from vehicle types used for passenger transport: emissions from SUVs and trucks rose by 374.0% and 69.3%, respectively, whereas emissions from four-door cars, two-door cars, station wagons, and vans all decreased. These increases from larger vehicles in GHG emissions were partially offset by a 124.7 Kt CO_2 eq decrease in emissions from four-door cars, two-door cars, station wagons, and vans, ultimately resulting in a 25% increase overall in the emissions of the private vehicle sector between 2001 and 2018.

In the long term, the subtle connections among economic, demographic, transportation, and energy factors play an important role in changes in air pollution levels in urban areas. To evaluate the relationship between environmental pressure from on-road vehicles and economic growth, decoupling analysis was conducted at both the city level and country level. Both Regina in particular and Canada in general experienced strong decoupling (Regina in 2010, 2013, and 2016, and Canada in 2011, 2012, and 2014). Additionally, after 2016, the decoupling level decreased both in Regina in particular and in Canada in general. Following decoupling analysis, the long-term downtown air pollutant levels, including concentrations of CO, NO_X, PM_{10}, $PM_{2.5}$, and SO_2 in rush hour, were predicted using the XGBoost machine learning model. The overall prediction results reveal the good performance of the XGBoost model in predicting the annual concentrations of air pollutants. Regarding the prediction of NO_X, for instance, the MAPE value decreased from 2.52% in 2016 to 0.91% in 2018. To provide more specific information to aid in policymaking on traffic-related air pollution, the factors influencing air pollutant levels in terms of vehicle fleet composition, demography, economics, and energy were identified. It is necessary to uncover and replenish the cause-effects among these several diverse types

of factors. The top five factors were FDFC, VRQ, TRQ, SWRQ and DP, with changes in the fuel economy of popular vehicle body types and changes in the composition of the vehicle fleet found to be the most important factors. With the development and frequency of personal and family travel demand over the last two decades, governments in "personal vehicle-oriented" cities with large numbers of private vehicles, not only in Canada but globally, should place a renewed emphasis on the establishment of a robust multi-mode travel system.

CHAPTER 4. ASSESSING THE IMPACT OF COVID-19 PANDEMIC ON URBAN TRANSPORTATION AND AIR QUALITY IN CANADA

4.1. Background

The global outbreak and spread of COVID-19 have brought serious threat to public health and major disruption to global economic activities. The impact on global supply chains and trade lasted for a long time, which also caused the anxiety not only in public health environment but also in global economic growth (Smith et al., 2020; Wang and Su, 2020). During this pandemic, different levels of restrictions on the movement of people in various countries also had significant impact on daily life (Fernandes, 2020). With the downturn in economy and reductions in daily travel caused by COVID-19, there was the reduced environmental pollutant emission, which could be "a blessing in disguise" (Muhammad et al., 2020).

It was found that the daily global CO_2 emissions decreased during the pandemic (Le Quéré et al., 2020). Zambrano-Monserrate et al. (2020) analyzed the indirect effect of COVID-19 on the air quality, beaches and environmental noise reduction, especially in China, USA, Italy and Spain. Bauwens et al. (2020) compared the dynamic changes in NO_2 concentration level over China, South Korea, western Europe and the United States during the coronavirus disease outbreak based on data from the spaceborne NO_2 column observations. In addition, the changes in air pollution at different cities during the epidemic were reported (Dai et al., 2020; Wang et al., 2020). In terms of the changes in urban vehicle emissions, Xiang et al. (2020a) evaluated the impact of this pandemic on the traffic-related air pollution in downtown of Seattle, and compared the median traffic volume, road occupancy and the pollutants before and after lockdown. Tanzer-Gruener et al. (2020) compared concentrations of PM2.5, CO and NO_2 between closure and business-as-usual periods in Pittsburgh.

From the perspective of energy consumption and emissions, the impact of unexpected

disaster on energy consumption was studied previously. For example, Taghizadeh-Hesary et al. (2017) compared the elasticity of oil consumption with crude oil price before and after the Fukushima Daiichi nuclear disaster. During the present pandemic, fuel demand and oil price plummeted in April 2020. Ou et al. (2020) incorporated the pandemic scenarios and the trip activities for projecting future fuel usage in the United State based on a machine-learning-model. In a global scale, fossil fuel consumption and CO_2 emissions are expected to return to pre-crisis levels in a two-year extent (Alberta Capital Airshed, 2020; Smith et al., 2020).

Although there were some studies about the impact of COVID-19 on environmental problems, the relation between this pandemic and urban air pollution is still not clear. This study aims to provide a new insight into the urban air pollutant emission of representative Canadian cities impacted by the pandemic. The consumption of urban transportation fuel will be analyzed and the corresponding CO_2 emissions will be evaluated. The changes in urban traffic volume and air pollutant concentrations before and after the outbreak of this pandemic will be investigated.

4.2. Methods

4.2.1. Study area

The COVID-19 virus in Canada was firstly reported in January 2020 and then the community transmission was confirmed in mid-March 2020, followed by the states of emergency in all Canadian provinces. In summer, the new cases steadily declined across the country, while the whole country experienced a resurgence of cases in autumn. The long-lasting pandemic had a significant impact on the environment of urban areas in Canada. In order to investigate the impact of the COVID-19 pandemic on urban transportation and air quality, some representative cities including Vancouver in British Columbia, Edmonton in Alberta, Saskatoon in Saskatchewan, Winnipeg in Manitoba, Toronto in Ontario, Montréal in Quebec, Halifax in Nova Scotia and St. John’s in Newfoundland and Labrador, were chosen. Considering the time when different cities

declared the state of emergency and relaunch strategy, the time frame in this research was from February to September, 2020.

The changes of air quality in different provinces of Canada were studied. Figure 25 shows the overall emissions of SOx, NOx and CO in British Columbia, Alberta, Saskatchewan, Manitoba, Ontario, Montréal, Nova Scotia and Newfoundland and Labrador in 1990 and 2017 (Environment and Climate Change Canada, 2019a). In 2017, Ontario and Alberta accounted for 44% of national SO_X emissions. Between 1990 and 2017, Ontario experienced the largest reduction and SO_X emissions decreased by 84%, while the only increase (24%) was observed in Saskatchewan (Chen et al., 2020b). The reduction in SO_X emissions in Ontario from 1990 to 2017 was mainly due to the technological upgrades and new air pollution control measures for the non-ferrous smelting and refining industry. For example, the closure of major smelter and the phase-out of coal electricity generation in Ontario both resulted in the decrease in SO_X emissions. The increasing electric utilities has become the most important source of emissions in Saskatchewan (Environment and Climate Change Canada, 2019b). In terms of NO_X emissions, Alberta accounted for 36% of national emissions which wat the highest NO_X emission among provinces in 2017. The most important source of NO_X emissions in Alberta was the oil and gas industry, accounting for 59% of the province's NO_X emissions in 2017. In recent years, the reduction in NO_X emissions from transportation and electric utilities sectors has been offset by the continuous increase in emissions from the oil and gas industry sector (Environment and Climate Change Canada, 2019a). Therefore, NO_X emissions in Alberta have been ranking first for many years in Canada. Ontario ranked the second largest proportion of NO_X emissions in 2017, accounting for 17% of the country's total emissions. Transportation, including roads, rail, aviation and marine, was the most important source, followed by off-road vehicles and mobile equipment. However, the NO_X emissions in Ontario decreased by 52% from 1990 to 2017 as a result of emission reductions from transportation, electric utilities, off-road vehicles and mobile equipment. In addition to NO_X emissions, CO emission reduction from transportation was also a main factor attributing to significant decrease in CO emissions between 1990 and 2017 in these eight provinces. During this period, the larger reductions of 69%, 61%, and 42% took place in British Columbia, Ontario, and Quebec, respectively.

CO emissions was mainly from the home firewood burning in Quebec and from the transportation (road, rail, air and marine) in Ontario.

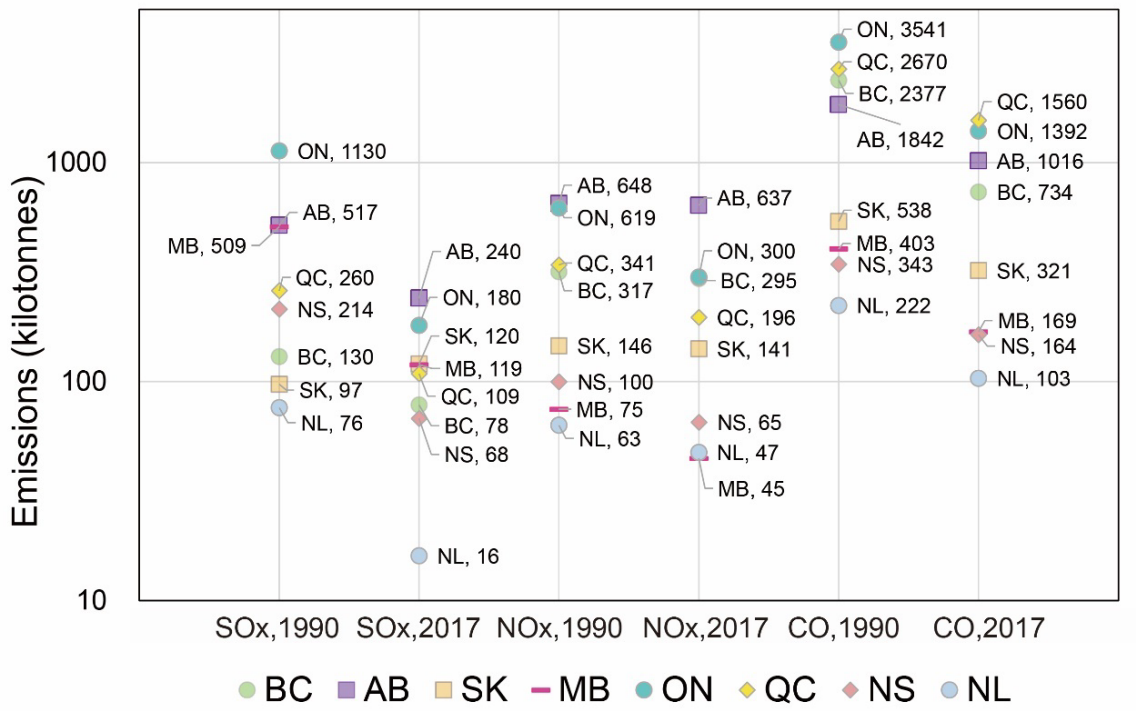

Figure 25. Ranking of SOx emissions, NOx emissions and CO emissions by province, Canada, 1990 and 2017 (Environment and Climate Change Canada, 2019a)

4.2.2. Data sources and processing

The air quality data of eight cities from February to August in 2018, 2019 and 2020 were collected. The hourly pollutant concentrations monitored on each day was used to calculate the corresponding monthly average levels. The pollution data in Vancouver, British Columbia were taken from Robson Square monitoring station (B.C. Air Quality Data, 2020). The air quality data in Edmonton, Alberta were accessed from both Alberta Air Data Warehouse and Alberta Capital Airshed (ACA) (Alberta Capital Airshed, 2020; Government of Alverta, 2020). The data were from the core long term program in Central station and McCauley station of Edmonton. The real-time and historic air quality data in Saskatoon, Saskatchewan was from the National Air Pollution Surveillance (NAPS) network on the Air Quality Index (AQI) website (Government of Saskatchewan, 2020).

The monitoring station in Winnipeg, Manitoba was on the Ellen Street which was close to downtown area. In Ontario, the station chosen for O_3 and NO_2 data was Toronto Downton station. Due to the lack of data in Toronto Downton station, the Toronto West station was chosen for the supplementary data of CO. The website didn't provide the daily average data of air quality and thus the hourly data was collected and calculated to get the daily average data. The station chosen in Montréal, Quebec was Station 31 St-Dominique located in downtown area. The station chosen in Nova Scotia was the Halifax station located in Johnston Building (Nova Scotia Environment, 2020). The air monitoring sites located in St. John's, Newfoundland and Labrador was one of the NAPS stations (Environment and Climate Change Canada, 1969; Government of Newfoundland and Labrador, 2020). The Air Quality Health Index (AQHI) monthly data from February to September in 2019 and 2020 were collected. Due to the lack of historical data in Montréal, the representative cities including Vancouver, Edmonton, Saskatoon, Winnipeg, Toronto, Halifax and St. John's were chosen for the comparison of AQHI (Environment and Climate Change Canada, 2019c).

The consumptions of domestic motor gasoline in different months were from a monthly cross-sectional designed survey which collected data on the activities of all Canadian refineries and oil sands processing plants involved in the production of refined petroleum products and of selected major blending terminals of these products (Statistics Canada, 2020b). The level of average traffic congestion in different cities was a representation of traffic volume in this study. The traffic index data was obtained from TOMTOM (2020), covering six cities in Canada, namely Vancouver, Edmonton, Winnipeg, Toronto, Montréal and Halifax. The baseline was calculated per city by analyzing free-flow travel times of all vehicles on the entire road network which was recorded 24 hours a day and 365 days a year. The whole data source came from 600 million drivers around the world who used their tech in navigation devices, in-dash systems and smartphones. The satellite imagery of averaged NO_2 concentrations were collected on an online platform which used data from the Copernicus Sentinel-5P satellite (European Commission & European Space Agency, 2020). These satellite maps show the concentration of NO_2 in the lowest kilometers of the atmosphere. The changes and trends of concentrations can be better presented by this 14-

day moving average than shorter time periods because the average of concentrations gives an overview over the whole time period. LabelMe (MIT, US) was used first to outline the administrative boundaries of Vancouver and Toronto by continuous points in the scene of the NO_2 satellite images. The coordinates of points associated with the boundaries were saved and overlaid on top of NO_2 satellite images. Then the MATLAB (Mathworks, US) was used to segment the images under three different threshold levels and calculate the pixels of each threshold in the whole city. The percentage of the pixels with NO_2 concentration higher than thresholds to the pixels of the whole city were calculated.

4.3. Results and discussion

4.3.1. Situation of COVID-19 in Canada

As of October 9, 2020, there have been 178117 confirmed COVID-19 cases and 9585 deaths in Canada. Most COVID-19 cases in Canada are in Ontario and Quebec, which are two most populous provinces. After the first case of community transmission confirmed in British Columbia, all provinces in Canada declared state of emergency in mid-March and prohibited gathering with varying degrees. The emergency orders included the closure of non-essential workplaces, outdoor amenities in parks and recreational areas and public places. Residents were encouraged to stay at home and keep social distance when going out. These emergency orders allowed provinces to ban gathering and different provinces have their own gathering banned policies. For example, on March 12, Quebec required banning gatherings of 10 people in a private location and 250 people in a public location. Soon after, on March 17, Ontario had their banning gatherings of 50 people indoors and over 100 people outdoors. This pandemic had a deep impact on the Canadian economy. For the economic recovery, gradual and stage-by-stage approaches to loosen emergency measures were put in place in different provinces in May 2020. The total cases in each province on the first of each month were counted as logarithmic numbers in Figure 26. Quebec, Ontario and British Columbia had 1, 15 and 8 COVID-19 cases on the first of March, representatively. There was zero COVID-19 case on the first of March in Alberta, Saskatchewan, Manitoba, Nova Scotia and Newfoundland and Labrador. As a result, in

Figure 26, the curves of Quebec, Ontario and British Columbia start from March and the rest curves of other provinces start from April.

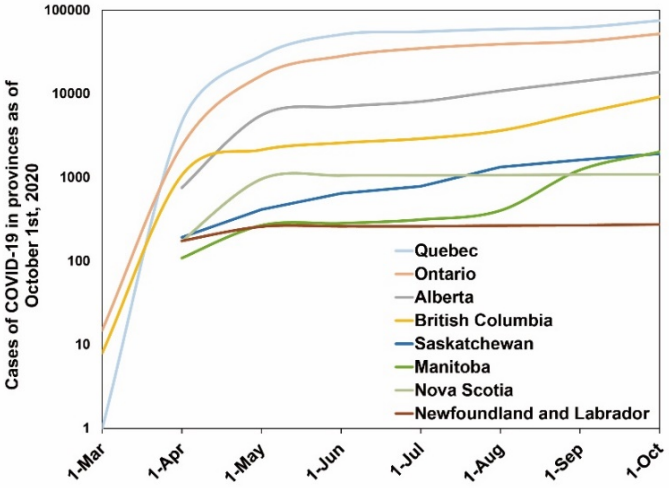

Province	State of emergency declared	Reopening in stage 1
Quebec	2020/3/12	2020/5/11
Ontario	2020/3/17	2020/5/8
Alberta	2020/3/17	2020/5/14
British Columbia	2020/3/18	2020/5/16
Saskatchewan	2020/3/18	2020/5/4
Manitoba	2020/3/20	2020/5/4
Nova Scotia	2020/3/22	2020/5/1
Newfoundland and Labrador	2020/3/18	2020/5/11

Figure 26. Cases of COVID-19 in eight provinces as of October 1st, 2020 and policies related COVID-19 declared by provincial and territorial governments (Government of Canada, 2020b)

4.3.2. Changes in domestic consumption of transportation fuels

Due to the global lockdowns caused by the COVID-19 pandemic, the demand and consumption of fuel have plummeted since March 2020. It has become the most severe plunge in energy consumption since the Second World War which has been on pace to trigger multi-decade lows for the world's consumption of oil, gas and coal (Bakx, 2020). During this period, several studies have assessed the impact of COVID-19 on fossil fuel consumption. Güngör et al. (2020) collected the daily gasoline consumption data during 2014 to 2020 and forecasted the effects of COVID-19 pandemic on Turkish gasoline market. In their estimation, there was 0.8% difference compared with the actual gasoline consumption data before the COVID-19 outbreak while there was approximately 30% difference after the COVID-19 outbreak. Ou et al. (2020) quantified and forecasted the US demands of motor gasoline in varying pandemic scenarios. Under the optimistic scenario, the projected motor gasoline demand was about 98% of the demand compared with the non-pandemic scenario in late September 2020. The projected proportion number under

the pessimistic scenario was about 78% of the demand under the non-pandemic scenario. From global scale, Smith et al. (2020) assessed the impact of COVID-19 on coal, natural gas and oil consumption and estimated CO_2 emissions worldwide over a two-year range. The samples were divided into advanced economics like Canada and European Union (EU) countries and emerging economies like China and Mexico. The EU countries appeared to be impacted most than the advanced group and emerging economies due to the spread of COVID-10, displaying significant negative drops in oil and natural gas consumption. Only the top three populous metropolitans in Canada were included. Therefore, a comparison of transportation fuel consumption indifferent provinces during pandemic in Canada was included in this research to know how the outbreak of COVID-19 impacted the demand for fossil fuels.

Figure 27 shows the monthly consumption of transportation fuels, namely motor gasoline, diesel fuel and kerosene-type jet fuel, in Canada from February 2019 to June, 2020 (Statistics Canada, 2020a, b). The domestic consumption of each petroleum product was calculated as production plus imports minus the sum of stock change, inputs and exports. All three types of transportation fuels decreased from February to March 2020 and remained at historically low levels in April 2020. Since December 2019, the domestic consumption of motor gasoline has been continued downward. In April 2020, it fell 44.4% while the consumption of diesel fuel oil was down 20.5% compared with 2019 (Statistics Canada, 2020b). The demand for transportation fuels remained low in June 2020. The domestic consumption of motor gasoline in June 2020 fell 14.5% compared with June 2019, and diesel fuel oil was down 9.6% as well. The demand for transportation fuels remained low in June 2020 compared with the same period in 2019. Although overall refining activity increased from May to June in 2020 along with economies reopening, it would still take long time to recover to pre-pandemic levels.

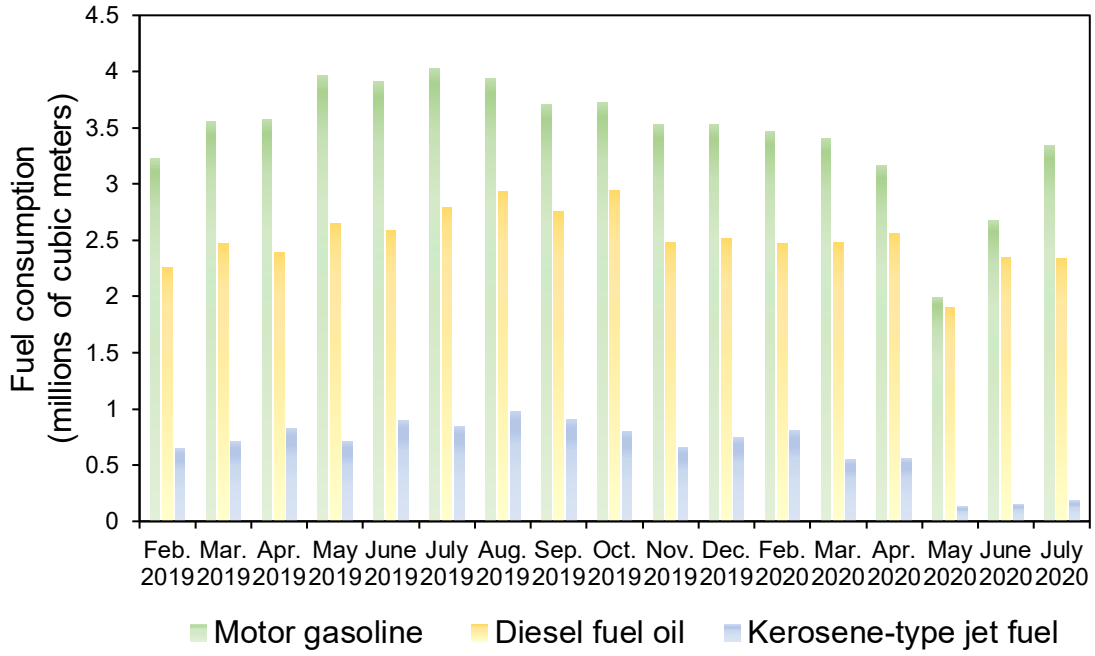

Figure 27. Domestic consumption of motor gasoline, diesel fuel and kerosene-type jet fuel in Canada, monthly (Statistics Canada, 2020a, b).

In the first quarter of 2020, there was a 57% decrease in global oil demand from mobiles compared with the same period in 2019, which was the consequence of lockdown measures globally. During the confinement period, the gasoline demand was declined by 70% in both France and the United Kingdom. The decline for road gasoline consumption in Canada is less than that for the world as well as other developed countries (International Energy Agency, 2020a). In 2017, the vehicles in Canada have the highest fuel consumption and CO_2 emissions with an average consumption of 8.9 litres of gasoline per 100 kilometers driven (L/100 km) and a value of 206 grams per kilometer, respectively. For other developed countries, the fuel consumption averaged 8.6 L/100 km in the United States, 5.9 L/100 km in Germany and 4.9 L/100 km in Portugal (International Energy Agency, 2019a). Canadians are much more dependent on vehicles than many other countries and less fuel-efficient vehicles such as SUV and trucks are often preferred in Canada. In 2017, trucks, which gradually became the preferred vehicle choice of Canadians, even accounted for 70% of newly registered vehicles in Canada (Canada Energy Regulator, 2019). Such vehicle preference is also one of the main reasons for the higher average fuel economy in

Canada. The current study presents the impact of this pandemic on the cities with high fuel-economy vehicles. The air pollution and emissions from vehicles can be further reduced by strengthening green stimulus policies in adjusting vehicle purchase and promoting the fuel-efficient vehicles (Ji et al., 2020).

4.3.3. Changes in urban traffic volume

The reduction in traffic volume impacted by this pandemic has been seen in cities all over the world. The effect of self-isolation, social distancing, and the shuttering of shops, restaurants and offices from the pandemic could be seen in the traffic data (Parr et al., 2020). The condition of traffic flows also has the relation with air pollutant emission (Sadullah et al., 2003). In Canada, there was a slow downward trend followed by a large and fairly sudden drop in traffic congestion. In the present study, the average congestion condition was used to represent the traffic volume of urban transportation. The levels of daily and weekly congestion were calculated based on the hourly data, with each week starting from Monday and ending on Sunday in this data collection (TOMTOM, 2020). The daily and weekly standard congestion levels were considered. The cut-off date in this research is the end of August 2020 which is also the week 35 in the figure.

Figure 28 shows the average congestion level of Vancouver, Edmonton, Winnipeg, Toronto, Montréal and Halifax in 2020 and the relative difference of average congestion levels in 2020 from corresponding standard congestion levels in 2019. In Vancouver, the peak rush-hour congestion decreased 54% compared to the average weekday rush hour in week 12, which was the start of COVID-19 restrictions. Compared with the other five cities, the trend of decline during restriction and the trend of recovery during reopening period in Vancouver was relatively moderate. In week 12, the traffic congestion level decreased 69% and 75% in Toronto and Montréal, respectively, compared with 2019. In the first week after the restriction policy declared in Toronto, the traffic congestion level dropped significantly, while in Montréal, the congestion was reduced 32% in the first week and dropped significantly until the second week. During the pandemic period, the traffic congestion level in Edmonton showed the largest drop of 71% in week 15, while the

congestion level in week 35 was 35% less than standard weekly level in 2019. The impact on traffic from this pandemic in Winnipeg was the smallest among these six cities, with the lowest decrease of 60%. Toronto and Halifax are the only two cities in which the traffic congestion levels began to decline before week 12 compared to 2019. After the opening policy was announced, the traffic congestion in Halifax has returned to levels before the pandemic on the Friday of week 35. Among these six cities, Montréal and Halifax are the top two cities where traffic volume levels have the fastest recovery after the reopening. As of week 35, the congestion level declined by 25% in Montréal and 27% in Halifax compared with the standard weekly congestion level in 2019. Although it can be seen that the traffic volume was gradually recovering, the change for the remaining time of the year will be contingent on the duration and extent of the restriction (Le Quéré et al., 2020)

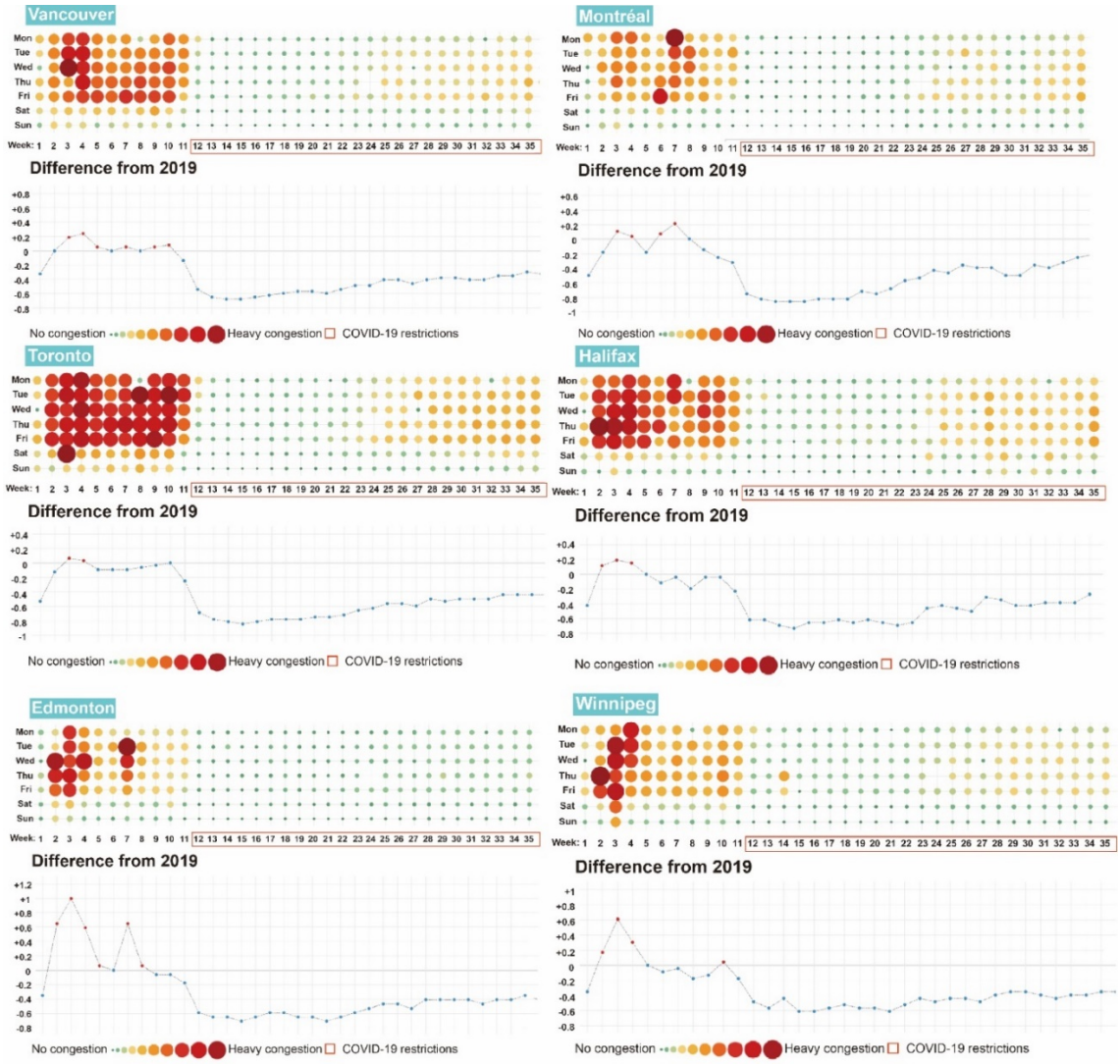

Figure 28. Average congestion level in 2020 and the relative difference of average congestion levels in 2020 from standard congestion levels in 2019 in Vancouver, Edmonton, Winnipeg, Toronto, Montréal and Halifax.

4.3.4. Changes in CO_2 emissions from vehicle fuel consumption

Vehicle emissions can be estimated and calculated according to either the fuel consumed or the distance travelled by the vehicles. Generally, the first approach represented by fuel consumption is appropriate for the estimation of CO_2 emissions (Eggleston et al., 2006b). The Tier 1 approach recommended by Intergovernmental Panel on Climate Change (Eggleston et al., 2006b) as used to calculate the CO_2 emissions based on the domestic

consumption of motor gasoline with a CO_2 emission factor. The calculation of CO_2 emission for fuel consumption is shown in Equation 9.

$$Emission = \sum_{a} [Fuel_a * EF_a] \quad (9)$$

where *Emission* is the total emission of CO_2 (kg); $Fuel_a$ is the fuel sold (L); EF_a is the emission factor for refined petroleum products (kg/L); a is the type of fuel. The CO_2 emission factors are mainly influenced by the fuel properties, followed by combustion technology. To ensure consistency with the guidelines from IPCC in 2006, Environment and Climate Change Canada (2016) directed and developed the value of the major class of refined petroleum products using data provided by industry to the Canadian Industrial Energy End-Use Data Analysis Centre (CIEEDAC).

Figure 29 presents an estimation of the CO_2 emissions from the motor gasoline consumption from February 2019 to June 2020 in Canada. There was a significant drop in estimated CO_2 emissions from 7,303.73 million kg in March to 4,593.01 million kg in April in 2020 due to the lockdown in different provinces. The estimated CO_2 from motor gasoline consumption in April 2019 is 8,253.52 million kilograms, which is almost twice that in April 2020. With the implementation of reopening policy, CO_2 emissions gradually rebounded in May 2020. Different from previous economic crises, the economic critical stage concomitant by COVID-19 was more deeply anchored in constrained individual behavior. At present, even though the emissions level rebounded, it is still unclear how the second wave of COVID-19 in Canada will affect CO_2 emissions. Being aware of changing emission levels can be helpful for the government to determine the future emissions trajectories in carbon-intensive pathways through the post-pandemic period (Feng et al., 2020; Le Quéré et al., 2020).

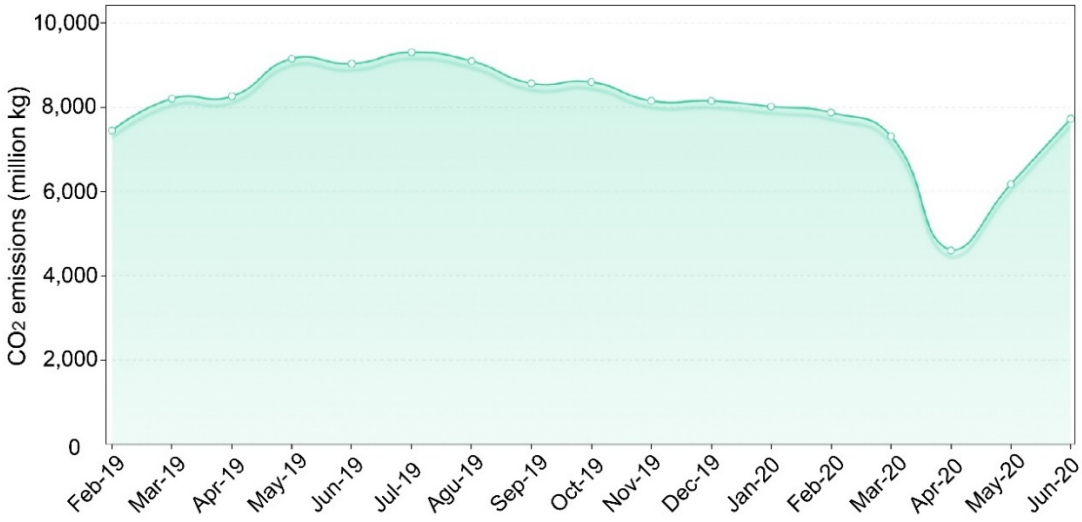

Figure 29. Estimated CO_2 emission from the motor gasoline consumption from February 2019 to June 2020 in Canada, monthly.

4.3.5. Changes in urban air pollution indicators——NO_2 concentration

Most NO_2 emissions come from burning of fossil fuels, especially from vehicles. In 2018, about 51% of NO_x emission derived from the transportation mobile equipment in Canada (Environment and Climate Change Canada, 2020a). The COVID-19 restriction could result in the change of average NO_2 concentration. It was found the NO_2 concentration in cities of China deceased 40% compared with the same period in 2019. Similar decrease (20% to 38%) was also observed in western Europe and the United States (Xiang et al., 2020b). However, , the monitoring results in Iran didn't show less emissions from vehicles (Bauwens et al., 2020). In this study, the NO_2 concentrations at the same time period in 2018, 2019 and 2020 were compared among eight cities in Canada and the results are shown in Fig. 6. It can be seen these cities experienced NO_2 decreases in 2020 compared with the same period in 2019 and 2018 except for Toronto and Winnipeg. During the period in 2020, the most significant change was in Edmonton with a 78.6% decline from February to July. Although the date of emergency declared in Toronto was earlier than that of other cities apart from Montréal, Toronto was the only city that had consistently exceeded pollution levels from April to June. From February to August in 2020, Vancouver, Edmonton and St. John's were the cities with NO_2 concentration level not exceeding the

previous two years. British Columbia had good pandemic control since the outbreak. Among the most populous provinces with serious pandemic, the changes in the level of pollutant concentrations can also reflect the level of public health and control measures in different regions.

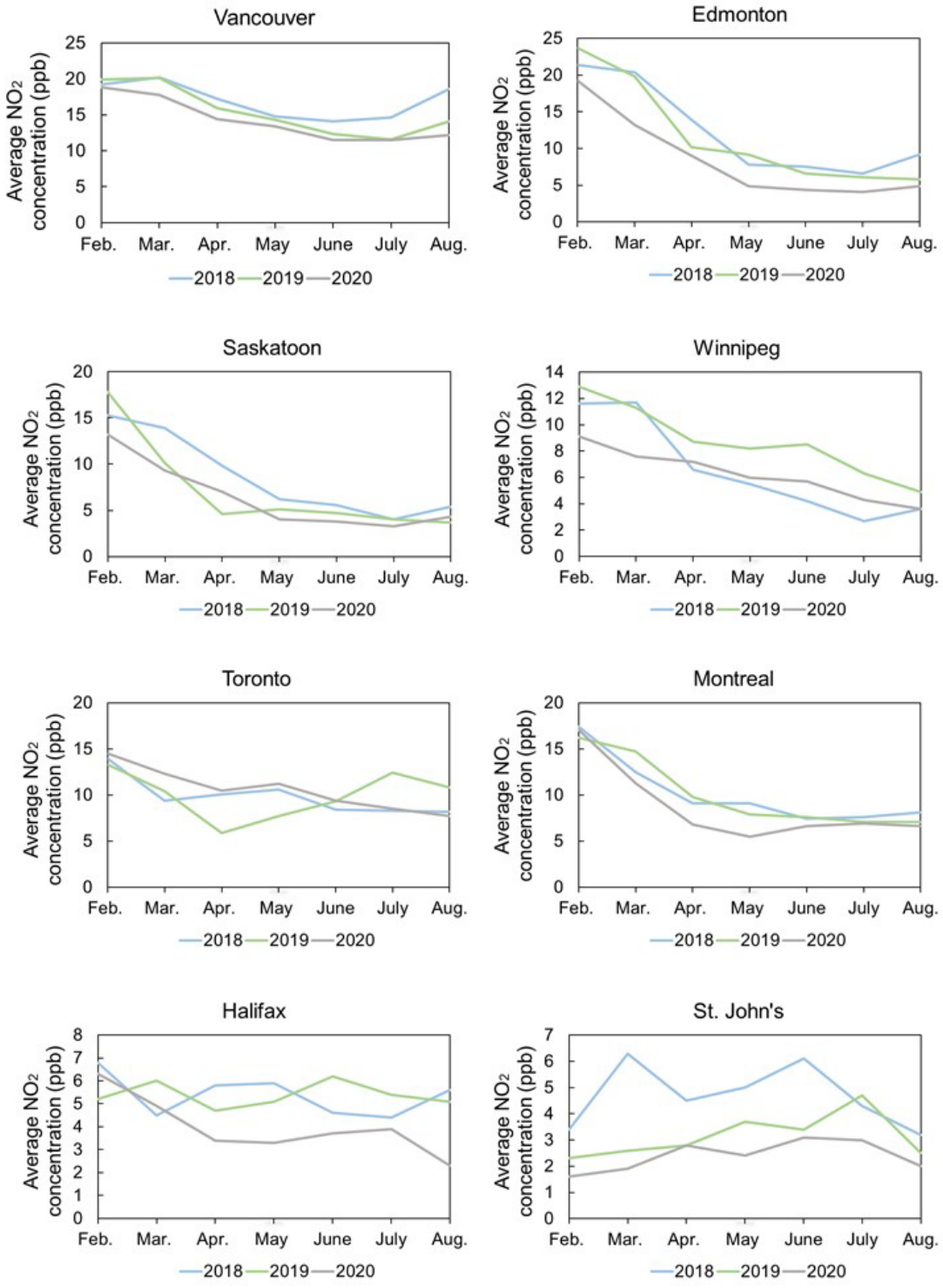

Figure 30. Change in average NO_2 concentration from February to August in 2018, 2019 and 2020 (ppb)

4.3.6. Spatial–temporal variation of NO_2 concentration

The maps based on the data from the Copernicus Sentinel-5P satellite of European Space Agency (ESA) can show a 14-day average NO_2 concentration across Canada (European Commission & European Space Agency, 2020). The variations of air pollutants such as NO_2 are not only the manifestation of changes in emissions, but also the indicators of economic and urban development (Ye et al., 2020). In Figure 31, the satellite images of four cities, Vancouver, Edmonton, Toronto and Montréal, are presented. The satellite images showing the amount of NO_2 from March to June in 2019 and 2020 in four cities were compared. The average levels of atmospheric NO_2 in these major Canadian cities and their surrounding areas have plummeted during this pandemic compared to a year ago. Since The change in NO_2 concentration is consistent in these four cities. In April, the month after the emergency declared, the concentrations of pollutants in these cities of Canada have decreased to a certain extent. As there was a gradual control for the pandemic and a need for economy recovery, the stage-by-stage reopening was put on the agenda in May in different cities. The NO_2 concentration level had a certain degree of rebound after July 2020. In fact, it can be seen that the effect of short-term quarantine in reducing air pollution was significant, but could be only temporary (Yang, 2019).

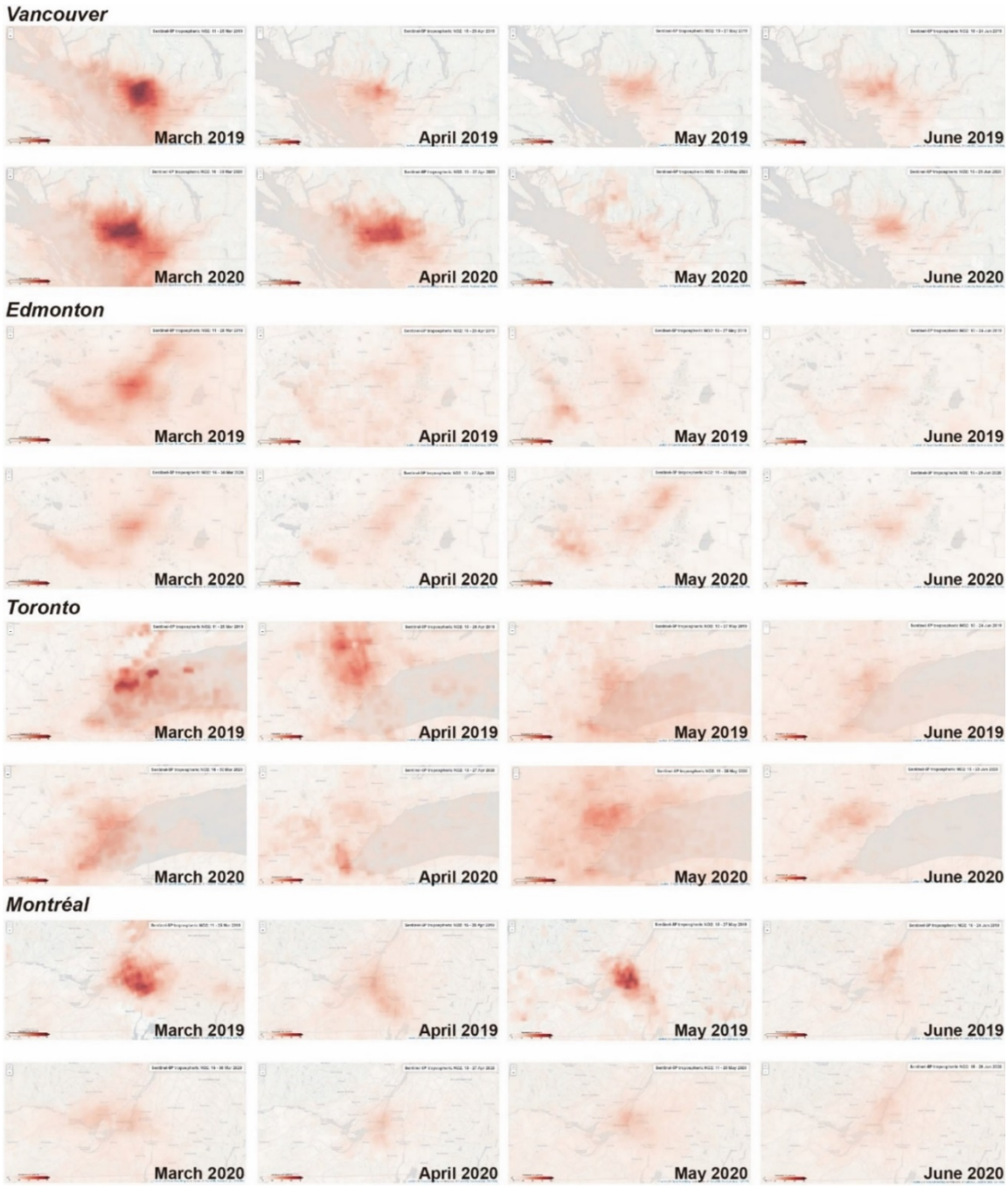

Figure 31. Changes in NO_2 emission levels in representative cities in Canada (European Commission & European Space Agency, 2020)

In order to better reveal the changes of NO_2 concentration in the urban areas, the image binarization was conducted for further analysis based on the satellite images in Figure 31. Image binarization is a thresholding method, which is a form of segmentation to divide the

image into constituent objects. In this study, the pollutant analysis based on image binarization could help analyze the area variation under different thresholds of NO_2 concentration. The concentration range of tropospheric NO_2 in the Copernicus Sentinel-5P satellite is from 0-180 μmol/m^2. 30, 50 and 70 μmol/m^2 were selected as the threshold levels. Vancouver and Toronto were chosen as the representative cities to compare the NO_2 changes from March to June in 2019 and 2020. Figure 32 to Figure 33 show the results of image binarization analysis. It can be seen for both Vancouver or Toronto from March to May in 2019, the above-threshold area percentage exhibits an overall downward trend. In April 2020, due to the start of emergency measures in Toronto, the above-threshold area ratios all dropped sharply. At the same time in Vancouver, due to the impact of wildfires, the above-threshold area ratio did not decrease even during the lockdown period. With the start of the first-stage reopening in Toronto, the areas above different NO_2 threshold concentrations rapidly expanded in May 2020 due to increasing travel and retaliatory consumption behaviors (Wang and Wang, 2020). However, in Vancouver, there was a continuous downward trend from May 2020.

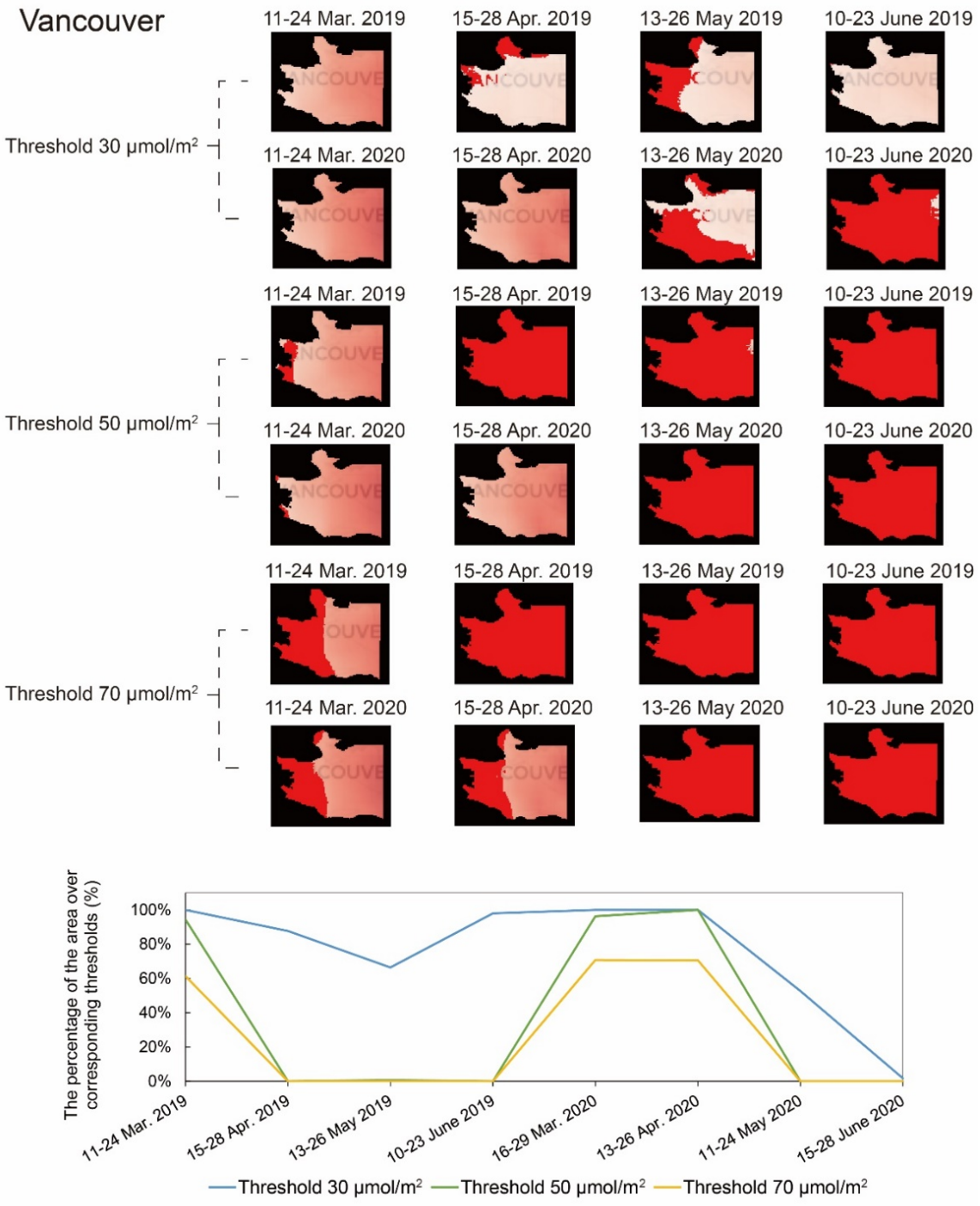

Figure 32. Area with NO_2 concentration and the percentage of aera over corresponding thresholds in Vancouver from March to June in 2019 and 2020 (the red area is the area with the NO_2 concentration less than corresponding threshold level and the remaining area is the area that meets the threshold with the NO_2 concentration higher than certain level.)

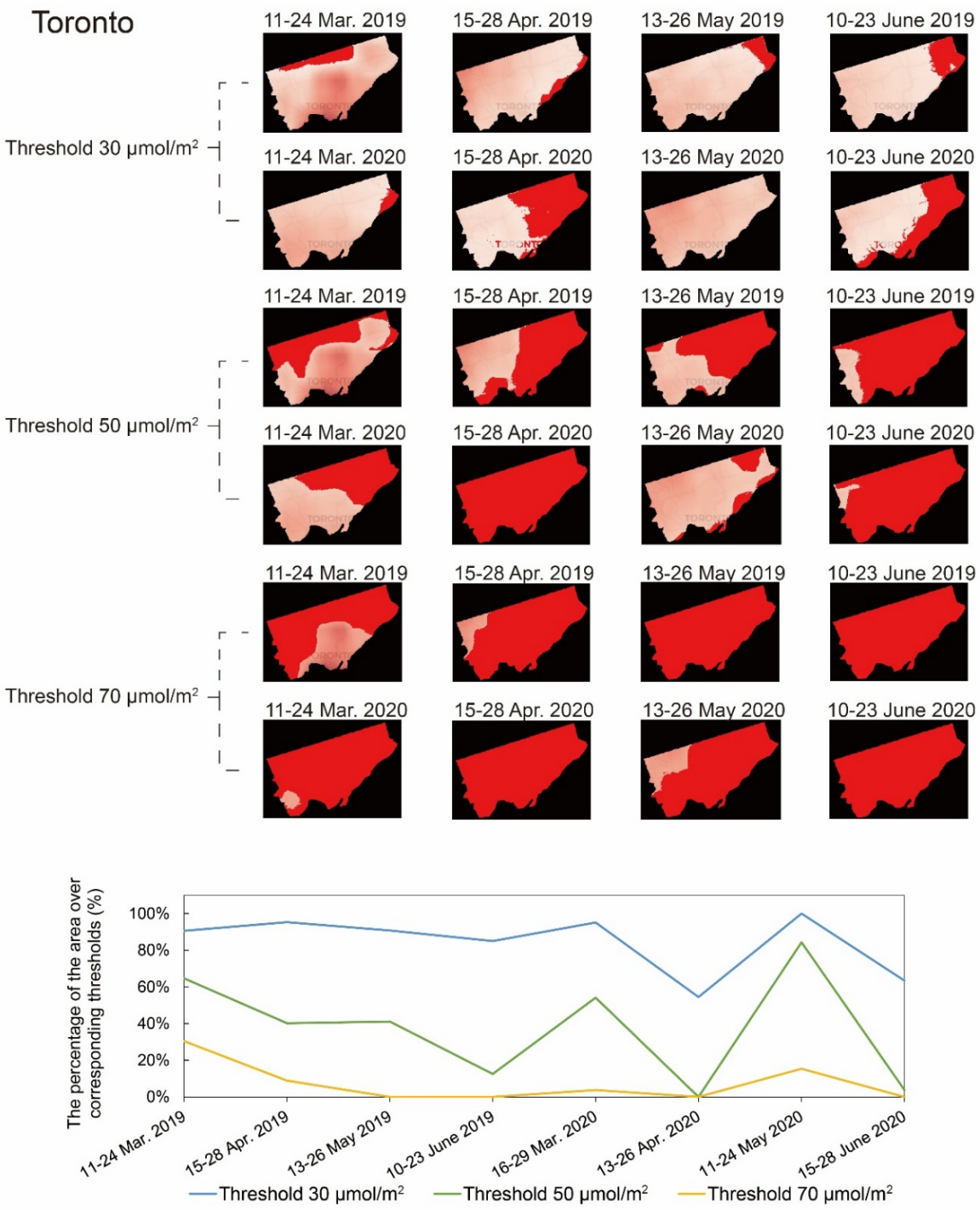

Figure 33. Area with NO_2 concentration and the percentage of aera over corresponding thresholds in Toronto from March to June in 2019 and 2020 (the red area is the area with the NO_2 concentration less than corresponding threshold level and the remaining area is the area that meets the threshold with the NO_2 concentration higher than certain level.)

4.3.7. Changes in urban air pollution indicators——CO concentration

CO in the air can enter the bloodstream and reduce oxygen delivery, which is the cause of fatal poisoning reported in many countries (Raub et al., 2000). In northern United States, the rate of accidental death resulted from CO emitted from motor vehicles is high in the northern and usually peaks in the winter (Ernst and Zibrak, 1998). Most CO is produced by the incomplete combustion of fossil fuels. Approximately 5.8 Mt of CO were emitted in Canada in 2018, which decreased by 54% compared with that in 1990. The Air Pollutant Emissions Inventory Report in 2020 in Canada (Environment and Climate Change Canada, 2020a) indicated that transportation and mobile equipment sector accounted for 56% of total CO emissions. Figure 34 presents the change in average CO concentration from February to August in 2018, 2019 and 2020 at Vancouver, Edmonton, Saskatoon, Toronto, Montréal and Halifax. Winnipeg and St. John's were not included due to the lack of monitoring data or negligible magnitude of CO concentration level. The line graphs were not shown for several months in Toronto due to the lack of monitoring data for CO concentration. The CO concentration level of six cities all decreased from March 2020. The average CO concentration in Edmonton dropped from 0.14 to 0.07 ppm in March from 2018 to 2020, with a highest decreasing ratio of 50% among these cities. From May to August, the average concentration in this city remained around 0.04 ppm. Different from other cities, the average CO concentration level in Toronto had a significant rebound from 0.10 ppm in April to 0.16 ppm in June 2020. Before the pandemic began, the average CO concentrations of Vancouver, Halifax and Edmonton in 2020 were significantly lower than those in 2018 and 2019. During the period of lockdown, the decrease of CO concentration in these three cities was much faster. Based on the analysis aforementioned, the traffic congestion in Halifax during the pandemic has been reduced compared with same period in previous years, while the changes in Vancouver fluctuated without a decreasing trend. It indicated that the CO concentration in Halifax was more affected by residents' travel while Vancouver did not.

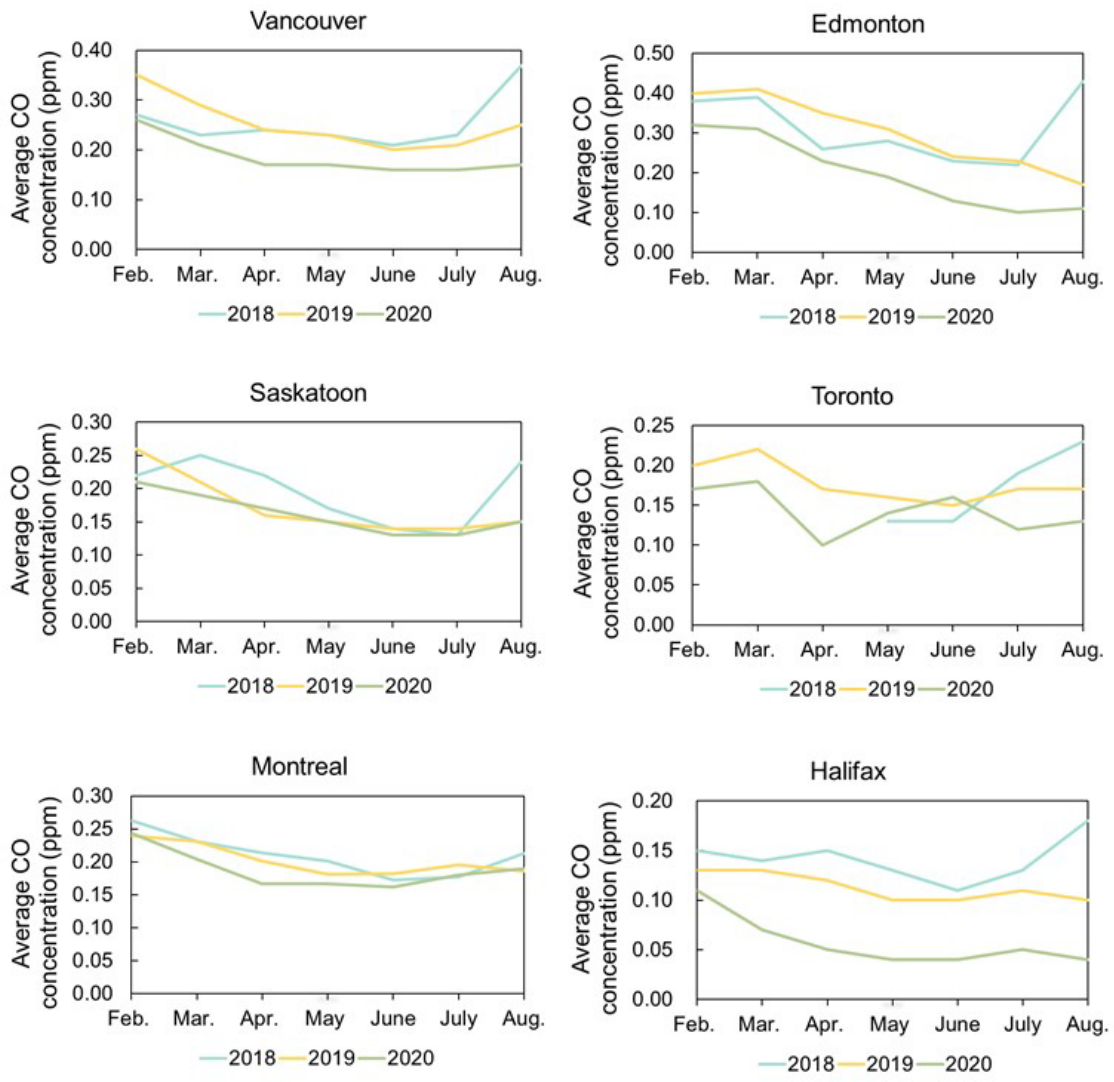

Figure 34. Change in average CO concentration from February to August in 2018, 2019 and 2020 (ppm)

4.3.8. Changes in urban air pollution indicators——SO_2 concentration

The variation of SO_2 concentration in different Canadian cities are shown in Figure 35. Due to the limited data, only Vancouver, Edmonton, Toronto, Montréal and Halifax were included in this analysis. The Alberta Air Data Warehouse and Alberta Capital Airshed (ACA) lacks SO_2 concentration data in 2018 in Edmonton and thus only the data of 2019 and 2020 were collected. It can be seen that the impact of this pandemic on SO_2 concentration in each city was not significant. From 1990 to 2018, the whole SO_X

emissions in Canada decreased by 73%. Ore- mineral and oil-gas industries are two of the largest contributors, each accounting for 32% of total SO_X emissions in Canada (Environment and Climate Change Canada, 2020a). Smaller anthropogenic sources of SO_2 emissions involve locomotives, ships and vehicles with heavy equipment that burn fuel with a high sulfur content. The concentration changes from 2018 to 2020 in Figure 35 did not show clear correlation between SO_2 concentration and this pandemic.

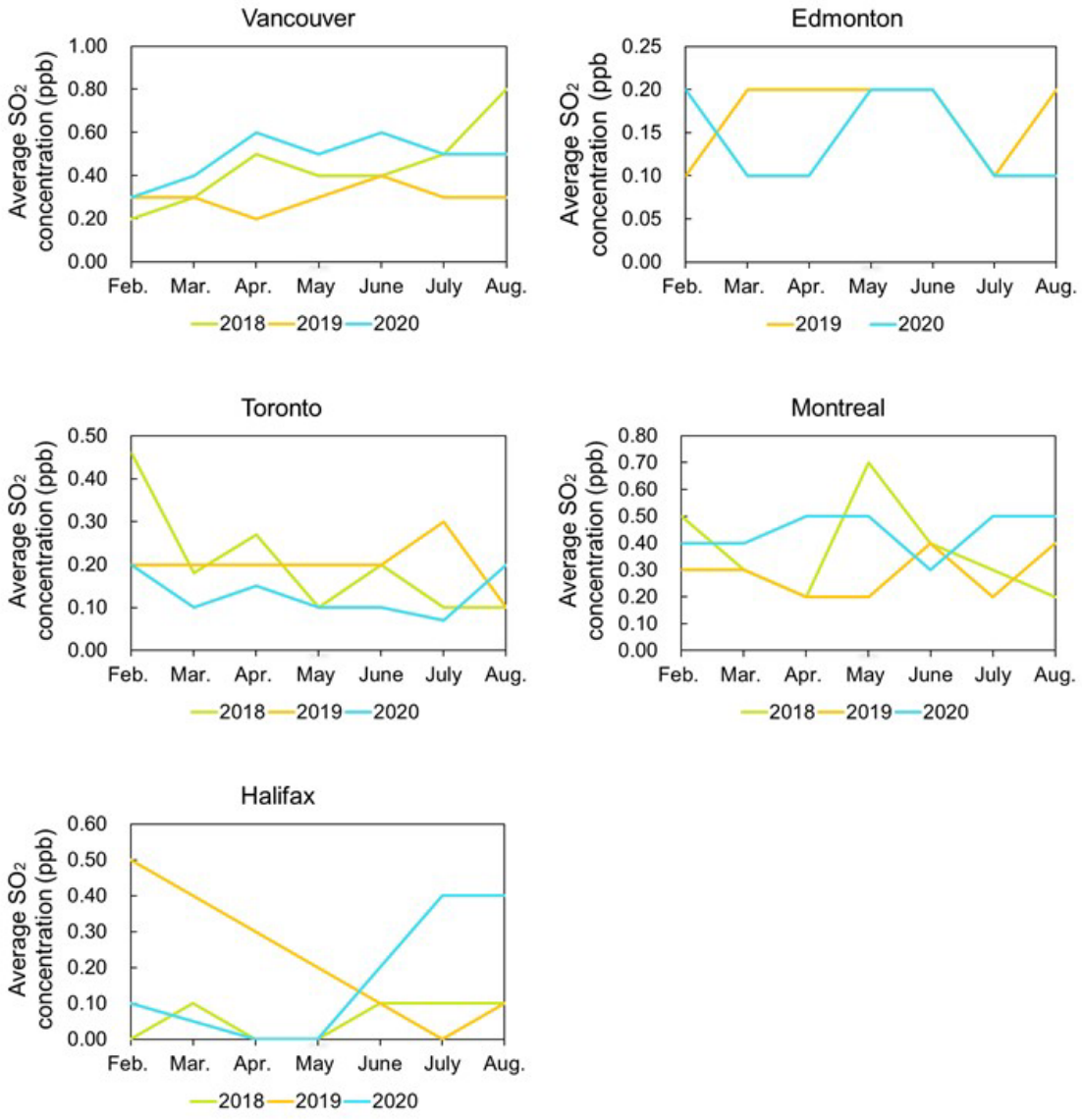

Figure 35. Change in average SO_2 concentration from February to August in 2018, 2019 and 2020 (ppb)

4.3.9. AQHI impacted by the pandemic

The AQHI is a scale designed to provide hourly air quality and related health information (Lerner et al., 2019). It is calculated based on a comprehensive consideration of various pollutants, including ozone at ground level, particulate matter and NO_2 (Xiao et al., 2020b). Different from the Air Quality Index (AQI) which communicates the air quality based on a single worst pollutant, the AQHI can reflect the health risk based on a mixture of pollutants associated with air pollution (Chen et al., 2013).The AQHI helps people to know the levels of air pollution in their surrounding environment on a scale ranging from 1-10+. The health risk associated with the air quality increases as the AQHI rises (Asif and Chen, 2020). There are four groups of the index reading which are low risk (1-3), moderate risk (4-6), high risk (7-10) and very high risk (10+). Figure 36 presents the AQHI from February to September in Vancouver, Edmonton, Saskatoon, Winnipeg, Toronto, Halifax and St. John's in 2019 and 2020. The AQHI of most cities declined to varying degrees after February 2020, except for Winnipeg and St. John's. Among these cities, Edmonton showed the largest decline which dropped from 3.7 in February to 2.4 in May. In Halifax, Edmonton, and Saskatoon, the AQHI during pandemic period in 2020 was lower than that in 2019.

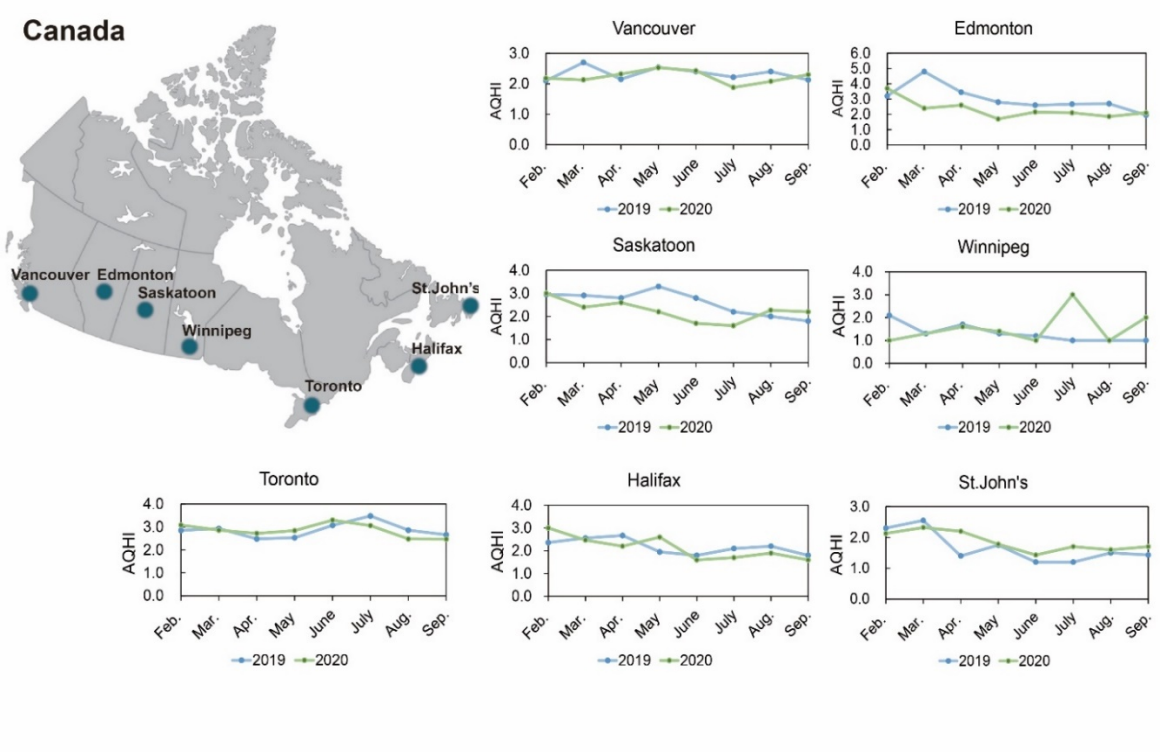

Figure 36. Comparison of Air Quality Health Index (AQHI) in representative cities of Canada in 2019 and 2020 (Environment and Climate Change Canada, 2019c)

4.4. Summary

This chapter proposed a new perspective regarding the dynamic impacts of the COVID-19 pandemic on the urban transportation and emission. Due to the lockdown after the outbreak of COVID-19, the domestic consumption of motor gasoline and estimated CO_2 emissions from urban vehicles in Canada has continuously decreased with a lowest level in April 2020, and rebounded in May 2020. Although the overall refining activity increased from May to June in 2020 along with reopening, it will still take a long time to recover to pre-pandemic levels duo to the upcoming second wave of pandemic and further change. The pandemic significantly reduced the traffic volume and congestion level in Vancouver, Edmonton, Winnipeg, Toronto and Montréal compared with the same period in 2019. The AQHI and concentration level of NO_2 and CO had strong relevance with the COVID-19 period while SO_2 did not show significant relation. The urban air quality throughout the country improved a lot during the pandemic period, which will be still unclear how the

rebound will be. It also indicates that emissions from urban vehicles account for a large proportion air pollutant emission in urban areas.

In the short term, the current improvement in these results is mainly brought about by the reduction in travel due to lockdown and remote working, but this is not a long-term panacea. The closed environment of public transportation has been identified as a high-risk environment for transmission, resulting in significant reductions in passenger traffic in Canada and elsewhere during the pandemic period. Public transit ridership down 75% compared to June 2019 in Canada. Meanwhile, the "remote working" caused by the COVID-19 will persist, and future transportation patterns are likely to be bifurcated: the recovery of personal travel modes such as the private car will be faster. It is expected to further promote the development of public transportation facilities and use the energy-saving and emission-reducing vehicles in these cities. Perhaps staggering commuting, controlling public transportation ridership, and reducing public transportation congestion should all be considered as part of the “new normal” transportation policy, in order to make “new normal” doable and maintain sustainable, which could better serve human life as well as meet the challenges of a changing environment (the “new normal” means a new and adjustable way of living and continuing our lives as long as the COVID-19 has not been defeated). This pandemic experience should make policy-makers recognize the importance of green and innovative transportation for resilient cities. We need to improve the whole systemic resilience of transportation systems in terms of infrastructure networks, cooperative transport system networks and the way urban transportation governance is organized. The comprehensive analysis of changing fuel consumptions, traffic volume and emission levels will help the government assess the impact and make corresponding strategy for such a pandemic in the future.

CHAPTER 5. ASSESSMENT OF REDUCTIONS IN NO_2 EMISSIONS FROM THERMAL POWER PLANTS IN CANADA BASED ON THE ANALYSIS OF POLICY, INVENTORY, AND SATELLITE DATA

5.1. Background

Emission of nitrogen oxides (NO_x) from power plants burning fossil fuel has broad effects on human health, atmospheric composition, acid deposition, air/water quality, and even the economy (Chui and Gao, 2010; Godowitch et al., 2008; Kim et al., 2006). In spite of the associated ill effects, NO_x emissions are continuing at concerning rates. For instance, Zhang et al. (2009) suggested that nearly 50% of the increase in NO_x emissions in China over time was attributable to new power plants constructed since the year 2000. It has been reported elsewhere that as much as 25% of NO_x emissions in the United States in 1999 was tied to electric power generation (Kim et al., 2006). In Europe, 24 of the countries that signed on to the European Commission Directive exceeded the NO_2 emission threshold specified in the directive in 2008. For the electricity sector in particular, as a resource- and environmentally-intensive industry, air pollution is an issue of critical concern. Amid global efforts to improve energy efficiency and achieve carbon-free energy generation in recent years, the United States saw an 87% drop in NO_x emissions from power plants between 1996 and 2020 (Environmental Protection and Agency, 2021). The NO_2 emission reduction ratio of the power plants after ultra-low emissions retrofitted in China ranged from 29.0% to 79.3% through the satellite data evaluation(Jiao et al., 2020). Most of the decline in emissions of key air pollutants from electricity generation facilities in Canada has occurred from 2005 onward. Compared with 1990 levels, NO_x emissions from these facilities had decreased by 50% by 2018 (Environment and Climate Change Canada, 2020b).

Recent studies have demonstrated that the short existing time of NO_x in the atmosphere made the emissions recorded in ground data at the emission source is closely correlated to the amount of NO_2 observed at a high spatial resolution in satellite imagery (Richter et al.,

2005). The satellite inversion of tropospheric NO_2 has been applied by many scholars for monitoring and tracing the interannual and geospatial variation, especially the emissions from anthropogenic activities such as coal-fired power generation (Jiao et al., 2020; Lu and Streets, 2012; Russell et al., 2010). Moreover, the emergence of remote sensing presents a novel approach for quantitative monitoring of emissions or empirical study of other ecological issues (Karimi et al., 2020; Tian et al., 2021; Xiao et al., 2020a). Apart from direct quantitative monitoring, many scholars have taken a combined approach comparing ground data with emission estimates based on satellite observation. For instance, an approach comparing satellite retrievals with emissions estimates from a bottom-up inventory has been used to double-measure the emission variation from power plants (Liu et al., 2018; Lu and Streets, 2012). More recently, satellite pollutant monitoring has been used to verify the effect of technologies and policies intended to control and reduce emissions from coal-fired power plants (Jiao et al., 2020; Wu et al., 2019). However, there is a lack of studies having used a combined (ground–satellite) approach to further process and validate the threshold changes on a smaller spatial scale. Meanwhile, satellite pollutant observation is also regarded as a supplementary information management tool that can be used to draw connections with national pollutant release inventory, showing thresholds or concentration trends for specific pollutants and a particular jurisdiction from both digital and visual perspectives (Danilina and Grigoriev, 2020; Tang and Mudd, 2014).

To assist in identifying the amount of point pollution sources and assess the air quality, the National Pollutant Release Inventory (NPRI) was enacted in Canada as an information management tool under federal administration (Walker, 2018). This NPRI program has been regarded as a success for having brought a reduction of 38% in official emissions in the first three years of its use (Harrison and Antweiler, 2003). For the study described in this paper, power plants representing five fuel types (biomass, coal, diesel, fuel oil, and natural gas) and spanning eight Canadian provinces were selected to analyze the effects of policies on NO_2 emission trends in the area surrounding the point source based on data from the NPRI and satellite inversion. As we describe below, the introduction of regulatory mechanisms and domestic and international agreements for emission reduction and the scaling back of coal-fired electricity generation have been the main factors in Canada's

progress in NO_2 emission reduction (Cuddihy et al., 2005). Our analysis began with the collection of quantitative data on energy consumption and energy intensity in a global context. Then, the trends of NO_2 emissions from Canada's fossil fuel-dependent electricity sector spanning the period 2008 to 2017 were analyzed. After that, the policies and incentives from international, federal, and provincial levels in Canada were assessed to explain the transition pathways. Third, to verify the performance of these policies and incentives, a comparison between annual NPRI NO_2 data and tropospheric vertical column densities (TVCDs) of NO_2 as recorded by an Ozone Monitoring Instrument (OMI) to identify which provinces most closely align was conducted. Five power plants—one from each of the identified provinces—were selected for the purpose of carrying out a NO_2 concentration threshold trend analysis within a 50 km radius. These results were deployed in a combined approach integrating the NPRI environmental management tool with satellite observation to verify changes in the amount of NO_2 in the area surrounding power plants. Meanwhile, the effect of the corresponding policies and incentives was explored, not only in terms of emission reduction, but also in terms of concentration thresholds.

5.2. Methods

5.2.1. Data preparation

Data from 97 power plants in the Canadian provinces of British Columbia (BC), Alberta (AB), Saskatchewan (SK), Ontario (ON), Quebec (QC), New Brunswick (NB), Nova Scotia (NS), and Newfoundland and Labrador (NL) were collected to analyze the trends of on-site NO_2 emission inventory from 2008 to 2017. The fuel types used at these power plants included biomass, coal, diesel, fuel oil, and natural gas. Information such as geographical location and the date a power plant was retired or will be retired was compiled. In the process of satellite inversion, a criterion was applied to rule out signals from nearby emission sources, hence the number of power plants under consideration was narrowed down from 97 to 41. The criterion was that the value of tropospheric NO_2 in one-pixel size must only reflect the target power plant within a given 13×13 km area. The information of the power plants is shown in Table 5 and Table 6.

Table 5. Information of 97 power plants

Facility	Address	Fuel type	Latitude	Longitude
Williams Lake Power Plant	Williams Lake, BC	Biomass	52.1608	-122.1724
Whitecourt Electric Power Generating Facility	Whitecourt, AB	Biomass	54.1624	-115.7339
Grand Prairie Cogen Power Plant	Grande Prairie, AB	Biomass	55.1602	-118.8184
Centrale de cogénération à la biomasse	Sherbrooke, QC	Biomass	45.4808	-71.9519
Société de Cogénération de St-Félicien	St-Félicien, QC	Biomass	48.6375	-72.4338
Centrale de Senneterre	Senneterre, QC	Biomass	48.3837	-77.223
Usine de cogénération de Chapais	Chapais, QC	Biomass	49.7709	-74.8562
Brooklyn Energy Centre	Brooklyn, NS	Biomass	44.0515	-64.6956
Sundance Thermal Electric Power Generating Plant	Duffield, AB	Coal	53.5085	-114.5571
Nanticoke Coal Generating Station (1973-2013)	Nanticoke, ON	Coal	42.7961	-80.05
Boundary Dam Coal Power Station	Estevan, SK	Coal	49.0961	-103.0305
Genesee Thermal Generating Station	Warburg, AB	Coal	53.344	-114.305
Poplar River Coal Power Station	Coronach, SK	Coal	49.0472	-105.4883
SHEERNESS GENERATING STATION	Hanna, AB	Coal	51.5317	-111.7861
Keephills Coal Power Plant Canada	Duffield, AB	Coal	53.4487	-114.4491
Battle River Generating Station	Forestburg, AB	Coal	52.5647	-112.1414
Trenton Coal Generating Station	Trenton, NS	Coal	45.6202	-62.6498
Belledune Coal Generating Station	Belledune, NB	Coal	47.9058	-65.867
Lambton Coal Generating Station (1969-2013)	Courtright, ON	Coal	42.7961	-82.4697
Lingan Coal Generating Station	Lingan, NS	Coal	46.2358	-60.0386

Shand Coal Power Station	Estevan, SK	Coal	49.0879	-102.864
Wabamun Coal Power Plant Canada (1956-2010)	Wabamun, AB	Coal	53.56	-114.4862
Dalhousie Generating Station	Dalhousie, NB	Coal	48.0519	-66.3702
Point Tupper Coal Generating Station	Port Hawkesbury, NS	Coal	45.5872	-61.3489
H.R.Milner Coal Generating Station Canada	Grande Cache, AB	Coal	54.0071	-119.104
Point Aconi Coal Generating Station	Halifax, NS	Coal	46.3225	-60.3039
Thunder Bay Generating Station (2018 decommission)	Thunder Bay, ON	Coal	48.3592	-89.2219
Atikokan Generating Station	Atikokan, ON	Coal	48.8361	-91.5656
Grand Lake Coal Generating Station	Newcastle Creek, NB	Coal	46.0572	-66.0051
Kirkland Lake Generating Station	Kirkland Lake, ON	Natural Gas	48.1347	-80.0425
Palisades Generating Station	Jasper National Park, AB	Natural Gas	52.9412	-118.043
Tunis Power Plant	Tunis, ON	Natural Gas	48.8704	-80.8942
Meridian Cogeneration Plant	Lloydminster, SK	Natural Gas	53.2593	-109.9512
Sarnia Regional Cogeneration Facility	Sarnia, ON	Natural Gas	42.9346	-82.4381
Cardinal Power of Canada, L.P.	Cardinal, ON	Natural Gas	44.7846	-75.3773
Electric Utility - Generation	Medicine Hat, AB	Natural Gas	50.0409	-110.7219
LAKE SUPERIOR OPERATIONS - SAULT STE MARIE	Sault Ste Marie, ON	Natural Gas	46.5183	-84.3626
Joffre Site; Cogeneration	Lacombe, AB	Natural Gas	52.3083	-113.55
Nipigon Power Plant	Nipigon, ON	Natural Gas	49.1512	-88.3418

Société en commandite Boralex énergie	Dolbeau-Mistassini, QC	Natural Gas	48.8794	-72.2166
Mississauga Cogeneration Plant	Mississauga, ON	Natural Gas	43.7016	-79.6433
Queen Elizabeth Power Station	Saskatoon, SK	Natural Gas	52.0944	-106.705
Cogénération Kingsey Falls	Kingsey Falls, QC	Natural Gas	45.8603	-72.0643
MacKay River Power Plant	Fort McMurray, AB	Natural Gas	57.0398	-111.9087
McMahon Cogen Plant	Taylor, BC	Natural Gas	56.1447	-120.6686
Rainbow Lake Generating Station (Units 4&5)	Rainbow Lake, AB	Natural Gas	58.4471	-119.2383
Cory Cogeneration Station	Saskatoon, SK	Natural Gas	52.0919	-106.8475
Ottawa Health Sciences Centre (OHSC) Cogeneration Facility	Ottawa, ON	Natural Gas	45.4032	-75.6541
Becancour Power Plant	Bécancour, QC	Natural Gas	46.368	-72.405
Scotford Complex	Fort Saskatchewan, AB	Natural Gas	53.7989	-113.0844
Cavalier Power Plant	Strathmore, AB	Natural Gas	51.0056	-113.1716
Cochrane Generating Station	Cochrane, ON	Natural Gas	49.0622	-81.0057
Hamilton Community Energy	Hamilton, ON	Natural Gas	43.2608	-79.8732
Sarnia Cogen	Sarnia, ON	Natural Gas	42.9586	-82.4146
Rainbow Lake Generating Station (Units 1, 2 & 3)	Rainbow Lake, AB	Natural Gas	58.4603	-115.2383
Iroquois Falls G.S.	Iroquois Falls, ON	Natural Gas	48.7696	-80.6669
West Windsor Power	Windsor, ON	Natural Gas	42.2807	-83.0876
Carseland Power Plant	Carseland, AB	Natural Gas	50.9012	-113.3928

Greenfield Energy Centre	Courtright, ON	Natural Gas	42.7683	-82.4542
Brighton Beach Power	Windsor, ON	Natural Gas	42.2798	-83.0946
Island Cogeneration No. 2 Inc.	Campbell River, BC	Natural Gas	50.069	-125.282
WHITBY COGENERATION L.P.	Whitby, ON	Natural Gas	43.8593	-78.9032
Gerald Parisien Energy Facility	Cornwall, ON	Natural Gas	45.0278	-74.727
Calgary Energy Centre	Calgary, AB	Natural Gas	51.1805	-113.9373
Brock University	St. Catharines, ON	Natural Gas	43.1192	-79.2483
Centrale de Cap-aux-Meules Power Plant	Cap-aux-Meules, les-de-la-Madeleine, QC	Diesel	47.3709	-61.8828
Nunavut Power Corp./Iqaluit?	Iqaluit, NU	Diesel	63.7537	-68.5071
Jackfish Plant	Yellowknife, NT	Diesel	62.469	-114.3809
Inuvik Plant	Inuvik, NT	Diesel	68.3554	-133.7271
Masset Diesel Generating Station	Masset, BC	Diesel	54.02	-132.1137
Cambridge Bay	Cambridge Bay, NU	Diesel	69.1157	-105.056
Rankin Inlet	Rankin Inlet, NU	Diesel	62.8126	-92.0806
Centrale d'Obedjiwan	Obedjiwan, QC	Diesel	48.6605	-74.9322
Centrale de Kuujjuaq	Kuujjuaq, QC	Diesel	58.1111	-68.406
Centrale de La Romaine	La Romaine, QC	Diesel	50.2157	-60.6867
Sandy Lake Diesel Generating Station	Sandy Lake, ON	Diesel	53.063	-93.3569
Ramea Diesel Generating Station	Ramea, NL	Diesel	47.5229	-57.3921
Charlottetown Diesel Generating Station	Charlottetown, NL	Diesel	48.4409	-54.0115
Makkovik Diesel Generating Station	Makkovik, NL	Diesel	55.0832	-59.1745

Centrale de Kuujjuarapik	Kuujjuarapik, QC	Diesel	55.2809	-77.756
Centrale d'Inukjuak	Inukjuak, QC	Diesel	58.4546	-78.1106
Centrale de Puvirnituq	Puvirnituq, QC	Diesel	60.0372	-77.2749
Cape Dorset	Cape Dorset, NU	Diesel	64.2329	-76.5432
Pangnirtung	Pangnirtung, NU	Diesel	66.1453	-65.7056
Arviat	Arviat, NU	Diesel	61.1083	-94.0583
Baker Lake	Baker Lake, NU	Diesel	64.3194	-96.0208
Igloolik	Igloolik, NU	Diesel	69.3833	-81.8
Pond Inlet	Pond Inlet, NU	Diesel	72.7001	-77.9582
Fort Simpson Plant	Fort Simpson, NT	Diesel	61.8625	-121.3486
Kugluktuk	Kugluktuk, NU	Diesel	67.8229	-115.118
Holyrood Thermal Generating Station	Holyrood, NL	Fuel Oil	47.4506	-53.0963
Tufts Cove Oil Generating Station	Dartmouth, NS	Fuel Oil	44.6764	-63.5961
Coleson Cove Oil Generating Station	Saint John, NB	Fuel Oil	45.1534	-66.2025
Centrale de Tracy Oil Generating Station	Tracy, QC	Fuel Oil	45.9972	-73.1722
Lennox Oil Gas Generating Station	Greater Napanee, ON	Fuel Oil	44.1439	-76.8492
COURTENAY BAY GENERATING STATION UNIT#2	Saint John, NB	Fuel Oil	45.2757	-66.0269
Fort Chipewyan Generating Station	Fort Chipewyan, AB	Fuel Oil	58.7276	-111.1364

Table 6. Information of 41 power plants after selection

Facility	Address	Fuel type	Latitude	Longitude
Centrale de cogénération à la biomasse	Sherbrooke, QC	Biomass	45.4808	-71.9519
Société de Cogénération de St-Félicien	St-Félicien, QC	Biomass	48.6375	-72.4338
Centrale de Senneterre	Senneterre, QC	Biomass	48.3837	-77.223
Usine de cogénération de Chapais	Chapais, QC	Biomass	49.7709	-74.8562
Sundance Thermal Electric Power Generating Plant	Duffield, AB	Coal	53.5085	-114.5571
Nanticoke Coal Generating Station (1973-2013)	Nanticoke, ON	Coal	42.7961	-80.05
Boundary Dam Coal Power Station	Estevan, SK	Coal	49.0961	-103.0305
Genesee Thermal Generating Station	Warburg, AB	Coal	53.344	-114.305
Poplar River Coal Power Station	Coronach, SK	Coal	49.0472	-105.4883
SHEERNESS GENERATING STATION	Hanna, AB	Coal	51.5317	-111.7861
Keephills Coal Power Plant Canada	Duffield, AB	Coal	53.4487	-114.4491
Battle River Generating Station	Forestburg, AB	Coal	52.5647	-112.1414
Shand Coal Power Station	Estevan, SK	Coal	49.0879	-102.864
Point Aconi Coal Generating Station	Halifax, NS	Coal	46.3225	-60.3039
Grand Lake Coal Generating Station	Newcastle Creek, NB	Coal	46.0572	-66.0051
Tunis Power Plant	Tunis, ON	Natural Gas	48.8704	-80.8942
Nipigon Power Plant	Nipigon, ON	Natural Gas	49.1512	-88.3418
Société en commandite Boralex énergie	Dolbeau-Mistassini,	Natural Gas	48.8794	-72.2166

	QC			
Cogénération Kingsey Falls	Kingsey Falls, QC	Natural Gas	45.8603	-72.0643
MacKay River Power Plant	Fort McMurray, AB	Natural Gas	57.0398	-111.9087
McMahon Cogen Plant	Taylor, BC	Natural Gas	56.1447	-120.6686
Rainbow Lake Generating Station (Units 4&5)	Rainbow Lake, AB	Natural Gas	58.4471	-119.2383
Becancour Power Plant	Bécancour, QC	Natural Gas	46.368	-72.405
Cavalier Power Plant	Strathmore, AB	Natural Gas	51.0056	-113.1716
Rainbow Lake Generating Station (Units 1, 2 & 3)	Rainbow Lake, AB	Natural Gas	58.4603	-115.2383
Carseland Power Plant	Carseland, AB	Natural Gas	50.9012	-113.3928
Island Cogeneration No. 2 Inc.	Campbell River, BC	Natural Gas	50.069	-125.282
Masset Diesel Generating Station	Masset, BC	Diesel	54.02	-132.1137
Centrale d'Obedjiwan	Obedjiwan, QC	Diesel	48.6605	-74.9322
Centrale de Kuujjuaq	Kuujjuaq, QC	Diesel	58.1111	-68.406
Centrale de La Romaine	La Romaine, QC	Diesel	50.2157	-60.6867
Sandy Lake Diesel Generating Station	Sandy Lake, ON	Diesel	53.063	-93.3569
Charlottetown Diesel Generating Station	Charlottetown, NL	Diesel	48.4409	-54.0115
Centrale de Kuujjuarapik	Kuujjuarapik, QC	Diesel	55.2809	-77.756
Centrale d'Inukjuak	Inukjuak, QC	Diesel	58.4546	-78.1106
Centrale de Puvirnituq	Puvirnituq, QC	Diesel	60.0372	-77.2749
Cape Dorset	Cape Dorset, NU	Diesel	64.2329	-76.5432
Holyrood Thermal Generating Station	Holyrood, NL	Fuel Oil	47.4506	-53.0963

Coleson Cove Oil Generating Station	Saint John, NB	Fuel Oil	45.1534	-66.2025
COURTENAY BAY GENERATING STATION UNIT#2	Saint John, NB	Fuel Oil	45.2757	-66.0269
Fort Chipewyan Generating Station	Fort Chipewyan, AB	Fuel Oil	58.7276	-111.1364

Annual on-site NO_2 release data from 2008 to 2017 were collected from the National Pollutant Release Inventory (NPRI), which provides annual open (i.e., publicly accessible) data on industrial emissions to the air, surface, water, and land (Johnston Edwards and Walker, 2020; Taylor et al., 2020). With the enactment of the *Canadian Environmental Protection Act* in 1999, owners or operators are required to report release data if their facilities have emitted one or more of the substances listed in the NPRI (Tang and Mudd, 2014). NPRI is an information-based tool that reports on the release, disposal, and transfer of pollutants from over 7,000 facilities in Canada, power plants being one of the categories of reporting facilities (Government of Canada, 2019). It is a valuable tool that can be adopted in local environmental monitoring to analyze the pollution burden and improve environmental outcomes (Tang and Mudd, 2014). Although there has been a lack of consideration of toxicity releases in NPRI (Taylor et al., 2020), its effectiveness and authenticity in other chemical releases have been explored and tested by previous scholars (Brown et al., 2014; Walker, 2018).

The vertical column densities of NO_2 data from the OMI satellite, developed by the Royal Netherlands Meteorological Institute (KNMI), were used in this research for analysis purposes. The nominal spatial resolution of 13×24 km was converted to a 13×13 km resolution to observe and track pollution sources. The satellite NO_2 data were downloaded in the form of monthly level-3 (i.e., variables mapped on uniform space-time grid scale) OMI data, available from the Tropospheric Emission Monitoring Internet Service (TEMIS) (https://www.temis.nl/index.php). In this platform, the satellite data are presented as a monthly average of daily measurements from OMI. The differential optical absorption spectroscopy technique was used for NO_2 slant columns and the TVCDs were derived from KNMI using the retrieval–assimilation–modeling approach (Boersma et al., 2007). Looking at previous studies, summertime NO_2 retrievals are frequently used to quantitatively analyze NO_x emissions (in consideration of the impact of snow cover and seasonal variation) (Lamsal et al., 2010; Lu and Streets, 2012). Because of missing data in non-summer months in Canada and the seasonal variations mentioned above, NO_2 data from July, August, September, and October were selected from the monthly level-3 OMI data to ensure the reliability of the data.

5.2.2. Satellite inversion of tropospheric NO_2 and threshold processing

To verify the annual NPRI NO_2 data and variation trends in different provinces, the NO_2 TVCDs as recorded in OMI data were used. The average monthly TVCD of NO_2 was calculated based on selected monthly data following the raster weighted mean approach and employing the Map Algebra tool available in the ArcGIS platform. The values of multiple raster data sets were summed based cell-by-cell criteria.

$$S = \frac{\sum_{i=1}^{n} R_i}{n} \tag{10}$$

where, n is the total number of months, R_i is the value of raster data in month i map, S is the raster unit value in output map.

All pixels were allocated into 0.125×0.125 grids with corner coordinate information. Each pixel over the same grid was weighted by its overlapping area to achieve the average NO_2 columns. In order to identify the provinces where power plants had a significant influence on the air quality in the surrounding area for the period under study (i.e., 2008 to 2017), the linear relationship between NPRI NO_2 emissions from power plants and the average TVCD of NO_2 over power plant areas was examined by linear regression and coefficient of determination (R^2) (Lu and Streets, 2012). Images from satellite remote sensing show a clear concentration gradient in different zones where point source emission levels differ. Thus, the provinces in which this correlation was strong were selected for further investigation, while the power plants in those provinces where releases over 5000 tonnes of NO_2 based on NPRI in 2007 were subjected to a threshold trend analysis, examining the area within a 50 km radius of a given plant. In our study, it should be noted, the focus was on relative changes in concentration over the study period rather than on the absolute values describing the dilution of emissions in the atmosphere (Jiao et al., 2020).

5.2.3. Policies and incentives governing Canada's energy transition

International, federal, and provincial policies and incentives in Canada that support sustainable transition pathways for the fossil fuel-dependent electricity sector were

categorized and assessed. The types of policies and incentives are diverse, ranging from technology push to market pull policies (Jordaan et al., 2017). The market created through demand-pull policies helps to improve the demand for lower-emission technologies. This study mainly focused on past, present, and future demand-pull policies that have been devised from the public sector to create a market for target-based emission reduction instruments, where the instruments may be direct or indirect approaches. Direct approaches include renewable portfolio standards, while indirect approaches include agreements or programs at the international level that contribute to the green development of the electricity sector, such as national carbon trading and emissions taxes. The policies and incentives were accessed through the joint database of renewable energy policies and measures maintained by the International Renewable Energy Agency and the International Energy Agency (2021), as well as from a review of the Acts and regulations in force in Canada concerning indigenous people and the international agreements to which Canada is a party. This approach combining analysis of implemented policies with emission reduction performance evaluation is applicable to other jurisdictions endeavoring to meet international emission reduction commitments.

5.3. Results and discussion

5.3.1. Characteristics of Canadian energy consumption in a global context

Canada's primary energy consumption is currently more than three times what it was in the 1960s, and it continues to grow (The British Petroleum Company plc, 2021). As a developed country, Canada's overall energy consumption growth rate has been slowing since the year 2000, and its per capita consumption of electricity has been gradually decreasing since the year 2000. Notwithstanding these encouraging trends, further electrification of the transportation, industrial, residential, and commercial sectors will be critical to achieving Canada's emission reduction targets (Asif and Chen, 2020). In most countries, energy consumption and economic activity are highly correlated, where “energy intensity” refers to the characterization of this relationship (Farajzadeh and Nematollahi, 2018; Tan and Lin, 2018). It effectively measures the energy used to produce a given level of economic output. A higher energy intensity means that more energy is being consumed

per unit of GDP. As can be seen in Figure 37, among developed countries, energy intensity has been trending downward since the year 2000 (Ritchie and Roser, 2020). However, Canada has consistently lagged behind other developed countries in lowering its energy intensity despite having a low-carbon electricity mix of 60.1% hydro and 15.8% nuclear. One possible explanation is Canada's reliance on the primary sector due to its northerly latitude and cold climate. Moshiri and Duah (2016) investigated the factors driving energy intensity in Canada and found that the reductions in energy intensity that have been seen in recent years are largely attributable to improvements in energy efficiency rather than to more efficient use of energy in economic sectors. Looking at inter-provincial disparities, the main drivers of regional inequalities in energy intensity have been differences in the energy-efficiency of the technologies employed throughout the economic sectors and the prevalence of energy-intensive industries (Su et al., 2021).

It should be noticed that although the electricity sector in Alberta generated more emissions than any other province for its size and reliance on coal-fired generation, since the 1940s the whole country has benefited from the growth in Alberta's oil and gas sector that belongs to the energy-intensive industry. Because a number of different fuels are used in electricity generation, there are significant differences in consumption-related emissions among Canadian provinces (Cai et al., 2021; Vazifeh et al., 2021). The GHG intensity of electricity generation ranges from 790 g CO_2 per kWh to 1.2 g CO_2 per kWh (Canada Energy Regulator, 2017). There are also fewer east–west interties among the electricity transmission networks because of the heterogeneous population distribution in Canada. In this context, the various federal and provincial climate change and energy policies in force are intended to further decarbonize the electricity system and close the gap between provinces.

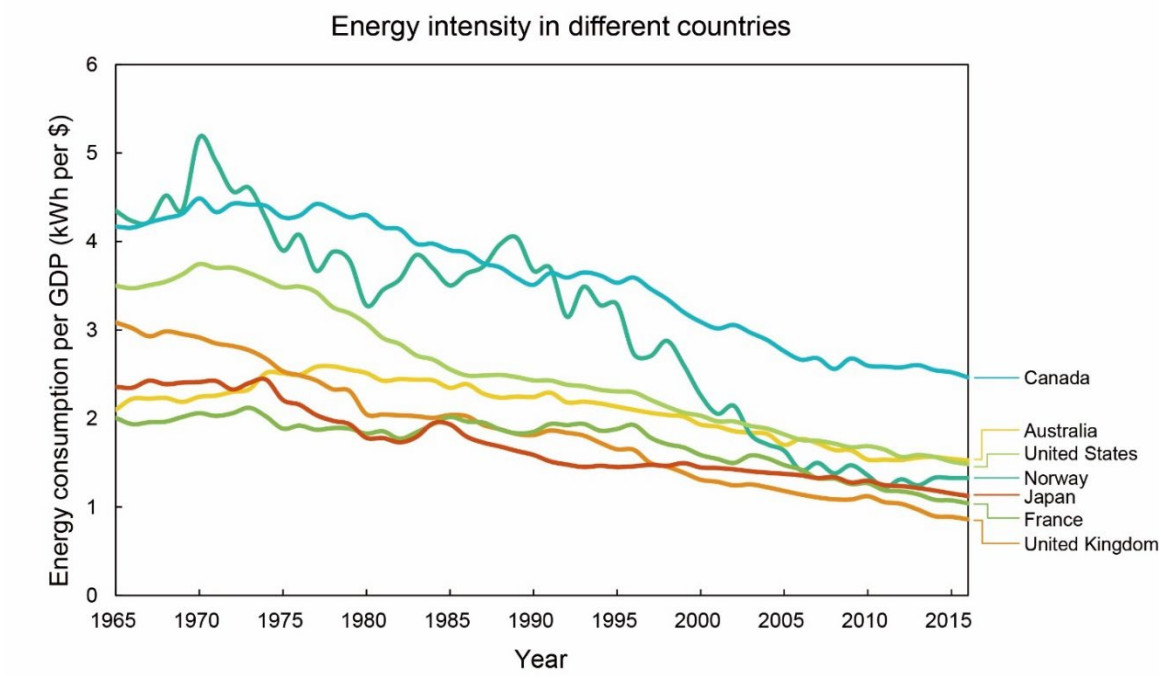

Figure 37. Energy intensity in different countries from 1965 to 2016 (Ritchie and Roser, 2020).

5.3.2. Trends of NO_2 emissions from power plants

According to the data from NPRI, 97 electricity generation facilities across Canada were targeted in this study to quantify their NO_2 emissions during the period, 2008 to 2017. The population in Canada increased around 10% in 2017 compared with 2008 and the variation in degree of urbanization in Canada is not significant from 2008 to 2017 (Statistics Canada, 2021c) . Coal, natural gas, biomass, fuel oil, and diesel were all represented among the facilities under study. The total NO_2 emissions from these facilities decreased from 204,590 to 135,866 tonnes/year during the study period, mostly as a result of increased generation from non-emitting sources. The NO_2 emissions from the electric utility sector as a percentage of total NO_2 emissions from all sectors (e.g., transportation, oil and gas, off-road vehicles and mobile equipment) decreased from 23.4% in 2008 to 20.7% in 2017. The total NO_2 emissions from the five electricity generation fuels mentioned above decreased by 33.6% during the ten-year study period. Figure 38 illustrates these changes in a Sankey diagram representing the NO_2 emitted from facilities by fuel type in all eight provinces under consideration, for the study period. In the figure, the widths of bands are linearly

proportional to the amounts of emission. The outer side of the diagram represents each province's share of the total NO_2 emissions from power plants. The inner side, however, represents the contributions of the different fuel types to the emissions flow from the power plants in different provinces. From Figure 38 it can be seen that coal-fired power plants were among the highest emitting sources of air pollutants both in 2008 and 2017. Having said that, it is also observed that emissions from coal-fired and diesel power plants dropped by 36% and 25.5%, respectively, over the study period. Diesel is typically used for electricity generation in areas, too remote to be connected to the grid.

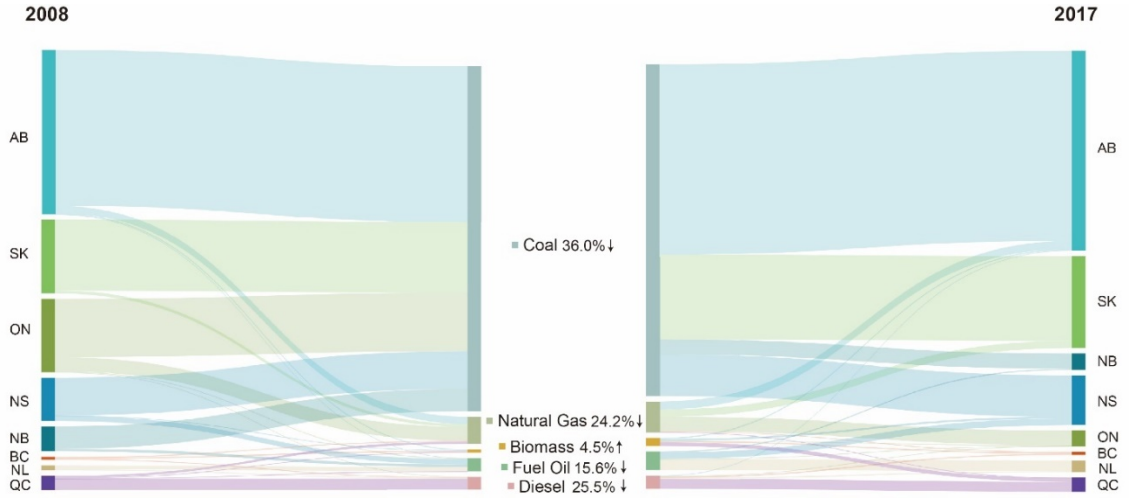

Figure 38. Change of NO_2 emissions emitted from power plants with different fuels in eight Canadian provinces in 2008 and 2017. (BC: British Columbia, AB: Alberta, SK: Saskatchewan, ON: Ontario, QC: Quebec, NB: New Brunswick, NS: Nova Scotia, NB: Newfoundland and Labrador)

The overall trend in Canada during this ten-year period has been encouraging, although the national average to some extent masks the disparities among provinces and the concerning trends that continue in some provinces. The emission fluctuation over the study period reflects progress in the mix of low-emitting electricity generation sources, such as hydropower, nuclear sources, and other renewable sources. With the phasing out of coal-fired electricity, Ontario has successfully transformed its regional electricity systems and increased the amount of electricity generated from renewable and low-emitting resources. By 2018, about 96% of electricity in Ontario was being generated from zero-carbon

emitting sources. Another trend during the study period had to do with the use of natural gas, as a lower-emitting alternative to coal, for electricity generation (Hibbard and Schatzki, 2012). The NO_2 emission from natural gas power plants in 2017 was approximately 76% of what it had been in 2008. Among the eight provinces studied, while the province of Newfoundland and Labrador saw an increase in emissions from thermal power generation over the study period, the remaining seven provinces experienced varying degrees of decline in emissions from thermal power generation. Although most Canadian provinces already generate the majority of their electricity from non-emitting sources, it should be noted, Alberta, Saskatchewan, New Brunswick, and Nova Scotia are lagging in terms of the transformation of their electricity system. For instance, most of British Columbia's electricity is produced by BC Hydro, and hydroelectric stations generate about 95% of Quebec's electricity, whereas the aforementioned Alberta, Saskatchewan, New Brunswick, and Nova Scotia combined account for 99.7% of total coal-fired electricity generation in Canada despite combining to account for only about 20% of Canada's population (Audit and Evaluation Branch and Natural Resources Canada, 2019; Statistics Canada, 2021b).

5.3.3. Analysis of policy at international, national, and provincial levels

Countries have different paths to renewable power development and different policy frameworks to meet various targets for energy security, air pollution emission reduction, and economic development (Lipp, 2007). There is no common electricity market in Canada, with each province and territory maintaining its own energy policies related to electricity mix, resource management, and regulatory framework. Given that Canada has a federalist political system, some researchers have argued that Canada's federal government should exercise its authority to carefully plan and coordinate among the provinces through climate policy to ensure that international and national GHG emissions goals are met (Jordaan et al., 2017; Tian et al., 2020). Canada has the advantage of an abundant low-carbon electricity supply in the form of hydroelectric facilities, nuclear facilities, and other renewable resources such as wind and solar. In this context, the continued shift toward low-carbon electricity generation will enable further emission reductions in other sectors

through end-use electrification (e.g., electric vehicles) (Yu et al., 2017).

In recent decades, Canada has developed or otherwise engaged in various emissions mitigation strategies at the international, federal, and provincial levels, such as emission reduction requirements for coal-fired units, regulations for natural gas-fired electricity and new natural gas-fired units, as well as the policies designed to encourage the establishment of coal-to-gas conversion. Figure 39 gives an overview of the policies, regulations, and incentives that have been introduced to transform the electricity system at different levels in Canada; these mechanisms—including financial incentives, subsidies, feed-in tariffs, and regulatory mechanisms (International Energy Agency, 2020b)—warrant careful consideration in any effort to qualitatively analyze the emission reduction performance and future pathways of Canada's electricity sector. Table 7 shows the total collected policies, regulations, and incentives at different levels in Canada.

According to Jordaan et al. (2017), these mechanisms can be broadly categorized as those that exert direct market pull and those that exert indirect market pull. Direct approaches are those can generate markets for clean energy through financial stimulants such as subsidies and investment fund (Ahmed et al., 2021). Most of the indirect approaches are in the form of international agreements or programs that contribute to the green development of the electricity sector such as carbon trading. The cumulative benefits of these policies, regulations, and incentives to reduce emissions include combatting climate change and its adverse effects as well as bringing about health and environmental benefits through reduced air pollution (Nikzad and Sedigh, 2017). In this regard, Environment and Climate Change Canada (2018) published a report in which it endeavored to quantify the future benefits of complying with emission reduction targets. According to its projection, by 2055, compliance will have brought about 555 kt and 206 kt reductions in the emission of sulphur oxides (SO_x) and NO_x, respectively. In addition to the direct environmental benefits, Matz et al. (2020) have noted that emission reduction also brings about various indirect socio-economic benefits, such as increased crop yields, lower levels of surface soiling, and improved air quality and visibility.

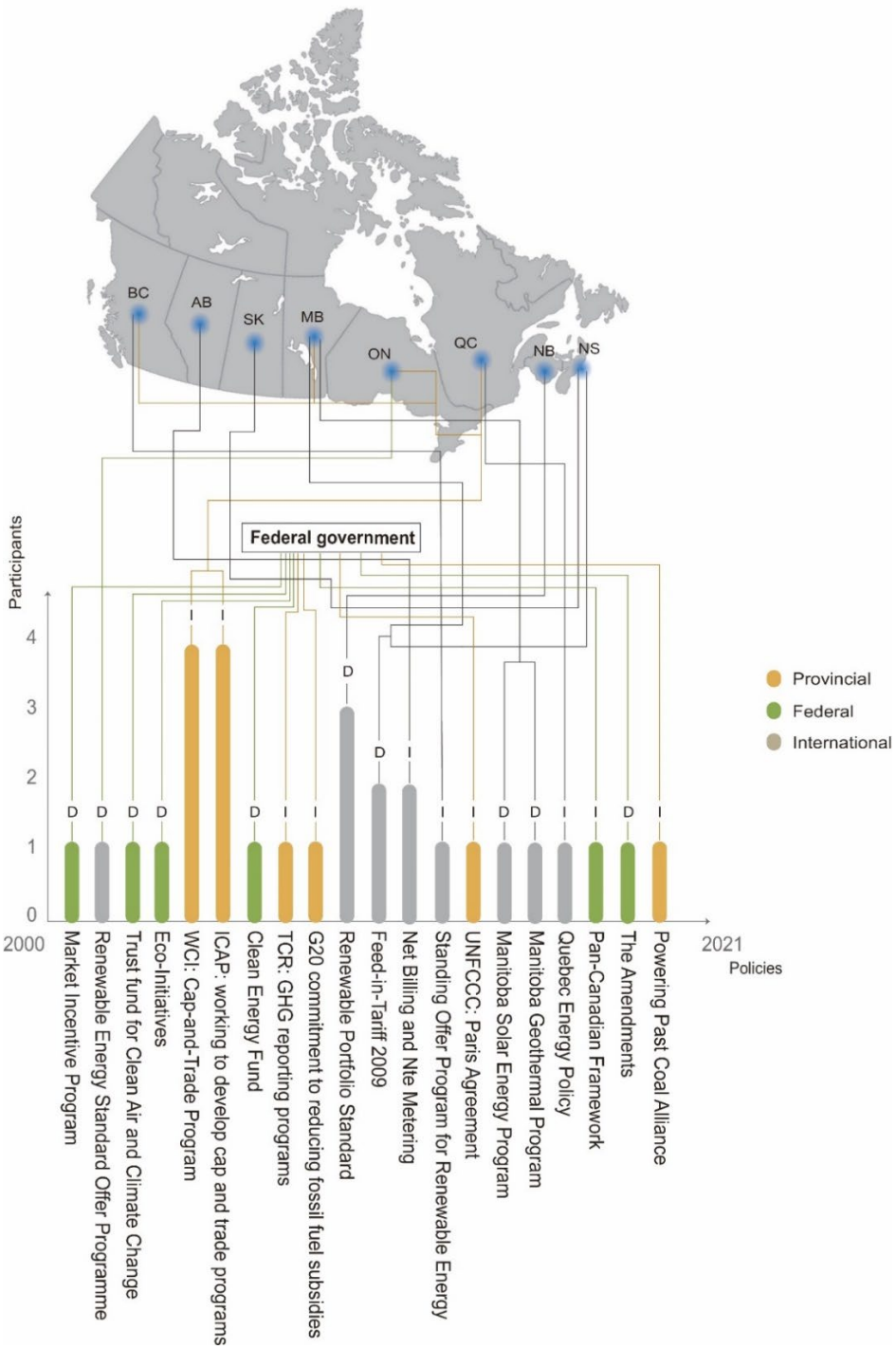

Figure 39. Policies and incentives in terms of transforming the electricity energy systems in international, provincial and federal levels in Canada. (BC: British Columbia, AB: Alberta, SK: Saskatchewan, ON: Ontario, QC: Quebec, NB: New Brunswick, NS: Nova Scotia, NB: Newfoundland and Labrador)

Table 7. Total collected direct and indirect policies, regulations and incentives at international, federal and provincial levels in Canada

International	**Canadian participants**	**Year**	**D/I**
United Nations Framework Convention on Climate Change (UNFCCC): Paris Agreement	Federal government	2015	I
The Western Climate Initiative (WCI): Cap-and-Trade Program	B.C., Manitoba, Ontario, Quebec	2007	I
International Carbon Action Partnership (ICAP): working to develop cap and trade programs	B.C., Ontario, Quebec, Manitoba	2007	I
The Climate registry (TCR): GHG reporting programs	Canadian provinces	2009	I
G20 commitment to reducing fossil fuel subsidies	Federal government	2009	I
Powering Past Coal Alliance (PPCA)	Federal government	2017	I
Federal			
Canadian Green Power Marketing Programs		1996	I
Market Incentive Program		2002	D
Electricity Performance Standard for Coal Fired Generation		2012	D
Eco-Initiatives (Program closed in 2014)		2007	D
Regulations Amending the Reduction of Carbon Dioxide Emissions from Coal-fired Generation of Electricity Regulations		2016	D
Pan-Canadian Framework		2016	I
Regional Electricity Cooperation and Strategic Infrastructure (RECSI)		2016	I

Trust fund for Clean Air and Climate Change		2007	D
Accelerated Capital Cost Allowance (CCA)		2005	I
Clean Energy Fund - Renewable Energy and Clean Energy Systems Demonstration Projects		2009	D
Clean fuel standard		2017	D
Provincial			
Climate Leadership Plan (proposed policy package)	Alberta	2015	D&I
Net billing	Alberta	2009	I
Market framework that includes an energy market and a capacity market	Alberta	2016	D
BC Clean Energy Act (policy package)	British Columbia	2010	D&I
BC Carbon Tax (update to $45/tonne)	British Columbia	2008	I
Standing Offer Program for Renewable Energy	British Columbia	2013	I
BC Oil and Gas Commission's Flaring, Incinerating and Venting Reduction Guideline	British Columbia	2021	I
B.C. emissions offsets regulations	British Columbia	2008	I
Climate and Green Plan	Manitoba	2017	D
Low Carbon Fuel Standards	Manitoba	2020	I
Request for proposals to develop 1000 MW of wind power over a decade	Manitoba	2005	D
Penalties for suppliers who do not meet minimum renewable fuel content	Manitoba	2009	D
Manitoba Solar Energy Program	Manitoba	2015	D
Manitoba Geothermal Program	Manitoba	2016	D
Renewable Portfolio Standard (RPS)	New Brunswick	2006	D

Policy Commitment to Increase RPS	New Brunswick	2015	D
Renewable portfolio standard (40% of electricity from renewable energy by 2020)	Nova Scotia	2009	D
Demand-side management policies for electricity	Nova Scotia	2009	I
Cap on Electricity Sector Greenhouse Gas Emissions	Nova Scotia	2018	I
Community Feed-in-Tariff (COMFIT)	Nova Scotia	2011	D
Enhanced Net Metering Program	Nova Scotia	2019	I
Green Energy and Green Economy Act	Ontario	2009	D&I
Coal-Fired Phase Out	Ontario	2007	D
Renewable Energy Standard Offer Programme (RESOP)	Ontario	2006	D
Feed-In-Tariff Energy Efficiency Standards and Smaller Projects (FIT)	Ontario	2009	D
Net metering for Smaller Producers	Ontario	2005	I
Energy Savings Rebate program	Ontario	2019	D
Cap and Trade	Quebec	2013	I
Carbon carbon tax	Quebec	2007	I
Low Carbon Fuel Standards	Quebec	2007	I
Québec's 2006-2015 Energy Strategy (4000 MW of wind by 2015)	Quebec	2006	D
Net metering for Small Producers	Quebec	2016	I
Quebec Energy Policy 2030	Quebec	2016	D
Demand Side Management policies for electricity	Saskatchewan	2019	I
Policy commitment (50% of renewable energy in electricity by 2030, 30%)	Saskatchewan	2015	D
Net metering for Small Producers	Saskatchewan	2015	I

The combination of financial mechanisms to push the development of renewable energy technology and a robust carbon cap and emissions trading system can also bring various economic, social, and environmental benefits. The phasing out of coal-fired electricity generation in Canada has already progressed markedly in recent years as a result of these emission reduction strategies, and this trend is projected to continue. However, the disparities between provinces remain an issue; for instance, the consumption intensity of the coal-fired plants in Saskatchewan is 330 times that of the hydro-powered plants in Manitoba. On the other hand, Alberta, Saskatchewan, New Brunswick, and Nova Scotia, although they all currently rely on coal-fired power generation, do all have clean energy policies in place. Alberta is committed to supplying 30% of its electricity from renewable sources by 2030, while Saskatchewan is targeting a threshold of 50% within the same time frame. Nova Scotia declared the target in 2030 is about 37% below the 2017 levels, and New Brunswick has 2030 emission reduction targets of between 25% and 40% below 1990 levels. Progress in reducing the emissions of Canada's electricity sector has been driven largely by international and federal initiatives to phase out coal-fired electricity generation combined with provincial electricity policies that are innovative in their approach to reducing emissions (Plumptre and Flanagan, 2017; Yu et al., 2017).

Apart from market pull policies, the adoption of a mix of generation sources/technologies is an important strategy in Canada's energy transition and emission reduction efforts. For instance, as an alternative to simply transitioning from coal-fired electricity to natural gas, Davis et al. (2020) has argued based on an analysis of various electricity generation scenarios in the Alberta context that a mix of wind, hydro, and solar power is the most promising scenario in terms of high emission abatement potential and low cost. While the design of solar photovoltaic power generation should also consider the application of demand-side management to realize the maximum demand-side peak reduction (Peinado-Guerrero et al., 2021).

5.3.4. Satellite inversion of NO_2 data changes in different provinces

Due to the short lifetime of NO_2 in the lower mixed layer, variations in density of the NO_2

column are considered to be indicative of changing trends in NO_2 sources, if the ground-level NO_2 emissions and NO_2 TVCDs in the column map are strongly correlated (Kim et al., 2006; Richter et al., 2005). Figure 40, Figure 41, and Figure 42 illustrate the extent and spatial distribution of monthly averages of NO_2 TVCDs over the eight Canadian provinces under the study for the period of 2008 to 2017, displaying the geographical location of the five types of power plants. According to these figures, although the extent of NO_2 TVCDs expanded in each province over the study period because of urbanization, decreasing column density in the satellite NO_2 hot spots was observed in some provinces. As shown in Figure 40 and Figure 41, particularly in Ontario and Quebec, a decrease in NO_2 column density in various hot spots in the satellite imagery was found to correspond reasonably well with reductions in on-site NO_2 release from power plants. The observation is also consistent with the coal consumption trend in Canada. The completion of Ontario's coal phase-out was a key development in this process, with the permanent closure of all of Ontario's coal-fired power plants by 2014 resulting in a 48% decrease in coal consumption in Ontario, compared with 2012 (Environment and Climate Change Canada, 2020c). Notwithstanding these gains in Ontario and Quebec, NO_2 emissions from electricity generation, as mentioned above, varies from province to province depending on the supply mix, which in turn is a function of the availability of natural resources, the transmission infrastructure, and the market structure in the given province (Government of Canada, 2018).

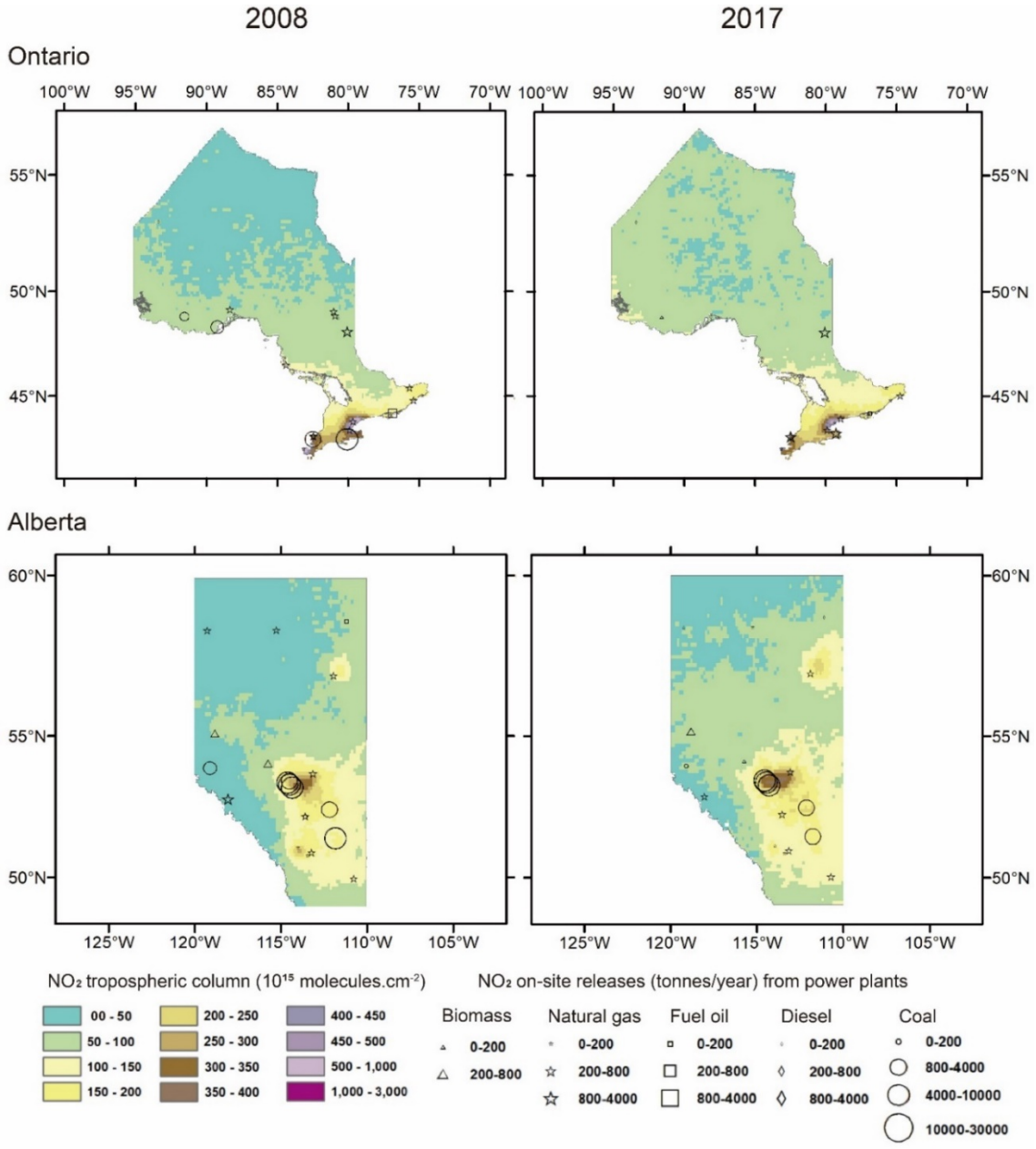

Figure 40. Spatial distribution of monthly averages of NO_2 TVCDs and geographical location of power plants in ON and AB in 2008 and 2017.

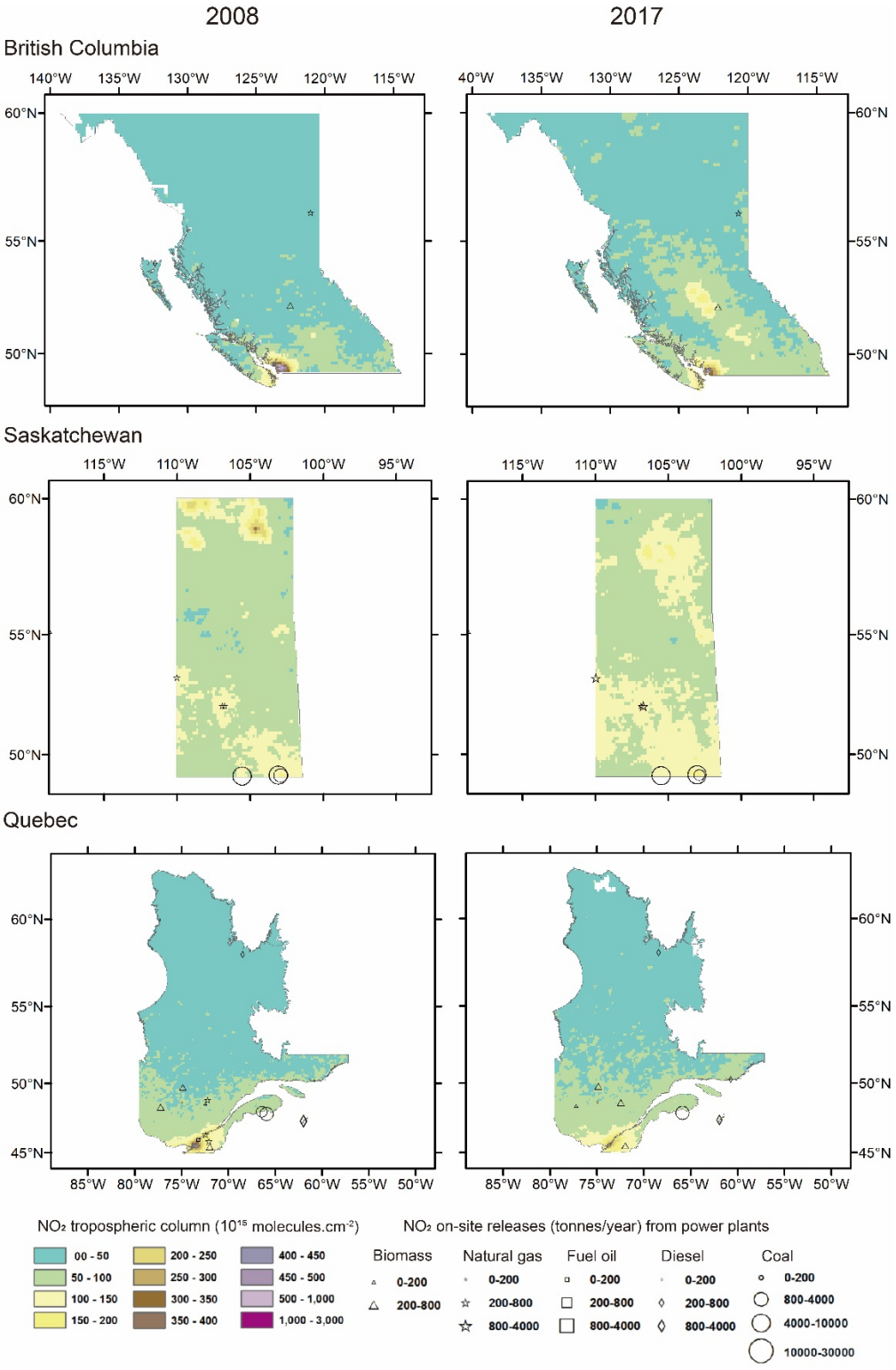

Figure 41. Spatial distribution of monthly averages of NO_2 TVCDs and geographical location of power plants in BC, SK and QC in 2008 and 2017.

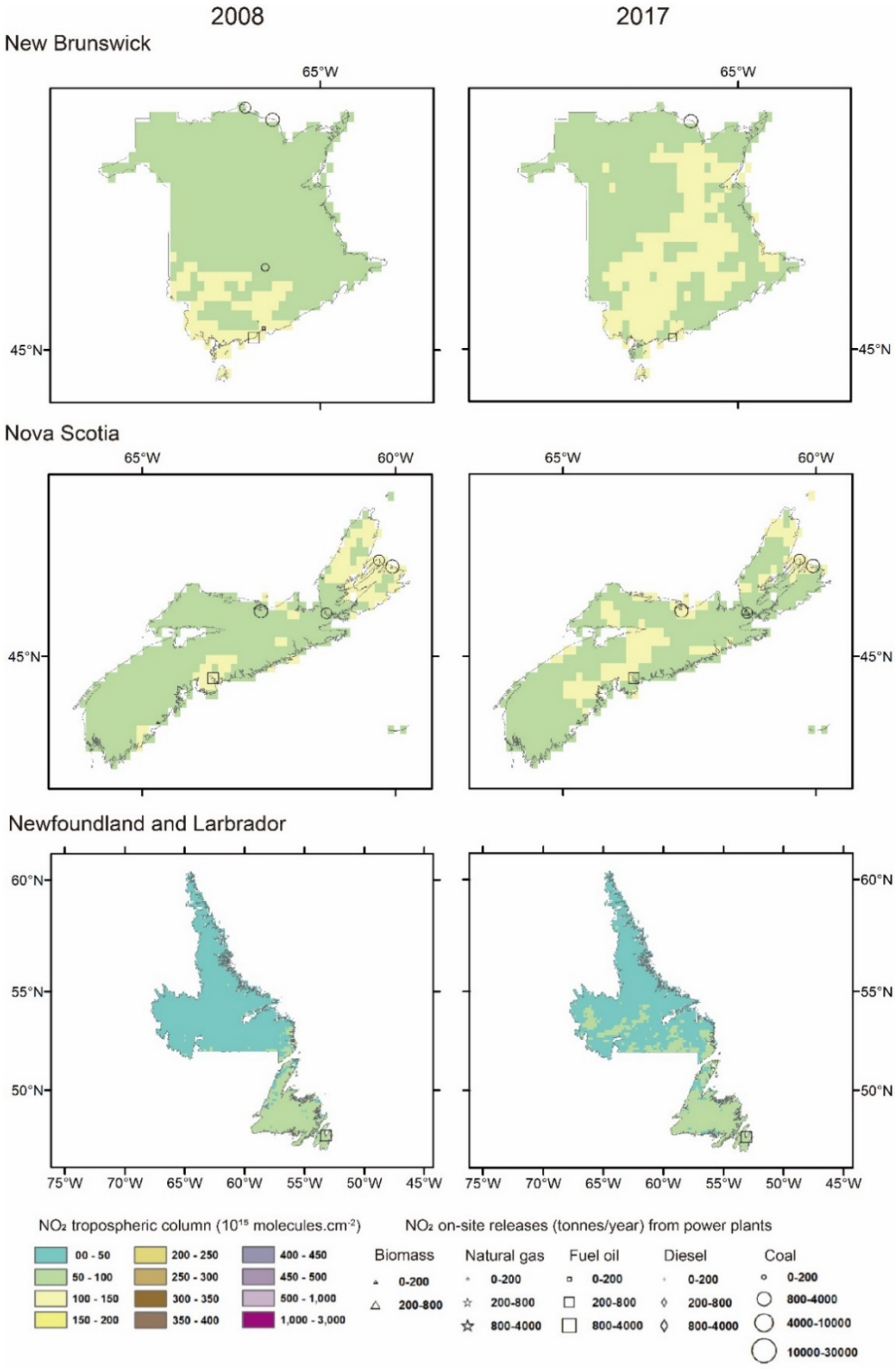

Figure 42. Spatial distribution of monthly averages of NO_2 TVCDs and geographical location of power plants in NB, NS and NL in 2008 and 2017.

In order to analyze the relationship between power plant emissions in different provinces and their impact on the surrounding area, scatter plots of annual on-site releases of NO_2 from power plants versus the average TVCD of NO_2 in the corresponding power plant raster areas for the study period were prepared in Figure 43. The entire range of on-site NO_2 releases was grouped into small values and the larger values in the left part of Figure 43. Although the absolute values obtained from satellite observations may not always be consistent with the emission values of a given power plant because of the effects of population density, wind direction, and atmospheric conditions, the variation trends between the two can be matched based on the findings of previous studies (Lu et al., 2013).

According to Lu and Streets (2012), data points with a R^2 up to 0.52 perform better in regression analysis. Among the provinces under study, the on-site release data were found to correlate more strongly with the TVCD of NO_2 in Ontario ($R^2 = 0.71$) and Alberta ($R^2= 0.61$) than in British Columbia, Saskatchewan, Quebec, New Brunswick, Nova Scotia, and Newfoundland. The relatively low NO_2 emissions during the study period may be the reason why the correlation was less pronounced in these latter provinces. Emission reductions on the part of neighboring provinces may be an additional cause of a weak correlation within a given province due to the long distances traveled by pollutants. Another consideration is that, although other types of point sources within the raster area in which a given power plant is located were excluded from the scope of the study, fugitive sources of NO_2 emissions beyond the 13 km radius and uncertainties in the NPRI data and satellite retrieval may still affect the results (Tang and Mudd, 2014; Walker, 2018)

The results for Ontario and Alberta indicate that the trend of on-site emissions from power plants is generally consistent with the variation in the TVCD of NO_2 over the corresponding areas. In Ontario between 2008 and 2017, the total on-site NO_2 releases from all types of power plants declined 98.4% and the total value of TVCDs of NO_2 in the corresponding areas saw a 70.5% decrease. However, in Alberta there was just an 11.5% drop in total on-site NO_2 releases over the same period, and the value of TVCDs of NO_2 in the corresponding areas in fact increased by 16.2%. Comparing the results from the two provinces, it can be inferred that even if there is a small decrease in NO_2 emissions from

power plants over a period of years, this will not be sufficient to offset the emissions from other sectors, and thus its effect on the NO_2 retrievals observed by satellites will be insignificant. The reliance on coal-fired generation and the size of coal-fired units in Alberta are the reasons for the less significant decrease in the electricity sector's emissions here compared to in other provinces. As of 2017, electricity generation still ranked second for emissions among industrial sectors in Alberta (Environment and Climate Change Canada, 2020c).

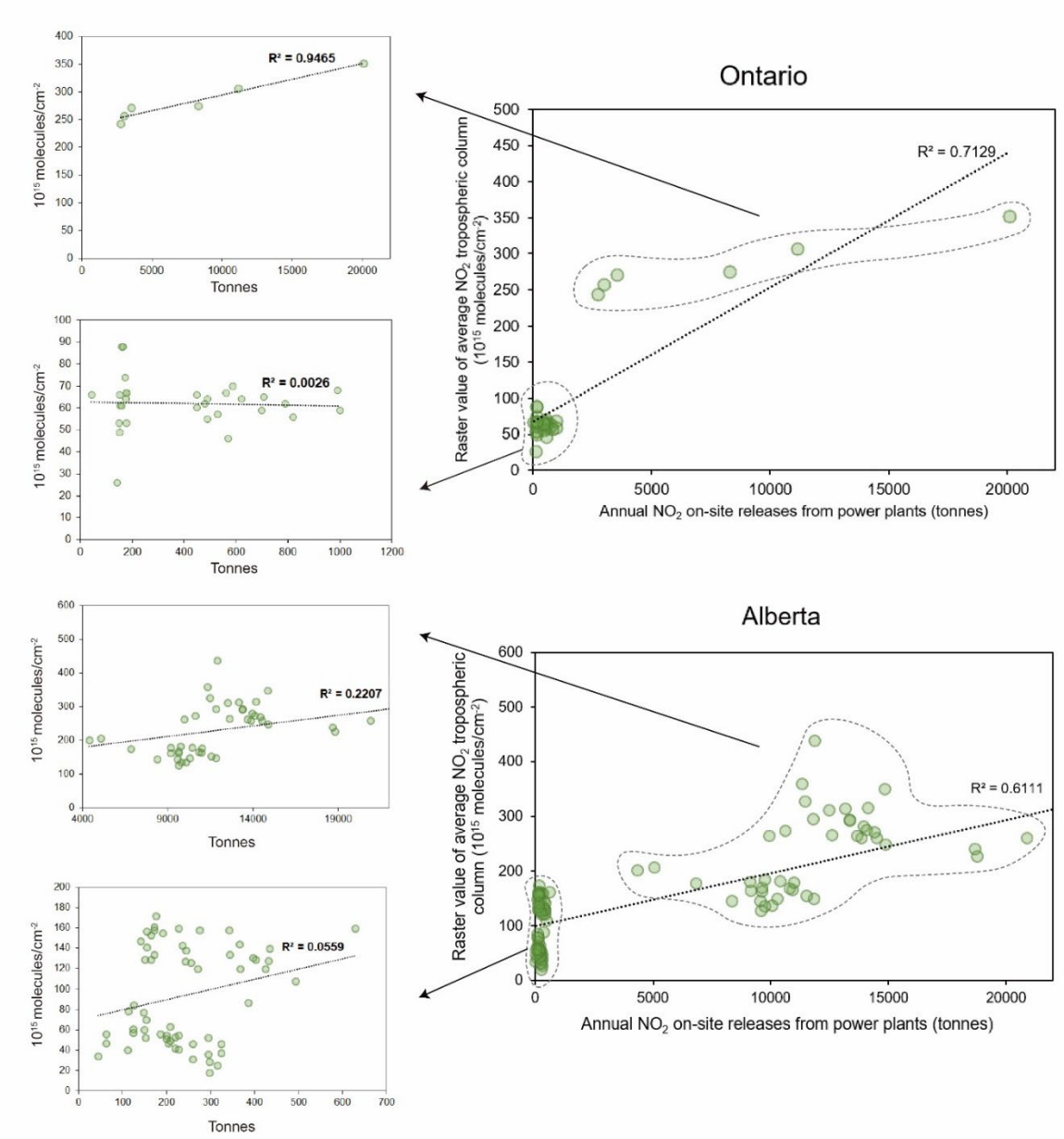

Figure 43. Scatter plots of annual on-site releases of NO_2 from power plants versus the average TVCD of NO_2 in corresponding power plant raster area from 2008 to 2017.

5.3.5. Tropospheric NO_2 over coal-fired power plants areas

Striking the appropriate balance between human activity and ecological preservation has always been a critical issue (Feng et al., 2020; Zhou and Li, 2020). Numerous studies and reports have discussed the environmental ramifications of power generation and its impact on the surrounding communities being served, and it is also frequently the subject of public discourse. To give a few examples, the location of some power plants in Ontario has met

with considerable local opposition in the past, with questions being raised about the environmental problems caused by emissions from burning fossil fuels, as well as the risks posed by freezing vapor plumes from cooling systems that may affect busy commuter rail lines and highways (National Post, 2010). Increased mortality was also found the largest component of the gross external damages from the discharges of SO_2, $PM_{2.5}$ and NO_x from electric power generation (Muller et al., 2011). Moreover, coal-fired plants with older equipment and geographic locations in areas with higher pollution baseline levels will have a more significant environmental impact. In addition to their impact on humans, studies have found that coal-fired power plants also have a negative impact on local flora and fauna. For instance, Llacuna et al. (1995) sampled three passerine bird species from areas within a polluted zone and within a non-polluted zone outside the 40 km radius of a power plant. Metal accumulation in the organs and tissues was found to be higher in birds from the polluted zone, especially Cr in the feathers and Al in the bone.

In our study, to compare the air pollution changes in the area near coal-fired power plants, five samples showing either significant decreases or increases in the NPRI emission data were selected for the purpose of threshold trend analysis of NO_2 in the surrounding area based on remote satellite sensing data. Power Plant L is a coal-fired power plant in Ontario. It began generating electricity in 1969 and had a total capacity of 1,976 MWh at the time of its closure. Following Ontario's decision to phase out coal-fired generation, Power Plant L shut down Unit 1 and Unit 2 in 2010, and the rest of the units were shut down in 2013. According to the NPRI, Power Plant L emitted 6,445 t of NO_2 in 2008, followed by a declining trend through to 2011. In 2012, emissions rose to 3,018 t, while, in 2013, 2,118 t of NO_2 were emitted, resuming the overall downward trend over the six-year period and marking a 67% decrease compared to the beginning of that period (i.e., 2008). Figure 44 shows the average NO_2 concentration in the 50×50 km range around Power Plant L in 2008 and 2013. It is clear based on the OMI satellite observations in Fig. 3 that, drawing toward the time of its closure, most of the pixel values in the 50 km range around this power plant decreased to varying degrees. The values of the NO_2 tropospheric column in these 32 pixels in 2008 and 2013 were also extracted for the purpose of comparison (Fig. 11). These values, which ranged from 216 to 452 (10^{15} molec.cm^{-2}), were divided into five groups. In 2008,

most of the values fell within the intervals, 316 to 366 and 366 to 416, while three pixels fell within the highest interval and only one in the lowest interval. In 2013, most of the values fell within the intervals of 266 to 316 and 316 to 366, and there were no pixels in the highest interval and six in the lowest interval. The average pixel value within 50 km decreased from 355 in 2008 to 311 in 2013, a decrease of 12.4%.

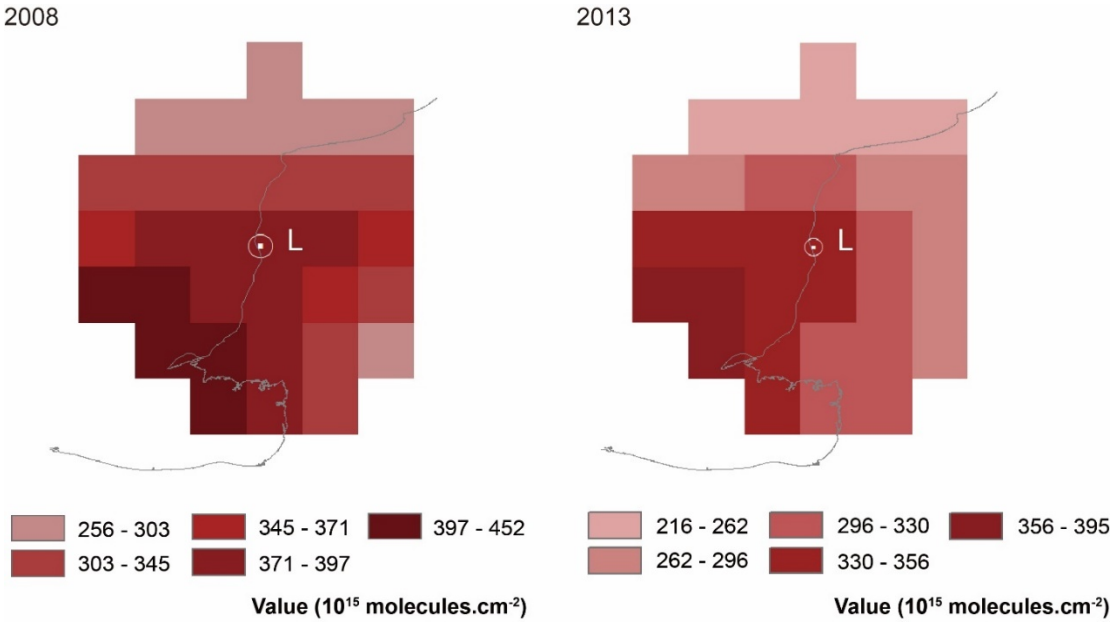

Figure 44. Average NO_2 concentration in the 50× 50 km range around L power plant in 2008 and 2013.

Power Plant N is another coal-fired power plant in Ontario. It was once the largest coal-fired power plant in the world and provided as much as 15% of Ontario's electricity, with a total capacity of 4,000 MWh at its peak. Like Power Plant L, Power Plant N was decommissioned in 2013 as part of the Ontario government's commitment to eliminate coal generation. The plant dropped from an NO_2 emission level of 20,087 t in 2008 to 2,761 t in 2013, a decrease of 86.3% over six years. The average NO_2 concentrations in the 50×50 km range around Power Plant N in 2008 and 2013 are shown in Figure 45. Compared to Figure 44, the drop in pixel values in Figure 45 is more pronounced. The values of these pixels, ranging from 204 to 396 (10^{15} molec.cm^{-2}) in the NO_2 tropospheric column in these two years, were extracted and divided into five groups for comparison as shown in Figure

47. In 2008, the two intervals accounting for the greatest numbers of pixels were the intervals, 284 to 324 and 324 to 364, while, in 2013, the lowest interval, 204 to 244, was the one with the greatest number of pixels falling within it. In 2008, no pixels fell within the lowest interval, while two pixels fell within the highest interval. However, in 2013, no pixels fell within the highest interval or even the second-highest interval. The average 32-pixel value within 50 km decreased from 319 in 2008 to 243 in 2013, a decrease of 23.8%. It is also necessary to consider the offsetting increase in NO_2 as a result of urban development, such as the increase in vehicles on the road. Comparing the NO_2 releases recorded by the NPRI between 2013 and 2008, the smallest reduction for these two power plants in Ontario was 67.1% from 6,445 tonnes in 2008 to 2,118 tonnes in 2013.Because of the impact of this offsetting source of emissions, we estimate that the degree of reduction in emissions in the ground data and satellite observation of the coal-fired power plants under study needs to be 60% or higher in order for its impact in reducing overall regional air pollution within the 50 km range to be significant.

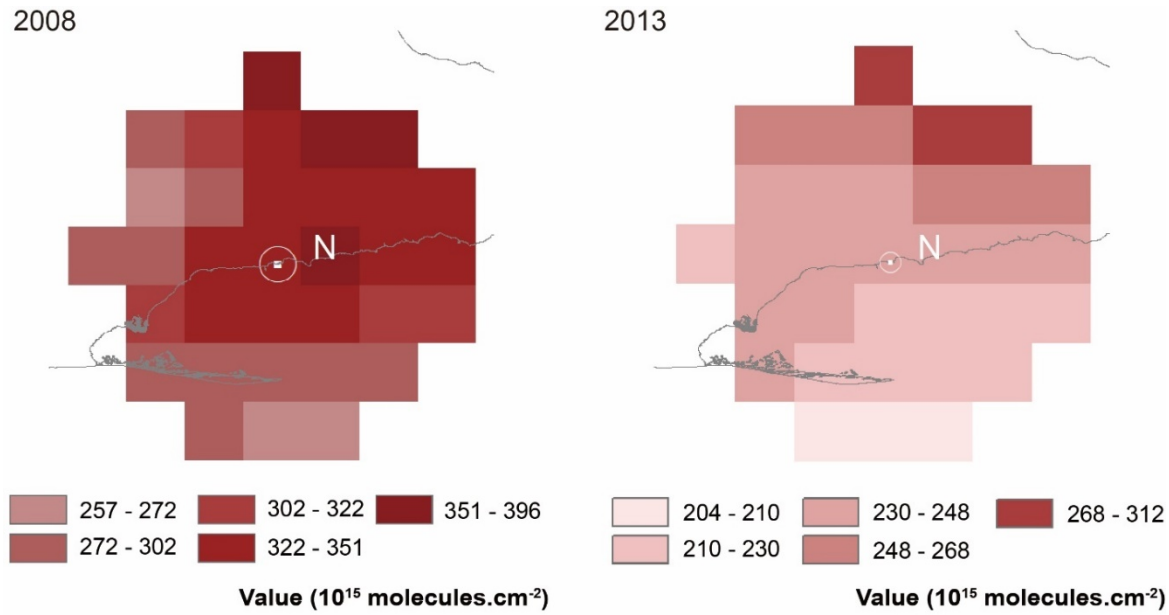

Figure 45. Average NO_2 concentration in the 50× 50 km range around N power plant in 2008 and 2013.

Alberta's coal fleets are the largest in Canada, with a total generating capacity of 5,555 MWh. In 2017, Alberta's electricity sector generated 44.3 megatonnes CO_2e emissions,

accounting for 60% of all GHG emissions from electrical generation in Canada. As of 2018, approximately 91% of Alberta's electricity was being generated from fossil fuels, 43% of that proportion from coal. Due to the reliance on coal generation, Alberta generates more GHG emissions from its electricity sector than any other province. The changes in NO_2 concentration near coal-fired power plants in Alberta as shown in satellite observation are concerning. However, under Alberta's climate change legislation, coal-fired power generation is scheduled to be phased out by 2030 (Canada Energy Regulator, 2021; Government of Canada, 2018). Thermal Electric Power Generating Plant S, Coal Power Plant K, and Thermal Generating Station G were selected because of their locations with the 50×50 km range in order to analyze the impact range of emissions from an aggregated area. This area was obtained by aggregating a 50 km radius around the location of these three power plants. According to the NPRI data, NO_2 emissions from Power Plant S decreased by 14% over the period of study from 27,189 t in 2008 to 23,374 t in 2017. The other two power plants showed an upward trend over the same period, with Power Plant G increasing from 12,620 t in 2008 to 14,860 t in 2017, and Power Plant K from 10,623 t to 11,347 t, increases of 17.7% and 7%, respectively.

Figure 46 shows the annual average NO_2 concentrations within the 50×50 km area centered on Plants S, K, and G, respectively, in 2008 and 2017. Quantitatively, the decrease in total NO_2 emissions from Power Plant S between 2008 to 2017 may have been sufficient. Nevertheless, hypothetically to offset the total increase in emissions from Power Plant K and Thermal Generating Station G, as observed from the OMI satellite imagery (Figure 46), the average NO_2 concentration in the vicinity of these three power plants did not in fact decrease. The pixel values within their 50 km range actually show a large increase over the ten-year period. In order to meet federal Clean Air Strategic Alliance (CASA) guidelines, coal-to-gas conversions are planned for Units 4, 5, and 6 in Power Plant S to reduce NO_2 emissions. Under this conversion program, Unit 4 will be converted to a natural gas unit in 2022, Unit 5 to a combined-cycle unit in 2023, and Unit 6 to a natural gas unit in 2021. According to the Third Quarter Report for 2020, Power Plant K also plans to complete the conversion of two of its units from coal to gas by 2021 (TransAlta Corporation, 2020). Similarly, with Power Plant G, Units 1 and 2 will be converted to

natural gas combined cycle (NGCC) technology and Unit 3 will be 100% natural gas by 2023 following a dual-fuel transition (Government of Canada, 2018). Indeed, most of the coal-fired power plants in Alberta are on-track to complete the conversion to gas, which will eliminate coal as a fuel source in Alberta's thermal fleet and expand the renewables fleet.

Figure 47 shows a comparison of the values in pixels extracted from the NO_2 tropospheric column. These values, ranging from 140 (10^{15} molec.cm^{-2}) in 2008 to 388 (10^{15} molec.cm^{-2}) in 2017, were also divided into five groups. In 2008, approximately 66% of the values fell within the 140 to 190 and 190 to 240 intervals, with no pixels falling within the highest interval. However, in 2017, only 8% of the values fell within the lowest interval (i.e., 140 to 190), with the rest of the pixel values evenly distributed among the other four intervals. The average pixel value within 50 km of the three power plants increased by 20.6% over the decade under study, from 223 in 2008 to 279 in 2017.

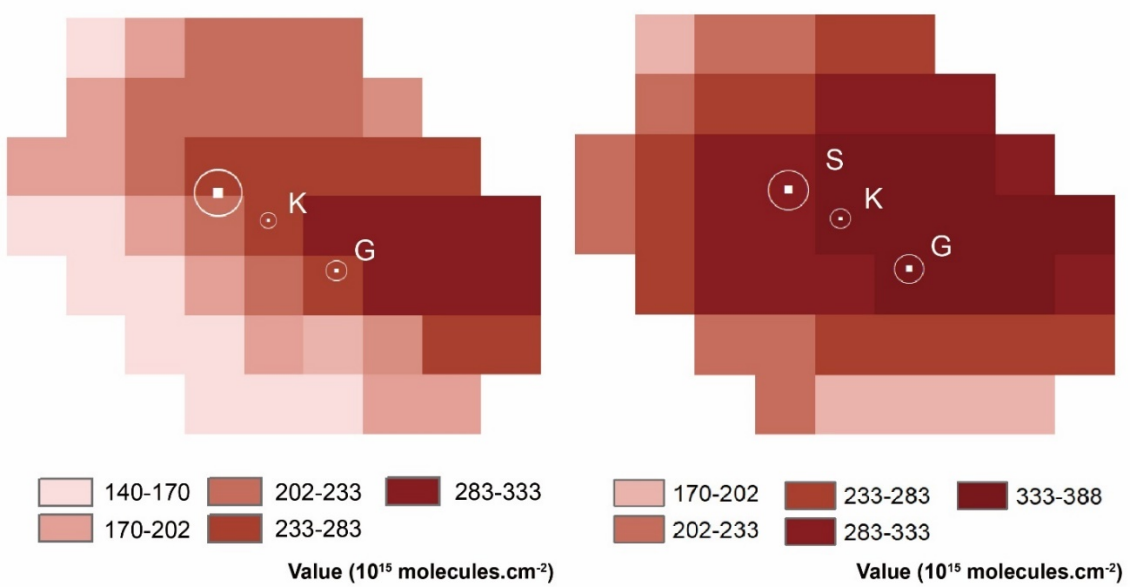

Figure 46. Average NO_2 concentration in the 50× 50 km range around S, K and G power plants in 2008 and 2017.

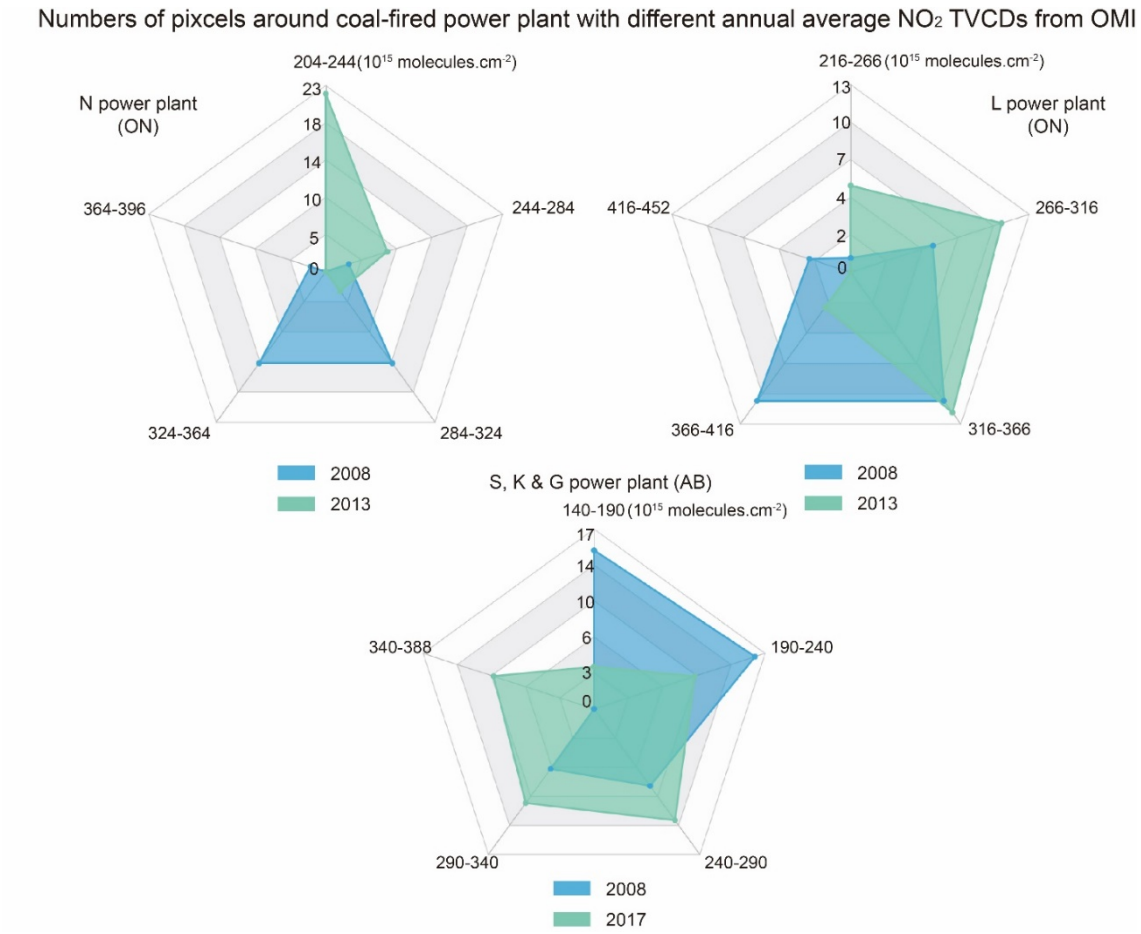

Figure 47. Comparison of trends of the NO_2 tropospheric column in 32 pixels around five power plants in 2008 and 2013.

5.4. Summary

This chapter demonstrates an approach to combine on-ground air pollutant emission inventory (i.e., NPRI) with satellite monitoring data to verify the impact on overall air pollution of implementing policies to reduce emissions from power plants. As the end-users of the urban services, citizen could have more chances to broaden their participation in the development of their community if information tools like NPRI can consider higher priority of public cognition (Zarei and Nik-Bakht, 2021). Given that NPRI data lack the robustness to capture changes in regional pollutant thresholds in the geographic vicinity of pollution source, the threshold trend analysis within a smaller scale described herein can be developed as a supporting platform to aid the public in understanding how the pollutant

concentration gradient has changed in their community as a result of emission reduction measures. This chapter provides insights for developing a verification method that uses digital and visual methods to characterize the changes in emissions concentration in the area surrounding an emission source as a result of emission reduction policies and incentives. Combining numerical data from an inventory tool with pollutant concentration thresholds at the geographical level can be helpful for monitoring emission reduction performance.

As demonstrated by the satellite observations, the decreasing column density in satellite NO_2 hot spots was obvious in some provinces, especially in Ontario, where total on-site NO_2 releases from all types of power plants decreased by 98.4% and the total value of TVCDs of NO_2 in the corresponding area saw a 70.5% decrease over the period of study (i.e., 2008 to 2017). The progress made in reducing emissions in Canada's electricity sector, reflected in these findings, has been largely attributable to the phase out of coal-fired power plants in response to international and federal climate action initiatives. With the advances brought by these direct and indirect demand-pull policies, coal-fired plants are being rapidly phased out in Canada, and this trend is projected to become more pronounced in future years. However, because the policies are fragmented and vary from province to province, there are still significant regional disparities in emission reductions. For instance, the satellite observation and NPRI data indicate that emissions from coal-fired plants and NO_2 concentration in the surrounding area continue to rise in Alberta. This trend may be reversed in the coming years, as Alberta, Saskatchewan, New Brunswick, and Nova Scotia have all made commitments to markedly increase the proportion of electricity supply from renewable sources in the future.

However, considering that new hydroelectric dam projects have met with public opposition due to their ecological impact, and that solar, wind, and biomass in Canada continue to lag behind the global average in terms of their market share, Canada's efforts to reduce emissions may need to focus on reducing consumption and maximizing incentives for energy efficiency and conservation (Li et al., 2018; Vazifeh et al., 2021). At the same time, Canada will need to make major capital investments in its power generation infrastructure

over the next 20 years. These investments also offer new opportunities for Canada, such as low-emission generation and smart grid technologies to ensure efficient use of network capacity. In addition, the non-distributability of some electricity sources can be addressed by integrating intermittent renewable resources through dispatchable energy or storage to ensure a reliable grid.

CHAPTER 6. CONCLUSIONS

6.1. Conclusions

In this thesis, a comprehensive review was conducted to assess the impact of elements in urban form on on-road vehicles GHG emissions. A small-medium North American city case study was given to track the progress in reducing real-world emissions over time and to estimate the future air quality impacts based on the trends of fleet mixes. It helps gain understanding of detailed source apportionment information to quantify the contributions to total emission made by different vehicle body types, different fuels, and manufacturer models in recent decades and how the fuel economy of the vehicle fleet has changed over the years. Following that, an assessment was conducted to analyze the impact of COVID-19 pandemic on GHG emissions from urban transportation and air quality in Canadian cities. The reduced traffic experienced throughout several lockdowns offers a glimpse of what air quality in cities would look like if the country switched to low-carbon transportation modes. Finally, the reductions in NO_2 emissions from thermal power plants in Canada were assessed to evaluate the government commitment of switching from fossil fuels to clean energy. The satellite observation was developed as a supplementary information management tool to verify the effect of technologies and policies on emissions changes from threshold perspective on a smaller spatial scale. Overall, this thesis provides some new insights on assessing air pollution and carbon emission levels from transportation and electricity sectors.

6.2. Recommendations for future research

- It is expected to further explore the impacts of evolution of urban form in the past decades on traffic-related emissions from road transportation.
- From global scale, it is necessary to provide a framework for evaluating the level of public transport service allocation, taking account of the effects of transit service allocation on private vehicle dependency and traffic-related emissions in different regions.

REFERENCES

Abdullahi, S., Pradhan, B., Mansor, S., Shariff, A.R.M., 2015. GIS-based modeling for the spatial measurement and evaluation of mixed land use development for a compact city. GIScience & Remote Sensing 52, 18-39.

Ahmed, Z., Cary, M., Shahbaz, M., Vo, X.V., 2021. Asymmetric nexus between economic policy uncertainty, renewable energy technology budgets, and environmental sustainability: Evidence from the United States. Journal of Cleaner Production, 127723.

Al-mulali, U., 2012. Factors affecting CO_2 emission in the Middle East: A panel data analysis. Energy 44, 564-569.

Alberta Capital Airshed, 2020. Live air data, https://capitalairshed.ca/about-us/our-role/.

Anderson, W.P., Kanaroglou, P.S., Miller, E.J., 1996. Urban form, energy and the environment: a review of issues, evidence and policy. Urban Studies 33, 7-35.

Anenberg, S.C., Miller, J., Minjares, R., Du, L., Henze, D.K., Lacey, F., Malley, C.S., Emberson, L., Franco, V., Klimont, Z., 2017. Impacts and mitigation of excess diesel-related NOx emissions in 11 major vehicle markets. Nature 545, 467-471.

Antich, M., 2019. Assessment of the commercial fleet market in Canada for 2019-2020. Automotive Fleet, https://www.automotive-fleet.com/344965/assessment-of-the-commercial-fleet-market-in-canada-for-2019-2020.

Asif, Z., Chen, Z., 2020. A life cycle based air quality modeling and decision support system (LCAQMS) for sustainable mining management. Journal of Environmental Informatics 35, 103-117.

Attoe, W., Logan, D., 1989. American urban architecture: Catalysts in the design of cities. Univ of California Press.

Audit and Evaluation Branch, Natural Resources Canada, 2019. Evaluation of the Regional Electricity Cooperation and Strategic Infrastructure (RECSI) Initiative, https://www.nrcan.gc.ca/nrcan/plans-performance-reports/strategic-evaluation-division/reports-plans-year/evaluation-reports-2019/evaluation-regional-electricity-cooperation-and-strategic-infrastructure-recsi-initiative/22363.

B.C. Air Quality Data, 2020. Current air quality data, https://envistaweb.env.gov.bc.ca/.

Bailey, B.K., 2018. Performance of ethanol as a transportation fuel, Handbook on Bioethanol. Routledge, pp. 37-60.

Bakx, K., 2020. COVID-19 wipes out demand for fossil fuels — will they bounce back?, CBC News, https://www.cbc.ca/news/business/covid-19-oil-gas-energy-transition-1.5552794.

Balsas, C.J.L., 2000. City center revitalization in Portugal: Lessons from two medium size cities. Cities 17, 19-31.

Baltagi, B.H., 2008. Econometric analysis of panel data. Springer.

Barla, P., Miranda-Moreno, L.F., Lee-Gosselin, M., 2011. Urban travel CO_2 emissions and land use: A case study for Quebec City. Transportation Research Part D: Transport and Environment 16, 423-428.

Bauwens, M., Compernolle, S., Stavrakou, T., Müller, J.F., Van Gent, J., Eskes, H., Levelt, P.F., van der A, R., Veefkind, J., Vlietinck, J., 2020. Impact of coronavirus outbreak

on NO_2 pollution assessed using TROPOMI and OMI observations. Geophysical Research Letters 47, e2020GL087978.
Bechle, M.J., Millet, D.B., Marshall, J.D., 2011. Effects of income and urban form on urban NO_2: Global evidence from satellites. Environmental Science & Technology 45, 4914-4919.
Bereitschaft, B., Debbage, K., 2013. Urban form, air pollution, and CO_2 emissions in large US metropolitan areas. The Professional Geographer 65, 612-635.
Berghauser Pont, M.Y., Haupt, P.A., 2009. Space, density and urban form.
Bishop, G.A., Haugen, M.J., 2018. The story of ever diminishing vehicle tailpipe emissions as observed in the Chicago, Illinois area. Environmental Science & Technology 52, 7587-7593.
Boarnet, M.G., 1994. The monocentric model and employment location. Journal of Urban Economics 36, 79-97.
Boersma, K., Eskes, H., Veefkind, J., Brinksma, E., Sneep, M.v., Van den Oord, G., Levelt, P., Stammes, P., Gleason, J., Bucsela, E., 2007. Near-real time retrieval of tropospheric NO_2 from OMI. Atmospheric Chemistry and Physics 7, 2103-2118.
Brown, D., Sadiq, R., Hewage, K., 2014. An overview of air emission intensities and environmental performance of grey cement manufacturing in Canada. Clean Technologies and Environmental Policy 16, 1119-1131.
Cai, M., An, C., Guy, C., 2020. Assessment of soil and water conservation practices in the loess hilly region using a coupled rainfall-runoff-erosion model. Sustainability 12, 934.
Cai, M., An, C., Guy, C., 2021. A scientometric analysis and review of biogenic volatile organic compound emissions: Research hotspots, new frontiers, and environmental implications. Renewable and Sustainable Energy Reviews 149, 111317.
Caïd, N., 2006. Decoupling the environmental impacts of transport from economic growth.
Canada Energy Regulator, 2017. Canada's Renewable Power Landscape 2017 – Energy Market Analysis, https://www.cer-rec.gc.ca/en/data-analysis/energy-commodities/electricity/report/2017-canadian-renewable-power/canadas-renewable-power-landscape-2017-energy-market-analysis-ghg-emission.html#:~:text=Greenhouse%20gas%20(GHG)%20emissions%20overview,are%20non%2Demitting%20when%20generating.
Canada Energy Regulator, 2019. Market Snapshot: How does Canada rank in terms of vehicle fuel economy?, https://www.cer-rec.gc.ca/en/data-analysis/energy-markets/market-snapshots/2019/market-snapshot-how-does-canada-rank-in-terms-vehicle-fuel-economy.html.
Canada Energy Regulator, 2021. Provincial and Territorial Energy Profiles – Alberta, https://www.cer-rec.gc.ca/en/data-analysis/energy-markets/provincial-territorial-energy-profiles/provincial-territorial-energy-profiles-alberta.html.
Carruthers, J.I., 2003. Growth at the fringe: The influence of political fragmentation in United States metropolitan areas. Papers in Regional Science 82, 475-499.
Cervero, R., 1988. Land-use mixing and suburban mobility. UC Berkeley: University of California Transportation Center, Berkeley, CA,
Cervero, R., Duncan, M., 2006. Which reduces vehicle travel more: Jobs-housing balance or retail-housing mixing? Journal of the American Planning Association 72, 475-490.

Chang, H.-S., Chen, T., 2016. Examine sustainable urban space based on compact city concept. Global Journal of Human-Social Science: B Geography, Geo-Sciences, Environmental Science & Disaster Management 16, 2-12.
Chen, F., Yin, Z., Ye, Y., Sun, D.J., 2020a. Taxi hailing choice behavior and economic benefit analysis of emission reduction based on multi-mode travel big data. Transport Policy 97, 73-84.
Chen, R., Wang, X., Meng, X., Hua, J., Zhou, Z., Chen, B., Kan, H., 2013. Communicating air pollution-related health risks to the public: An application of the Air Quality Health Index in Shanghai, China. Environment International 51, 168-173.
Chen, T., Guestrin, C., 2016. Xgboost: A scalable tree boosting system, Proceedings of the 22nd acm sigkdd international conference on knowledge discovery and data mining, pp. 785-794,
Chen, Z.K., An, C., Fang, H., Zhang, Y., Zhou, Z., Zhou, Y., Zhao, S., 2020b. Assessment of regional greenhouse gas emission from beef cattle production: A case study of Saskatchewan in Canada. Journal of Environmental Management 264, 110443.
Chui, E.H., Gao, H., 2010. Estimation of NOx emissions from coal-fired utility boilers. Fuel 89, 2977-2984.
Cirilli, A., Veneri, P., 2014. Spatial structure and carbon dioxide (CO_2) emissions due to commuting: An analysis of Italian urban areas. Regional Studies 48, 1993-2005.
Clark, L.P., Millet, D.B., Marshall, J.D., 2011. Air quality and urban form in US urban areas: Evidence from regulatory monitors. Environmental Science & Technology 45, 7028-7035.
Crane, R., Chatman, D.G., 2002. Traffic and Sprawl: Evidence from US Commuting from 1985-1997. University of Southern California, Los Angeles, CA.
Cuddihy, J., Kennedy, C., Byer, P., 2005. Energy use in Canada: environmental impacts and opportunities in relationship to infrastructure systems. Canadian Journal of Civil Engineering 32, 1-15.
Dabek-Zlotorzynska, E., Celo, V., Ding, L., Herod, D., Jeong, C.-H., Evans, G., Hilker, N., 2019. Characteristics and sources of $PM_{2.5}$ and reactive gases near roadways in two metropolitan areas in Canada. Atmospheric Environment 218, 116980.
Dai, Q., Liu, B., Bi, X., Wu, J., Liang, D., Zhang, Y., Feng, Y., Hopke, P.K., 2020. Dispersion normalized PMF provides insights into the significant changes in source contributions to $PM_{2.5}$ after the COVID-19 outbreak. Environmental Science & Technology 54, 9917-9927.
Danilina, V., Grigoriev, A., 2020. Information provision in environmental policy design. Journal of Environmental Informatics 36.
Davis, M., Moronkeji, A., Ahiduzzaman, M., Kumar, A., 2020. Assessment of renewable energy transition pathways for a fossil fuel-dependent electricity-producing jurisdiction. Energy for Sustainable Development 59, 243-261.
Dempsey, N., Brown, C., Raman, S., Porta, S., Jenks, M., Jones, C., Bramley, G., 2010. Elements of urban form, Dimensions of the sustainable city. Springer, pp. 21-51.
Doremus, J., Helfand, G., Liu, C., Donahue, M., Kahan, A., Shelby, M., 2019. Simpler is better: Predicting consumer vehicle purchases in the short run. Energy Policy 129, 1404-1415.
Dreessen, J., Sullivan, J., Delgado, R., 2016. Observations and impacts of transported Canadian wildfire smoke on ozone and aerosol air quality in the Maryland region

on June 9–12, 2015. Journal of the Air & Waste Management Association 66, 842-862.
Du, L., Wei, C., Cai, S., 2012. Economic development and carbon dioxide emissions in China: Provincial panel data analysis. China Economic Review 23, 371-384.
Dulal, H.B., Brodnig, G., Onoriose, C.G., 2011. Climate change mitigation in the transport sector through urban planning: A review. Habitat International 35, 494-500.
Duncan, M.J., Winkler, E., Sugiyama, T., Cerin, E., Leslie, E., Owen, N., 2010. Relationships of land use mix with walking for transport: do land uses and geographical scale matter? Journal of Urban Health 87, 782-795.
Ebrahimi-Khusfi, Z., Taghizadeh-Mehrjardi, R., Kazemi, M., Nafarzadegan, A.R., 2021. Predicting the ground-level pollutants concentrations and identifying the influencing factors using machine learning, wavelet transformation, and remote sensing techniques. Atmospheric Pollution Research 12, 101064.
Eggleston, H., Buendia, L., Miwa, K., Ngara, T., Tanabe, K., 2006a. 2006 IPCC guidelines for national greenhouse gas inventories.
Eggleston, S., Buendia, L., Miwa, K., Ngara, T., Tanabe, K., 2006b. 2006 IPCC guidelines for national greenhouse gas inventories. Institute for Global Environmental Strategies Hayama, Japan.
Environment, Canada, C.C., 2019. National inventory report 1990–2017: greenhouse gas sources and sinks in Canada. Environment and Climate Change Canada Gatineau, QC,
Environment and Climate Change Canada, 1969. National air pollution surveillance program, https://open.canada.ca/data/en/dataset.
Environment and Climate Change Canada, 2016. National Inventory Report 1990-2014: Greenhouse gas sources and sinks in Canada.
Environment and Climate Change Canada, 2018. Regulations Amending the Reduction of Carbon Dioxide Emissions from Coal-fired Generation of Electricity Regulations. Canada Gazatte, https://gazette.gc.ca/rp-pr/p2/2018/2018-12-12/html/sor-dors263-eng.html.
Environment and Climate Change Canada, 2019a. Canadian environmental sustainability Indicators: air pollutant emissions. ,
Environment and Climate Change Canada, 2019b. Canadian Environmental Sustainability Indicators: Air pollutant emissions. , www.canada.ca/en/environment-climate-change/services/environmental-indicators/airpollutant-emissions.html.
Environment and Climate Change Canada, 2019c. Local Air Quality Health Index conditions, https://weather.gc.ca/airquality/pages/index_e.html.
Environment and Climate Change Canada, 2020a. Canada's Air Pollutant Emissions Inventory Report 2020, Air pollutant emission inventory report, Gatineau, QC, https://www.canada.ca/en/environment-climate-change/services/air-pollution/publications/emissions-inventory-report-2020.html.
Environment and Climate Change Canada, 2020b. Canadian Environmental Sustainability Indicators: Air pollutant emissions., https://www.canada.ca/en/environment-climate-change/services/environmental-indicators/air-pollutant-emissions.html.
Environment and Climate Change Canada, 2020c. National Inventory Report 1990–2018: Greenhouse Gas Sources and Sinks in Canada: Executive Summary, Ottawa, p. 6, http://publications.gc.ca/site/eng/9.816345/publication.html.

Environmental Protection and Agency, 2021. Power Plant Emission Trends, https://www.epa.gov/airmarkets/power-plant-emission-trends.
Ernst, A., Zibrak, J.D., 1998. Carbon monoxide poisoning. New England Journal of Medicine 339, 1603-1608.
European Commission & European Space Agency, 2020. Copernicus sentinel-5P tropospheric nitrogen dioxide, https://maps.s5p-pal.com/.
Ewing, R., Cervero, R., 2001. Travel and the built environment: a synthesis. Transportation Research Record 1780, 87-114.
Ewing, R., Cervero, R., 2010. Travel and the built environment: A meta-analysis. Journal of the American Planning Association 76, 265-294.
Ewing, R., Pendall, R., Chen, D., 2003. Measuring sprawl and its transportation impacts. Transportation Research Record 1831, 175-183.
Ewing, R., Rong, F., 2008. The impact of urban form on US residential energy use. Housing Policy Debate 19, 1-30.
Ewing, R.H., Pendall, R., Chen, D.D., 2002. Measuring sprawl and its impact. Smart Growth America Washington, DC.
Fang, C., Wang, S., Li, G., 2015. Changing urban forms and carbon dioxide emissions in China: A case study of 30 provincial capital cities. Applied Energy 158, 519-531.
Farajzadeh, Z., Nematollahi, M.A., 2018. Energy intensity and its components in Iran: Determinants and trends. Energy Economics 73, 161-177.
Farren, N.J., Davison, J., Rose, R.A., Wagner, R.L., Carslaw, D.C., 2020. Underestimated ammonia emissions from road vehicles. Environmental Science & Technology 54, 15689-15697.
Feng, Q., An, C., Chen, Z., Wang, Z., 2020. Can deep tillage enhance carbon sequestration in soils? A meta-analysis towards GHG mitigation and sustainable agricultural management. Renewable and Sustainable Energy Reviews 133, 110293.
Fernandes, N., 2020. Economic effects of coronavirus outbreak (COVID-19) on the world economy. Available at SSRN 3557504.
Forster, P., Ramaswamy, V., Artaxo, P., Berntsen, T., Betts, R., Fahey, D.W., Haywood, J., Lean, J., Lowe, D.C., Myhre, G., 2007. Changes in atmospheric constituents and in radiative forcing. Chapter 2, Climate change 2007. The physical science basis.
Friedman, J.H., 2002. Stochastic gradient boosting. Computational Statistics & Data Analysis 38, 367-378.
Fujita, M., Ogawa, H., 1982. Multiple equilibria and structural transition of non-monocentric urban configurations. Regional Science and Urban Economics 12, 161-196.
Galster, G., Hanson, R., Ratcliffe, M.R., Wolman, H., Coleman, S., Freihage, J., 2001. Wrestling sprawl to the ground: defining and measuring an elusive concept. Housing Policy Debate 12, 681-717.
Glaeser, E.L., Kahn, M.E., 2010. The greenness of cities: Carbon dioxide emissions and urban development. Journal of Urban Economics 67, 404-418.
Godowitch, J., Gilliland, A., Draxler, R., Rao, S., 2008. Modeling assessment of point source NOx emission reductions on ozone air quality in the eastern United States. Atmospheric Environment 42, 87-100.
Gordon, P., Lee, B., 2015. Spatial structure and travel: Trends in commuting and non-commuting travels in US metropolitan areas, in: Hickman, R., Givoni, M., Bonilla,

D., Banister, D. (Eds.), Handbook on transport and development. Edward Elgar Publishing, Glos, UK.
Gordon, P., Richardson, H.W., 1997. Are compact cities a desirable planning goal? Journal of the American Planning Association 63, 95-106.
Gordon, S., 2017. Recession of 2008–09 in Canada. The Canadian Encyclopedia https://www.thecanadianencyclopedia.ca/en/article/recession-of-200809-in-canada.
Government of Alverta, 2020. Alberta air data warehouse, https://www.alberta.ca/alberta-air-data-warehouse.aspx.
Government of canada, 2013. Air pollution: regulations for vehicles and engines, https://www.canada.ca/en/environment-climate-change/services/air-pollution/sources/transportation/regulations-vehicles-engines.html.
Government of Canada, 2014. Regulations amending the on-road vehicle and engine emission regulations and other regulations made under the canadian environmental protection act, 1999, https://canadagazette.gc.ca/rp-pr/p1/2014/2014-09-27/html/reg1-eng.html.
Government of canada, 2017. Cleaner vehicles, engines and fuels, https://www.canada.ca/en/environment-climate-change/services/management-toxic-substances/sources/cleaner-vehicles-engines-fuels.html.
Government of Canada, 2018. Technical backgrounder: Federal regulations for electricity sector, https://www.canada.ca/en/environment-climate-change/services/managing-pollution/energy-production/technical-backgrounder-regulations-2018.html.
Government of Canada, 2019. About the National Pollutant Release Inventory, https://www.canada.ca/en/environment-climate-change/services/national-pollutant-release-inventory/about-national-pollutant-release-inventory.html.
Government of canada, 2020a. Compliance options to meet the Clean Fuel Standard, https://www.canada.ca/en/environment-climate-change/services/managing-pollution/energy-production/fuel-regulations/clean-fuel-standard/compliance-options.html.
Government of Canada, 2020b. Energy and greenhouse gas emissions (GHGs), https://www.nrcan.gc.ca/science-and-data/data-and-analysis/energy-data-and-analysis/energy-facts/energy-and-greenhouse-gas-emissions-ghgs/20063#L4.
Government of Canada, 2021a. Greenhouse gas emissions, https://www.canada.ca/en/environment-climate-change/services/environmental-indicators/greenhouse-gas-emissions.html.
Government of Canada, 2021b. National air pollution surveillance (NAPS) program, https://data-donnees.ec.gc.ca/data/air/monitor/national-air-pollution-surveillance-naps-program/?lang=en.
Government of Newfoundland and Labrador, 2020. Air monitoring, https://www.gov.nl.ca/mae/env-protection/science/airmon/.
Government of Saskatchewan, 2020. Current and historical saskatchewan air quality data, http://environment.gov.sk.ca/Default.aspx?DN=45dbacf9-7290-435e-b44b-0d526de3e5d1&l=English.
Government of saskatchewan, 2021. Air pollutant concentration, https://www.saskatchewan.ca/residents/environment-public-health-and-safety/state-of-the-environment/saskatchewans-state-of-the-environment/air-

pollutant-concentration.
Grange, S.K., Carslaw, D.C., Lewis, A.C., Boleti, E., Hueglin, C., 2018. Random forest meteorological normalisation models for Swiss PM_{10} trend analysis. Atmospheric Chemistry and Physics 18, 6223-6239.
Güngör, O., Ertugrul, H.M., Soytas, U., 2020. The impact of COVID-19 outbreak on Turkish gasoline consumption. Available at SSRN 3611788.
Hankey, S., Marshall, J.D., 2010. Impacts of urban form on future US passenger-vehicle greenhouse gas emissions. Energy Policy 38, 4880-4887.
Harrison, K., Antweiler, W., 2003. Incentives for pollution abatement: Regulation, regulatory threats, and non-governmental pressures. Journal of Policy Analysis and Management 22, 361-382.
Hastie, T., Tibshirani, R., Friedman, J., 2009. The elements of statistical learnin. Cited on, 33.
Haugen, M.J., Bishop, G.A., Thiruvengadam, A., Carder, D.K., 2018. Evaluation of heavy- and medium-duty on-road vehicle emissions in California's south coast air basin. Environmental Science & Technology 52, 13298-13305.
Hawkes, A., 2014. Long-run marginal CO_2 emissions factors in national electricity systems. Applied Energy 125, 197-205.
Hibbard, P.J., Schatzki, T., 2012. The interdependence of electricity and natural gas: current factors and future prospects. The Electricity Journal 25, 6-17.
Hu, M.M., Xia, B.C., 2020. Land-use variations in Regions with rapid economic development - A case study in the Pearl River Delta. Journal of Environmental Informatics Letters 3, 49-58.
Huang, J., Lu, X.X., Sellers, J.M., 2007. A global comparative analysis of urban form: Applying spatial metrics and remote sensing. Landscape and Urban Planning 82, 184-197.
International Energy Agency, 2019a. Fuel Economy in Major Car Markets, https://www.iea.org/reports/fuel-economy-in-major-car-markets.
International Energy Agency, 2019b. Fuel economy in major car markets: technology and policy drivers 2005-2017, p. 15, https://www.iea.org/reports/fuel-economy-in-major-car-markets.
International Energy Agency, 2020a. Global Energy Review 2020, Paris https://www.iea.org/reports/global-energy-review-2020.
International Energy Agency, 2020b. Policies database, https://www.iea.org/policies.
International Energy Agency, 2021. Policies database, https://www.iea.org/policies/about.
Ji, L., Huang, G., Niu, D., Cai, Y., Yin, J., 2020. A stochastic optimization model for carbon-emission reduction investment and sustainable energy planning under cost-risk control. Journal of Environmental Informatics 36, 107-118.
Jiao, X., Liu, X., Gu, Y., Wu, X., Wang, S., Zhou, Y., 2020. Satellite verification of ultra-low emission reduction effect of coal-fired power plants. Atmospheric Pollution Research 11, 1179-1186.
Johnston Edwards, S., Walker, T.R., 2020. An overview of Canada's National Pollutant Release Inventory program as a pollution control policy tool. Journal of Environmental Planning and Management 63, 1097-1113.
Jordaan, S.M., Romo-Rabago, E., McLeary, R., Reidy, L., Nazari, J., Herremans, I.M., 2017. The role of energy technology innovation in reducing greenhouse gas

emissions: A case study of Canada. Renewable and Sustainable Energy Reviews 78, 1397-1409.
Kahn, M.E., 2009. Urban growth and climate change. Annual Review of Resource Economics 1, 333-350.
Karimi, S., Nazemi, A., Sadraddini, A., Xu, T., Bateni, S., Fard, A., 2020. Estimation of forest leaf area index using meteorological data: assessment of heuristic models. Journal of Environmental Informatics 36, 119-132.
Kean, A.J., Harley, R.A., Kendall, G.R., 2003. Effects of vehicle speed and engine load on motor vehicle emissions. Environmental Science & Technology 37, 3739-3746.
Kim, S.W., Heckel, A., McKeen, S., Frost, G., Hsie, E.Y., Trainer, M., Richter, A., Burrows, J., Peckham, S., Grell, G., 2006. Satellite-observed US power plant NOx emission reductions and their impact on air quality. Geophysical Research Letters 33.
Kitamura, R., Akiyama, T., Yamamoto, T., Golob, T.F., 2001. Accessibility in a metropolis: Toward a better understanding of land use and travel. Transportation Research Record 1780, 64-75.
Krizek, K.J., 2003. Neighborhood services, trip purpose, and tour-based travel. Transportation 30, 387-410.
Lamsal, L., Martin, R., Van Donkelaar, A., Celarier, E., Bucsela, E., Boersma, K., Dirksen, R., Luo, C., Wang, Y., 2010. Indirect validation of tropospheric nitrogen dioxide retrieved from the OMI satellite instrument: Insight into the seasonal variation of nitrogen oxides at northern midlatitudes. Journal of Geophysical Research: Atmospheres 115.
Le Quéré, C., Jackson, R.B., Jones, M.W., Smith, A.J., Abernethy, S., Andrew, R.M., De-Gol, A.J., Willis, D.R., Shan, Y., Canadell, J.G., 2020. Temporary reduction in daily global CO_2 emissions during the COVID-19 forced confinement. Nature Climate Change, 1-7.
Leard, B., McConnell, V., Zhou, Y.C., 2019. The effect of fuel price changes on fleet demand for new vehicle fuel economy. The Journal of Industrial Economics 67, 127-159.
Lee, J., Kurisu, K., An, K., Hanaki, K., 2015. Development of the compact city index and its application to Japanese cities. Urban Studies 52, 1054-1070.
Lee, J.H., Lim, S., 2018. The selection of compact city policy instruments and their effects on energy consumption and greenhouse gas emissions in the transportation sector: The case of South Korea. Sustainable Cities and Society 37, 116-124.
Lee, S., Lee, B., 2014. The influence of urban form on GHG emissions in the US household sector. Energy Policy 68, 534-549.
Legras, S., Cavailhès, J., 2016. Environmental performance of the urban form. Regional Science and Urban Economics 59, 1-11.
Lerner, U., Hirshfeld, O., Fishbasinl, B., 2019. Optimal deployment of a heterogeneous air quality sensor network. Journal of Environmental Informatics 34, 99-107.
Li, G., Sun, W., Huang, G.H., Lv, Y., Liu, Z., An, C., 2018. Planning of integrated energy-environment systems under dual interval uncertainties. International Journal of Electrical Power & Energy Systems 100, 287-298.
Li, J., Hao, Y., Simayi, M., Shi, Y., Xi, Z., Xie, S., 2019a. Verification of anthropogenic VOC emission inventory through ambient measurements and satellite retrievals. Atmospheric Chemistry and Physics 19, 5905-5921.

Li, L., Shan, Y., Lei, Y., Wu, S., Yu, X., Lin, X., Chen, Y., 2019b. Decoupling of economic growth and emissions in China's cities: a case study of the Central Plains urban agglomeration. Applied Energy 244, 36-45.
Lipp, J., 2007. Lessons for effective renewable electricity policy from Denmark, Germany and the United Kingdom. Energy Policy 35, 5481-5495.
Liu, C., Shen, Q., 2011. An empirical analysis of the influence of urban form on household travel and energy consumption. Computers, Environment and Urban Systems 35, 347-357.
Liu, F., Choi, S., Li, C., Fioletov, V.E., McLinden, C.A., Joiner, J., Krotkov, N.A., Bian, H., Janssens-Maenhout, G., Darmenov, A.S., 2018. A new global anthropogenic SO_2 emission inventory for the last decade: a mosaic of satellite-derived and bottom-up emissions. Atmospheric Chemistry and Physics 18, 16571-16586.
Liu, Y., Chen, X., Wang, H., 2020. Perspective for emission and control of nitrous gas in biological wastewater treatment. Journal of Environmental Informatics Letters 2, 82-90.
Llacuna, S., Gorriz, A., Sanpera, C., Nadal, J., 1995. Metal accumulation in three species of passerine birds (Emberiza cia, Parus major, and Turdus merula) subjected to air pollution from a coal-fired power plant. Archives of Environmental Contamination and Toxicology 28, 298-303.
Longley, P.A., Mesev, V., 2000. On the measurement and generalisation of urban form. Environment and Planning A 32, 473-488.
Lu, Z., Streets, D.G., 2012. Increase in NOx emissions from Indian thermal power plants during 1996–2010: unit-based inventories and multisatellite observations. Environmental Science & Technology 46, 7463-7470.
Lu, Z., Streets, D.G., de Foy, B., Krotkov, N.A., 2013. Ozone Monitoring Instrument observations of interannual increases in SO_2 emissions from Indian coal-fired power plants during 2005–2012. Environmental Science & Technology 47, 13993-14000.
Ma, J., Ding, Y., Cheng, J.C., Jiang, F., Tan, Y., Gan, V.J., Wan, Z., 2020. Identification of high impact factors of air quality on a national scale using big data and machine learning techniques. Journal of Cleaner Production 244, 118955.
Makido, Y., Dhakal, S., Yamagata, Y., 2012. Relationship between urban form and CO_2 emissions: Evidence from fifty Japanese cities. Urban Climate 2, 55-67.
Manaugh, K., Miranda-Moreno, L.F., El-Geneidy, A.M., 2010. The effect of neighbourhood characteristics, accessibility, home–work location, and demographics on commuting distances. Transportation 37, 627-646.
Mapa Metro, 2021. Metros of America, https://mapa-metro.com/en/Canada/Toronto/Toronto-Subway-map.htm.
Marshall, J.D., McKone, T.E., Deakin, E., Nazaroff, W.W., 2005. Inhalation of motor vehicle emissions: effects of urban population and land area. Atmospheric Environment 39, 283-295.
Matsuhashi, K., Ariga, T., 2016. Estimation of passenger car CO_2 emissions with urban population density scenarios for low carbon transportation in Japan. IATSS Research 39, 117-120.
Matz, C.J., Egyed, M., Xi, G., Racine, J., Pavlovic, R., Rittmaster, R., Henderson, S.B., Stieb, D.M., 2020. Health impact analysis of $PM_{2.5}$ from wildfire smoke in Canada

(2013–2015, 2017–2018). Science of The Total Environment 725, 138506.
McConville, M.E., Rodriguez, D.A., Clifton, K., Cho, G., Fleischhacker, S., 2011. Disaggregate land uses and walking. American Journal of Preventive Medicine 40, 25-32.
Meijers, E.J., Burger, M.J., 2010. Spatial structure and productivity in US metropolitan areas. Environment and Planning A 42, 1383-1402.
Mills, D.E., 1981. Growth, speculation and sprawl in a monocentric city. Journal of Urban Economics 10, 201-226.
Miranda-Moreno, L.F., Bettex, L., Zahabi, S.A.H., Kreider, T.M., Barla, P., 2011. Simultaneous modeling of endogenous influence of urban form and public transit accessibility on distance traveled. Transportation Research Record 2255, 100-109.
Mizutani, F., Nakayama, N., Tanaka, T., 2015. An analysis of the effects of the compact city on economic activities in Japan, The Home of Regional Science in Europe. European Regional Science Association,
Mohamed, M., Higgins, C.D., Ferguson, M., Réquia, W.J., 2018. The influence of vehicle body type in shaping behavioural intention to acquire electric vehicles: A multi-group structural equation approach. Transportation Research Part A: Policy and Practice 116, 54-72.
Moshiri, S., Duah, N., 2016. Changes in energy intensity in Canada. The Energy Journal 37.
Muhammad, S., Long, X., Salman, M., 2020. COVID-19 pandemic and environmental pollution: a blessing in disguise? Science of The Total Environment, 138820.
Muller, N.Z., Mendelsohn, R., Nordhaus, W., 2011. Environmental accounting for pollution in the United States economy. American Economic Review 101, 1649-1675.
Muñiz, I., García López, M.-À., Calatayud, D., 2006. Sprawl: definición, causas y efectos. Department of Applied Economics at Universitat Autonoma of Barcelona, Working Papers.
Nasreen, S., Saidi, S., Ozturk, I., 2018. Assessing links between energy consumption, freight transport, and economic growth: evidence from dynamic simultaneous equation models. Environmental Science and Pollution Research 25, 16825-16841.
National Post, 2010. Urban Scrawl: Gas power plant needs buffer zone, https://nationalpost.com/posted-toronto/urban-scrawl-gas-power-plant-needs-buffer-zone.
Natural Resources Canada, 2009. 2009 Canadian vehicle survey: summary report.
Natural Resources Canada, 2021. Fuel consumption ratings search tool, https://fcr-ccc.nrcan-rncan.gc.ca/fr/.
Newman, P.W., Kenworthy, J.R., 1996. The land use—transport connection: An overview. Land Use Policy 13, 1-22.
Nikzad, R., Sedigh, G., 2017. Greenhouse gas emissions and green technologies in Canada. Environmental Development 24, 99-108.
Nova Scotia Environment, 2020. Nova scotia environment ambient air quality data, https://novascotia.ca/nse/airdata/.
OECD, G.G.S., 2012. Compact city policies: A comparative assessment. OECD Publishing, Paris,
Orun, A., Elizondo, D., Goodyer, E., Paluszczyszyn, D., 2018. Use of Bayesian inference

method to model vehicular air pollution in local urban areas. Transportation Research Part D: Transport and Environment 63, 236-243.
Ou, S., He, X., Ji, W., Chen, W., Sui, L., Gan, Y., Lu, Z., Lin, Z., Deng, S., Przesmitzki, S., 2020. Machine learning model to project the impact of COVID-19 on US motor gasoline demand. Nature Energy, 1-8.
Parr, S., Wolshon, B., Renne, J., Murray-Tuite, P., Kim, K., 2020. Traffic Impacts of the COVID-19 Pandemic: Statewide Analysis of Social Separation and Activity Restriction. Natural Hazards Review 21, 04020025.
Peinado-Guerrero, M.A., Villalobos, J.R., Phelan, P.E., Campbell, N.A., 2021. Stochastic framework for peak demand reduction opportunities with solar energy for manufacturing facilities. Journal of Cleaner Production, 127891.
Pérez, J., de Andrés, J.M., Borge, R., de la Paz, D., Lumbreras, J., Rodríguez, E., 2019. Vehicle fleet characterization study in the city of Madrid and its application as a support tool in urban transport and air quality policy development. Transport Policy 74, 114-126.
Plumptre, B., Flanagan, E., 2017. Using equivalency agreements to advance Canadian climate policy. JSTOR.
Preacher, K.J., Zhang, Z., Zyphur, M.J., 2011. Alternative methods for assessing mediation in multilevel data: The advantages of multilevel SEM. Structural Equation Modeling 18, 161-182.
Raub, J.A., Mathieu-Nolf, M., Hampson, N.B., Thom, S.R., 2000. Carbon monoxide poisoning—a public health perspective. Toxicology 145, 1-14.
Richter, A., Burrows, J.P., Nüß, H., Granier, C., Niemeier, U., 2005. Increase in tropospheric nitrogen dioxide over China observed from space. Nature 437, 129-132.
Ritchie, H., 2020. Cars, planes, trains: where do CO_2 emissions from transport come from?, https://ourworldindata.org/co2-emissions-from-transport.
Ritchie, H., Roser, M., 2020. Energy, https://ourworldindata.org/energy.
Ropkins, K., Beebe, J., Li, H., Daham, B., Tate, J., Bell, M., Andrews, G., 2009. Real-world vehicle exhaust emissions monitoring: review and critical discussion. Critical Reviews in Environmental Science and Technology 39, 79-152.
Russell, A.R., Valin, L.C., Bucsela, E.J., Wenig, M.O., Cohen, R.C., 2010. Space-based constraints on spatial and temporal patterns of NOx emissions in California, 2005− 2008. Environmental science & technology 44, 3608-3615.
Sadullah, A.F.M., Yahaya, N.Z., Latif, S.R.S.A., 2003. Air pollution from motor vehicles A mathematical model analysis: Case study in Ipoh City, Perak, Malaysia. Journal of the Eastern Asia Society for Transportation Studies 5, 2367-2391.
Schoettle, B., Sivak, M., 2017. Consumer preferences and motivations for owning light trucks versus passenger cars. Report No. SWT-2017-7). Ann Arbor: The University of Michigan Sustainable Worldwide Transportation.
Schweitzer, L., Zhou, J., 2010. Neighborhood air quality, respiratory health, and vulnerable populations in compact and sprawled regions. Journal of the American Planning Association 76, 363-371.
Senbel, M., Church, S., 2010. The relationship between urban form and GHG emissions. University of British Columbia,
Seo, Y., Kim, S.-M., 2013. Estimation of greenhouse gas emissions from road traffic: A

case study in Korea. Renewable and Sustainable Energy Reviews 28, 777-787.
Shan, Y., Fang, S., Cai, B., Zhou, Y., Li, D., Feng, K., Hubacek, K., 2021. Chinese cities exhibit varying degrees of decoupling of economic growth and CO_2 emissions between 2005 and 2015. One Earth 4, 124-134.
Shiraki, H., Matsumoto, K.i., Shigetomi, Y., Ehara, T., Ochi, Y., Ogawa, Y., 2020. Factors affecting CO_2 emissions from private automobiles in Japan: The impact of vehicle occupancy. Applied Energy 259, 114196.
Smith, L.V., Tarui, N., Yamagata, T., 2020. Assessing the impact of COVID-19 on global fossil fuel consumption and CO_2 emissions. ISER DP.
Song, P., Huang, G., An, C., Zhang, P., Chen, X., Ren, S., 2019. Performance analysis and life cycle greenhouse gas emission assessment of an integrated gravitational-flow wastewater treatment system for rural areas. Environmental Science and Pollution Research 26, 25883-25897.
Srinivasan, S., 2002. Quantifying spatial characteristics of cities. Urban Studies 39, 2005-2028.
Statistics Canada, 2014. Metropolitan gross domestic product, experimental estimates (x 1,000,000), https://www150.statcan.gc.ca/t1/tbl1/en/tv.action?pid=3610042301&pickMembers%5B0%5D=2.1&cubeTimeFrame.startYear=2001&cubeTimeFrame.endYear=2009&referencePeriods=20010101%2C20090101.
Statistics Canada, 2020a. Energy statistics, June 2020, https://www150.statcan.gc.ca/n1/daily-quotidien/200904/dq200904d-eng.htm.
Statistics Canada, 2020b. Gross domestic product (GDP) at basic prices, by census metropolitan area (CMA) (x 1,000,000), https://www150.statcan.gc.ca/t1/tbl1/en/tv.action?pid=3610046801&cubeTimeFrame.startYear=2009&cubeTimeFrame.endYear=2017&referencePeriods=20090101%2C20170101.
Statistics Canada, 2021a. Labour force characteristics, monthly, seasonally adjusted and trend-cycle, last 5 months, https://www150.statcan.gc.ca/t1/tbl1/en/tv.action?pid=1410028701&pickMembers%5B0%5D=1.9&pickMembers%5B1%5D=3.1&pickMembers%5B2%5D=4.8&pickMembers%5B3%5D=5.1&cubeTimeFrame.startMonth=01&cubeTimeFrame.startYear=2001&cubeTimeFrame.endMonth=12&cubeTimeFrame.endYear=2018&referencePeriods=20010101%2C20181201.
Statistics Canada, 2021b. Population estimates, quarterly, https://www150.statcan.gc.ca/t1/tbl1/en/tv.action?pid=1710000901.
Statistics Canada, 2021c. Population estimates, quarterly, https://www150.statcan.gc.ca/t1/tbl1/en/tv.action?pid=1710000901&cubeTimeFrame.startMonth=04&cubeTimeFrame.startYear=2008&cubeTimeFrame.endMonth=10&cubeTimeFrame.endYear=2017&referencePeriods=20080401%2C20171001.
Stone, B., Hess, J.J., Frumkin, H., 2010. Urban form and extreme heat events: are sprawling cities more vulnerable to climate change than compact cities? Environmental Health Perspectives 118, 1425-1428.
Stone Jr, B., 2008. Urban sprawl and air quality in large US cities. Journal of Environmental Management 86, 688-698.

Stone Jr, B., Rodgers, M.O., 2001. Urban form and thermal efficiency: how the design of cities influences the urban heat island effect. American Planning Association. Journal of the American Planning Association 67, 186.
Su, B., Ang, B., Liu, Y., 2021. Multi-region input-output analysis of embodied emissions and intensities: Spatial aggregation by linking regional and global datasets. Journal of Cleaner Production, 127894.
Su, Q., 2010. Travel demand in the US urban areas: A system dynamic panel data approach. Transportation Research Part A: Policy and Practice 44, 110-117.
Su, T., Zhang, J., Li, J., Ni, Y., 2011. Influence factors of urban traffic carbon emission: an empirical study with panel data of big four city of china. Industrial Engineering and Management 16, 134-138.
Sun, K., Tao, L., Miller, D.J., Pan, D., Golston, L.M., Zondlo, M.A., Griffin, R.J., Wallace, H.W., Leong, Y.J., Yang, M.M., 2017. Vehicle emissions as an important urban ammonia source in the United States and China. Environmental Science & Technology 51, 2472-2481.
Taghizadeh-Hesary, F., Yoshino, N., Rasoulinezhad, E., 2017. Impact of the Fukushima nuclear disaster on the oil-consuming sectors of Japan. Journal of Comparative Asian Development 16, 113-134.
Tan, R., Lin, B., 2018. What factors lead to the decline of energy intensity in China's energy intensive industries? Energy Economics 71, 213-221.
Tang, M., Mudd, G.M., 2014. Canadian power stations and the National Pollutant Release Inventory (NPRI): a success story for pollution intensity? Water, Air, & Soil Pollution 225, 1-17.
Tanzer-Gruener, R., Li, J., Eilenberg, S.R., Robinson, A.L., Presto, A.A., 2020. Impacts of modifiable factors on ambient air pollution: A case study of COVID-19 shutdowns. Environmental Science & Technology Letters 7, 554-559.
Tapio, P., 2005. Towards a theory of decoupling: degrees of decoupling in the EU and the case of road traffic in Finland between 1970 and 2001. Transport Policy 12, 137-151.
Taylor, S., Edwards, S.J., Walker, T.R., 2020. A toxicity-based analysis of Canada's National Pollutant Release Inventory (NPRI): a case study in Nova Scotia. Environmental Science and Pollution Research 27, 2238-2247.
The British Petroleum Company plc, 2021. Statistical Review of World Energy, https://www.bp.com/en/global/corporate/energy-economics/statistical-review-of-world-energy.html.
Thomas, C., 2009. Fuel cell and battery electric vehicles compared. International Journal of Hydrogen Energy 34, 6005-6020.
Tian, X., An, C., Chen, Z.K., Tian, Z., 2021. Assessing the impact of COVID-19 pandemic on urban transportation and air quality in Canada. Science of the Total Environment 765, 144270.
Tian, X.L., An, C.J., Chen, Z.K., 2020. Assessing the Impact of Urban Form on the Greenhouse Gas Emissions from Household Vehicles: A Review. Journal of Environmental Informatics.
TOMTOM, 2020. Tomtom traffic index, https://www.tomtom.com/en_gb/traffic-index/.
TransAlta Corporation, 2020. Management's Discussion and Analysis, https://www.transalta.com/wp-content/uploads/2020/11/2020.09.30-TAC-

Combined-MDA-and-FS-FINAL.pdf.
Travisi, C.M., Camagni, R., Nijkamp, P., 2010. Impacts of urban sprawl and commuting: a modelling study for Italy. Journal of Transport Geography 18, 382-392.
Tsai, Y.H., 2005. Quantifying urban form: compactness versus sprawl. Urban Studies 42, 141-161.
Vazifeh, Z., Mafakheri, F., An, C., 2021. Biomass supply chain coordination for remote communities: A game-theoretic modeling and analysis approach. Sustainable Cities and Society 69, 102819.
Veneri, P., 2010. Urban polycentricity and the costs of commuting: Evidence from Italian metropolitan areas. Growth and Change 41, 403-429.
Vorano, N., 2015. The shift from manual: Why the demise of stick shift is accelerating. The Globe and Mail, https://www.theglobeandmail.com/globe-drive/news/industry-news/the-shift-from-manual-why-the-demise-of-stick-shift-is-accelerating/article26795936/.
Vu, T.V., Shi, Z., Cheng, J., Zhang, Q., He, K., Wang, S., Harrison, R.M., 2019. Assessing the impact of clean air action on air quality trends in Beijing using a machine learning technique. Atmospheric Chemistry and Physics 19, 11303-11314.
Walker, T.R., 2018. Effectiveness of the national pollutant release inventory as a policy tool to curb atmospheric industrial emissions in Canada. PeerJ Preprints 6, e27372v27371.
Walks, A., 2015. Stopping the 'war on the car': Neoliberalism, Fordism, and the politics of automobility in Toronto. Mobilities 10, 402-422.
Wang, J.M., Jeong, C.-H., Hilker, N., Shairsingh, K.K., Healy, R.M., Sofowote, U., Debosz, J., Su, Y., McGaughey, M., Doerksen, G., 2018. Near-road air pollutant measurements: accounting for inter-site variability using emission factors. Environmental science & technology 52, 9495-9504.
Wang, Q., Su, M., 2020. A preliminary assessment of the impact of COVID-19 on environment–A case study of China. Science of the Total Environment, 138915.
Wang, Q., Wang, S., 2020. Preventing carbon emission retaliatory rebound post-COVID-19 requires expanding free trade and improving energy efficiency. Science of The Total Environment 746, 141158.
Wang, Y., Wen, Y., Wang, Y., Zhang, S., Zhang, K.M., Zheng, H., Xing, J., Wu, Y., Hao, J., 2020. Four-month changes in air quality during and after the COVID-19 lockdown in six megacities in China. Environmental Science & Technology Letters.
World Resources Institute, 2019. Everything You Need to Know About the Fastest-Growing Source of Global Emissions: Transport, https://www.wri.org/insights/everything-you-need-know-about-fastest-growing-source-global-emissions-transport.
Wu, Q., Xia, X., 2019. Response of surface water quality in urban and non-urban areas to heavy rainfall: Implications for the impacts of climate change. Journal of Environmental Informatics Letters 1, 27-36.
Wu, R., Liu, F., Tong, D., Zheng, Y., Lei, Y., Hong, C., Li, M., Liu, J., Zheng, B., Bo, Y., 2019. Air quality and health benefits of China's emission control policies on coal-fired power plants during 2005–2020. Environmental Research Letters 14, 094016.
Wu, Y., Arapi, A., Huang, J., Gross, B., Moshary, F., 2018. Intra-continental wildfire smoke transport and impact on local air quality observed by ground-based and satellite

remote sensing in New York City. Atmospheric Environment 187, 266-281.
Xiang, J., Austin, E., Gould, T., Larson, T., Shirai, J., Liu, Y., Marshall, J., Seto, E., 2020a. Impacts of the COVID-19 responses on traffic-related air pollution in a Northwestern US city. Science of the Total Environment 747, 141325.
Xiang, J., Austin, E., Gould, T., Larson, T., Shirai, J., Liu, Y., Marshall, J., Seto, E., 2020b. Impacts of the COVID-19 responses on traffic-related air pollution in a Northwestern US city. Science of the Total Environment, 141325.
Xiao, L., Christakos, G., He, J., Lang, Y., 2020a. Space-time ground-level $PM_{2.5}$ distribution at the Yangtze River Delta: a comparison of Kriging, LUR, and combined BME-LUR techniques. Journal of Environmental Informatics 36.
Xiao, L., Christakos, G., He, J., Lang, Y., 2020b. Space-Time Ground-Level PM2. 5 Distribution at the Yangtze River Delta: A Comparison of Kriging, LUR, and Combined BME-LUR Techniques. Journal of Environmental Informatics 36, 33-42.
Yang, W., Li, T., Cao, X., 2015. Examining the impacts of socio-economic factors, urban form and transportation development on CO_2 emissions from transportation in China: a panel data analysis of China's provinces. Habitat International 49, 212-220.
Yang, Z., 2019. DCT-based least-squares predictive model for hourly AQI fluctuation forecasting. Journal of Environmental Informatics.
Yang, Z., Bandivadekar, A., 2017. Light-duty vehicle greenhouse gas and fuel economy standards. ICCT report, 16.
Yao, Y., Huang, G., An, C., Chen, X., Zhang, P., Xin, X., Shen, J., Agnew, J., 2020. Anaerobic digestion of livestock manure in cold regions: Technological advancements and global impacts. Renewable and Sustainable Energy Reviews 119, 109494.
Ye, X., Chen, B., Lee, K., Storesund, R., Zhang, B., 2020. An integrated offshore oil spill response decision making approach by human factor analysis and fuzzy preference evaluation. Environmental Pollution, 114294.
Yu, L., Li, Y., Huang, G., An, C., 2017. A robust flexible-probabilistic programming method for planning municipal energy system with considering peak-electricity price and electric vehicle. Energy Conversion and Management 137, 97-112.
Zahabi, S.A.H., Miranda-Moreno, L., Patterson, Z., Barla, P., Harding, C., 2012. Transportation greenhouse gas emissions and its relationship with urban form, transit accessibility and emerging green technologies: a Montreal case study. Procedia-Social and Behavioral Sciences 54, 966-978.
Zambrano-Monserrate, M.A., Ruano, M.A., Sanchez-Alcalde, L., 2020. Indirect effects of COVID-19 on the environment. Science of the Total Environment, 138813.
Zarei, F., Nik-Bakht, M., 2021. Citizen engagement body of knowledge–A fuzzy decision maker for index-term selection in built environment projects. Cities 112, 103137.
Zhang, P., Huang, G., An, C., Fu, H., Gao, P., Yao, Y., Chen, X., 2019. An integrated gravity-driven ecological bed for wastewater treatment in subtropical regions: process design, performance analysis, and greenhouse gas emissions assessment. Journal of Cleaner Production 212, 1143-1153.
Zhang, Q., Streets, D.G., He, K., 2009. Satellite observations of recent power plant construction in Inner Mongolia, China. Geophysical Research Letters 36.

Zhang, T., Zeng, A., 2013. Spatial econometrics analysis on China transport carbon emissions. Urban Development, 10.

Zhou, N., Li, L., 2020. An ecosocial climax model based on concepts of climax community for analyzing communities in silas marner to ensure protection of ecosystem. Journal of Environmental Informatics 35, 45-55.

PUBLICATIONS

(1) ***Tian, X.***, An, C., and Chen, Z. K. (2020). Assessing the impact of urban form on the greenhouse gas emissions from household vehicles: A review. ***Journal of Environmental Informatics Letters*** (International Society of Environmental Information Sciences), 3(2), 70-85. DOI: 10.3808/jeil.202000029. (Adapted into CHAPTER 2)

(2) ***Tian, X.***, An, C., Chen, Z. K., Tian, Z. K. (2021). Assessing the impact of COVID-19 pandemic on urban transportation and air quality in Canada. ***Science of The Total Environment*** *(Elsevier)*, 765:144270. DOI: 10.1016/j.scitotenv.2020.144270. (Adapted into CHAPTER 4)

(3) ***Tian, X.***, An, C., Nik-Bakht, M., Chen, Z. K. (2021) Assessment of reductions in NO_2 emissions from thermal power plants in Canada based on the analysis of policy, inventory, and satellite data. ***Journal of Cleaner Production*** *(Elsevier).* Submitted in July 2021. Under review. Manuscript ID: JCLEPRO-D-21-13886 (Adapted into CHAPTER 5)

(4) Chen, Z. K., An, C., Chen, X., ***Tian, X.*** et al. (2021). Inexact inventory-theory-based optimization of oily waste management system in shoreline spill response. ***Science of The Total Environment*** *(Elsevier)*, 777:146078. DOI: 10.1016/j.scitotenv.2021.146078.

(5) Chen, Z. K., An, C., ***Tian, X*** et al. (2021). Exploring the use of cellulose nanocrystal as surface-washing agent for oiled shoreline cleanup. ***Journal of Hazardous Materials*** *(Elsevier)*, 402: 123464, DOI: 10.1016/j.jhazmat.2020.123464.

(6) Chen, Z. K., An, C., ***Tian, X*** et al. (2021). Spatiotemporal analysis of land use pattern and stream water quality in southern Alberta, Canada. ***Journal of Contaminant Hydrology*** *(Elsevier)* 242: 103852. DOI: 10.1016/j.jconhyd.2021.103852.